**Institut für Hydrologie**

Albert-Ludwigs-Universität Freiburg im Breisgau

**Simon Frey**

# Dating Techniques for Fast Components in Runoff

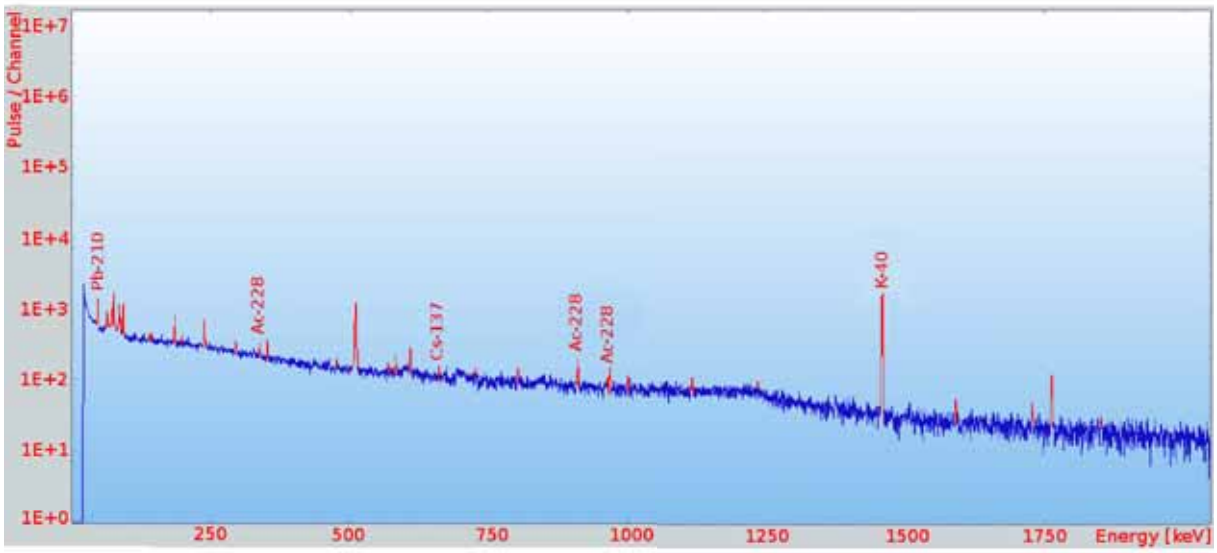


**Diplomarbeit unter Leitung von Dr. Ch. Külls**

**Freiburg i. Br., März 2010**

**Institut für Hydrologie**
Albert-Ludwigs-Universität Freiburg im Breisgau

Simon Frey

# Dating Techniques for Fast Components in Runoff

Referent: Dr. Ch. Külls

Koreferent: Prof. Dr. M. Weiler

**Diplomarbeit unter Leitung von Dr. Ch. Külls**

**Freiburg i. Br., März 2010**

# Ehrenwörtliche Erklärung

Hiermit erkläre ich, dass die Arbeit selbständig und nur unter Verwendung der angegebenen Hilfsmitteln angefertigt wurde.

Freiburg im Breisgau, den 12. März 2010,

Simon Frey

# Acknowledgements

First I would like to thank Dr. Christoph Külls for the direction of this thesis and helpful discussions. Further, I would like to thank Prof. Dr. Markus Weiler for co-supervising this thesis.

Special thanks to Dr. Clemens Schlosser and Helmut Schür from the Bundesamt für Strahlenschutz for the analysis via gamma spectroscopy, disussions and their time on Schauinsland. Also thanks to Dr. Udo Gerstmann from the Forschungszentrum für Umwelt und Gesundheit for the verification of the measurements made by the BfS.

For analysing my water samples in the laboratory, I would like to thank Stefan Kryszon from the Landesamt für Geologie, Rohstoffe und Bergbau and Barbara Herbstritt from the Institute of Hydrology. Further, special thanks to Emil Blattmann, the technician of the Institute of Hydrology, for his enthusiasm in building and modifying the sampling machine.

Thanks to Michael Daub from the Institute of Inorganic Chemistry for the provision of a centrifuge and a muffle furnace and his chemical advises.

I would like to thank Pablo Davila and Julian Haas for their critical reviews.

Also thanks to my former and recent flatmates and all my friends, who I had a great time with in Freiburg during my studies.

Special thanks to my family especially my parents Dietmar and Irma Frey and my grandfather Karl Frey for supporting me – emotionally and financially – during my whole study time.

Last, but not least, I would thank my girlfriend Mona von Harder for her time, listening to my hydrological issues, her endurance and her love.

# Table of contents

# List of figures

# List of tables



# List of figures in the appendix



# List of tables in the appendix

# List of abbreviations and units

| | |
|---|---|
| °C | degree Ceslius |
| a | year |
| Å | Ångström (0.1 nm = $10^{-10}$ m) |
| A | Ampère |
| AAS | Atomic Absorption Spectroscopy |
| BfS | Bundesamt für Strahlenschutz; Federal Authority for Radiation Protection |
| Bq | Becquerel (1 Bq = one decay per minute) |
| CFC | chlorofluorocarbon |
| Ci | Curie (1 Ci = 3.7 * $10^{10}$ Bq) |
| d | day |
| DC | direct current |
| DOC | dissolved organic carbon |
| DWD | Deutscher Wetterdienst; German Meteorological Service |
| eV | electron Volts (1 eV = 1.6 * $10^{-19}$ J) |
| g | gram |
| G | gravitational constant |
| GMWL | global meteoric water line |
| GSF | Forschungszentrum für Umwelt und Gesundheit; National Research Center for Environment and Health |
| h | hour |
| HPGe | high purity germanium |
| in. | inch (1 in. = 2.54 cm) |
| J | Joule |
| K | Kelvin |
| l | litre |
| m | metre |
| m a.s.l. | metres above sea level |

| | |
|---|---|
| min | minute |
| NaI(Tl) | sodium iodide doped with thallium |
| PALS | Positron Annihilations Lifetime Spectroscopy |
| s | second |
| S | siemens (multiplicative inverse of electrical impedance Ω) |
| SWAT | Soil and Water Assessment Tool |
| TPhB' | tetraphenylborate without a cation |
| u | unified atomic mass unit (1u = 1.660538782 * $10^{-24}$ g) |
| V | volt |
| VMOW2 | Vienna Standard Mean Ocean Water |

# List of variables

| | |
|---|---|
| $A_{eff}$ | effective activity [Bq] |
| $A_s$ | measured activity [Bq] |
| E | efficiency of the exchange resin [%] |
| K | water temperature [K] |
| $K_{sat}$ | saturated hydraulic conductivity [m $s^{-1}$] |
| $N_0$ | number of nuclides at time 0 [-] |
| $N_t$ | actual number of nuclides [-] |
| $Ox_{sat}$ | equilibrium saturation oxygen concentration at 1013 mBar [mg $l^{-1}$] |
| S | sample [-] |
| std | standard [-] |
| t | time [d] |
| V | volume of water, flew through the exchange resin [l] |
| λ | decay constant [-] |

# List of chemical symbols

| | |
|---|---|
| Al | aluminium |
| Am | americum |
| Ar | argon |
| Ba | barium |
| Be | beryllium |
| Ca | calcium |
| Cl | chloride |
| Cs | caesium |
| D | deuterium |
| H | hydrogen |
| He | helium |
| K | potassium |
| Kr | krypton |
| Mg | magnesium |
| Na | sodium |
| Ne | neon |
| O | oxygen |
| Pb | lead |
| Ra | radium |
| Rb | rubidium |
| Rn | radon |
| Ru | ruthenium |
| S | sulphur |
| Sr | strontium |
| U | uranium |
| Xe | xenon |

# Summary

Residence time is a useful information in catchment hydrology, helping provide better understanding in rainfall-runoff processes. A powerful tool for estimating the residence time is the usage of natural and anthropogenic radioactive tracers, like tritium. However, tritium concentrations in the hydrosphere almost reached their natural background levels, since atmospheric nuclear weapon tests were stopped in the mid 1960s. Therefore, there is a need for other tracers applying to age-dating, especially for young waters.

The goal of this work was the feasibility and verification of the usage of short-lived cosmogenic radionuclides, especially $^{22}$Na, for fast components in runoff, whereas fast means short residence times of less than ten years. In this order, field work as well as chemical treatment in the laboratory was done. This work was done in cooperation with the Bundesamt für Strahlenschutz (BfS, Federal Authority for Radiation Protection) in Freiburg and the Forschungszentrum für Umwelt und Gesundheit (GSF, National Research Center for Environment and Health) in Munich.

$^{22}$Na is one of the radionuclides that is produced by spallation in the upper atmosphere. After its formation it reaches the earth-surface through wet and dry deposition, whereas dry deposition is negligible. Its half-life is 2.602 years and it shows two decay modes, namely $\beta^+$-decay and electron capture. Both are linked with emissions of $\gamma$-rays at 1274.5 keV. Sodium is located in the first main group of the periodic table in the third period. It forms compounds with halogens, e.g. common table salt (NaCl). Nearly all compounds of sodium are well soluble in water.

Study area was the catchment of the river Dreisam near Freiburg, Germany. Within this catchment four locations were chosen showing water of different ages and different types of water – two groundwater sampling sites namely a spring at Schauinsland and one in the Zartener Becken (Hungerbrunnen) and two rivers, Brugga and Dreisam itself. Besides that precipitation in form of snow was collected and analysed.

Natural levels of $^{22}$Na are too low to be detected. Therefore, a method for the enrichment of minerals dissolved in water was established. Sample volume was 500 litres and an efficiency of ~70 % of the enrichment could be achieved. Because of the Compton backscattering effect, $^{40}$K disturbs the exact measurement of $^{22}$Na. Potassium in general was separated using a modified version of a chemical separation method, presented by Sakaguchi et al. (2003). By analysing the samples via gamma spectroscopy at the BfS $^{22}$Na was only detected in precipitation with an activity of 19 mBq per sample. But, surprisingly, $^{7}$Be could be detected in most of the samples excluding those from Schauinsland. Due to its high sorption, $^{7}$Be was

believed to be hardly detectable in water after passing soil or bedrock. Activities were 61.4 Bq in precipitation, 6.82 and 0.83 Bq in riverine water from Dreisam and Brugga, respectively, and 0.11 Bq in samples from Hungerbrunnen. These results were checked by GSF finding similar values. Besides gamma spectroscopy analyses, other data, indicating changes in residence times were collected. These data were stable isotopes ($^{2}H/^{18}O$) radon ($^{222}Rn$) activities and main components including silicate. Although water from Schauinsland did neither contain $^{22}Na$ nor $^{7}Be$, these data indicated, that it is influenced by a fast runoff component. The observed $^{7}Be$ levels were used for water age-dating. Equated ages for the different samples are 165.24 and 323.61 days for both rivers Dreisam and Brugga and 475.57 days for Hungerbrunnen.

Results of this study show, that $^{22}Na$ in general is detectable using this enrichment and chemical separation method. But either water samples were too small or sodium is liable to cation exchange processes with sodium stored in the soil, without changing the mass balance or influencing recovery, but changing the isotope signature. Nevertheless, these results motivate to continue the research on both $^{7}Be$ and $^{22}Na$ focusing on a better understanding of rainfall-runoff processes.

Keywords: cosmogenic produced radionuclides, $^{7}Be$, $^{22}Na$, age-dating, enrichment method, chemical separation, catchment hydrology, rainfall-runoff processes

# Zusammenfassung

Die Verweilzeit stellt eine nützliche Information für die Einzugsgebietshydrologie dar, da sie für ein besseres Verständnis von Niederschlags-Abfluss-Prozessen eingesetzt werden kann. Die Verwendung von natürlichen und künstlichen radioaktiven Tracern, wie Tritium, kann dazu beitragen, diese Information zu erlangen. Tritiumkonzentrationen in der Hydrosphäre sind mittlerweile jedoch wieder fast auf ihrem natürlichen Niveau, da seit den 1960er Jahren keine nukleare Waffen mehr in der Atmosphäre gezündet worden sind. Aufgrund dessen beseht die Notwenigkeit, neue Tracer für die Altersdatierung vor allem von jungem Wasser zu finden.

Ziel der Arbeit war es, eine Machbarkeitsstudie durchzuführen, um die Eignung von kosmogenen Radionukliden, allen voran $^{22}$Na, zur Identifizierung schneller Abflusskomponenten zu überprüfen. Um dies zu erreichen, wurden Versuche im Gelände und die chemische Aufbereitung der Proben im Labor durchgeführt. Die Arbeit fand in Zusammenarbeit mit dem Bundesamt für Strahlenschutz (BfS) in Freiburg und dem Forschungszentrum für Umwelt und Gesundheit (GSF) in München statt.

$^{22}$Na entsteht durch Spallation in der oberen Atmosphäre, von wo es durch trockene und nasse Deposition auf die Erdoberfläche gelangt, wobei die trockene Deposition vernachlässigbar ist. Die Halbwertszeit beträgt 2,602 Jahre, wobei es durch $\beta^+$-Zerfall und Elektroneneinfang zerfällt. Bei beiden Zerfällen wird $\gamma$-Strahlung der Energie von 1274,5 keV emittiert. Natrium steht in der ersten Hauptgruppe an dritter Position im Periodensystem und bildet sehr gerne Verbindungen mit Halogenen, z.B. Speisesalz (NaCl). So gut wie alle Verbindungen von Natrium sind in Wasser sehr gut löslich.

Die Untersuchungen wurden im Einzugsgebiet der Dreisam durchgeführt. Innerhalb dieses Einzugsgebietes wurden vier Probenahmestellen gewählt, sodass Wässer mit verschiedenen Verweilzeiten und verschiedenen Wassertypen zur Verfügung standen. Diese Probenahmestellen waren eine Quelle am Schauinsland und ein Grundwasserbrunnen im Zartener Becken (Hungerbrunnen), sowie zwei Flüsse, die Brugga und die Dreisam, wobei die Brugga ein Zufluss zur Dreisam darstellt. Außerdem wurde Niederschlag in Form von Schnee gesammelt und beprobt.

Da die natürliche Konzentration von $^{22}$Na zu gering ist um gemessen zu werden, wurde eine Anreicherungsmethode etabliert. Proben mit einem Volumen von 500 Liter wurden genommen und eine Effizienz der Anreicherung von ungefähr 70 % konnte erreicht werden. Der Effekt der Compton Rückstreuung ist verantwortlich dafür, dass die Messung von $^{22}$Na durch die Anwesenheit von $^{40}$K gestört wird. Deshalb wurde dieses mittels einer modifizierten

Version eines chemischen Trennungsganges (Sakaguchi et al. 2003) abgetrennt. Durch Gammaspektrometrie im BfS konnte $^{22}$Na nur im Niederschlag mit einer Aktivität von 19 mBq pro Probe nachgewiesen werden. Überraschenderweise wurde auch $^{7}$Be in den meisten Proben, außer denen von Schauinsland, gefunden. Aufgrund der hohen Sorption von $^{7}$Be, wurde angenommen, dass dieses kaum in Wasser nachzuweisen wäre, das sich durch Böden und Gestein bewegt hatte. Aktivitäten waren 61,4 Bq im Niederschlag, 6,82 und 0,83 Bq in den beiden Flüssen Dreisam und Brugga, sowie 0,11 Bq in Wasser vom Hungerbrunnen. Diese Werte wurden von der GSF überprüft. Dabei wurden vergleichbare Werte gefunden. Außer den Werten durch Gammaspektrometrie wurden weitere Daten erhoben, die Aufschlüsse über Änderungen der Verweilzeit geben können. Diese waren stabile Isotope ($^{2}$H/$^{18}$O), Radon ($^{222}$Rn) und chemische Hauptkomponenten inklusive Silikat. Obwohl diese Daten darauf hinweisen, dass die Quelle am Schauinsland von schnellen Fließkomponenten beeinflusst ist, wurde hier weder $^{7}$Be noch $^{22}$Na detektiert. Dort, wo $^{7}$Be gefunden wurde, wurde dieses verwendet um das Alter der Proben zu bestimmen. Dieses war 165,24 und 323,61 Tage für die beiden Flüsse Dreisam und Brugga und 475,57 Tage für Wasser vom Hungerbrunnen.

Die Ergebnisse dieser Studie zeigen, dass $^{22}$Na generell, unter Anwendung dieser Anreicherungsmethode und der chemischen Abtrennung von Kalium, nachweisbar ist. Jedoch waren entweder die Probenvolumina zu klein gewählt, oder Natrium unterliegt einem Austauschprozess mit im Boden gespeichertem Natrium, ohne dass die Massenbilanz oder der Rückerhalt davon betroffen wären, sich die Isotopensignatur jedoch verändert. Trotzdem ermutigen die Ergebnisse zu weiteren Untersuchungen zu $^{7}$Be und $^{22}$Na im Hinblick auf ein besseres Verständnis der Niederschlag- Abfluss Prozesse.

Schlüsselworte: kosmogene Radionuklide, $^{7}$Be, $^{22}$Na, Altersdatierung, chemischer Trennungsgang, Anreicherungsmethode, Einzugsgebietshydrologie, Niederschlag-Abfluss-Prozesse

# 1. Introduction

## *1.1 Motivation and objectives*

One of the most important phenomena in hydrology is the rainfall-runoff relationship. In this case it is very important to understand water pathways residence time and hydrological components interacting in a catchment. The information is useful in a variety of situations (e.g. water supply, water protection). By knowing the residence time of water (e.g. by collecting information about the so called “age of water”) the risk of microbiological contamination and its pathways through the hydrological system can be better understood and adequate measures can be taken to reduce the impact. The approach used for water-age estimations depends on several conditions, such as the recharge particularities and boundaries of the catchment (altitude, precipitation, temperature, mixture of waters, etc.) where it is possible to find from very young water (from recent precipitation) to ancient waters (recharged several hundreds of years ago).

While tracers applied to estimate long residence times (hundreds to thousands of years) have been widely applied – with their respective particular limitations – most of the tracers used to estimate short residence times (weeks to several years) have great limitations and challenges. Most of these tracers applied in non-ancient water-age estimations are gases, like $^{85}$Kr, CFCs, $SF_6$, $^{3}$H/$^{3}$He. These gases have many limitations of use for age estimations, especially due to their nature, atmospheric input and international regulations as well as the challenge they represent for water age studies (e.g. due atmospheric concentration reduction or local sources of the gas. Stable isotopes are often used providing only proxy data as their spatiotemporal variations are needed to track water parcels and as many factors influence their behaviour (continental effects, fractionation, etc.). In fact the attenuation and or time shift of known input signals are being used for dating purposes and provide only indirect and relative information. Absolute information on residence times were provided by $^{3}$H for the past 40 years. However, in the meantime $^{3}$H activities have dropped to their natural background levels limiting the application of such tracers.

Natural tracers providing absolute information in the range of days to few years could help answering major questions related to runoff generation, recharge and storage in hydrological basins. Nimz (1998) has proposed the use of natural cosmogenic radionuclides such as isotopes of sodium, $^{22}$Na and $^{24}$Na, as well as $^{7}$Be and $^{35}$S to estimate young water-age. While preliminary studies have shown that $^{7}$Be has high limitations because of its high sorption

(Hohwieler 2005) and $^{35}S$ is recycled in the sulphur cycle of soils and plants (Hong & Kim 2005), no obvious and known limitations constrain the applications of $^{22}Na$, whereas $^{24}Na$ has a very short half-life of only about 15 hours, making it hard to detect.

The goal of this thesis is to evaluate the feasibility and verification of the usage of natural short-lived cosmogenic radionuclides, especially $^{22}Na$, for fast components in runoff (short residence times, young water-age).

## *1.2 State of the art*

For groundwater age-dating several methods have been developed. These methods are based on the use of tracer techniques. Besides classical tracers and stable isotopes (e.g. $SiO_2$ and $^{2}H$, respectively) radioactive isotopes (e.g. $^{222}Rn$ or $^{3}H$) have been widely used (Clark & Fritz 1997). The classical tracer techniques apply the contact time of water with bedrock. The longer water has contact with bedrock, the higher the amount of dissolved minerals (until the maximum concentration is reached). The information taken from stable isotopes ($^{2}H$ and $^{18}O$) leads to a proxy for age, which means the amplitudes of these stable isotopes have to be known in order to determine the age of the water. Dating with $^{3}H$ has two disadvantages. First, because its anthropogenic origin in the 1960s by atmospheric nuclear bomb testing, two ages are estimated, one when the atmospheric concentration was rising and the other when it was decreasing again. The second and bigger problem is, that $^{3}H$ fall back to its natural background making it hardly detectable. Another method that uses tritium as a tracer is the $^{3}H/He$-method (Solomon et al. 1992). The limitation of this method is, that water must be isolated from the atmosphere to avoid degassing of He.

Besides those methods anthropogenic gases like $SF_6$ or CFCs are widely used (Gooddy et al. 2006). These tracers have limitations to application for groundwater only, due to their gas phase being sensitive to atmosphere contact and their reduced solubility.

Unfortunately, most of the mentioned techniques are useless in surface water, where the water is in constant exchange with the atmosphere or had low contact time with the bedrock (fast flow). Since the early 1960s, there are many research programs to develop other techniques using airborne radionuclides and other tracers. The two most popular are $^{7}Be$ and $^{35}S$ with half-lives of 53 and 86,7 days, respectively (Wogman et al. 1968); both of them have serious limitations for water-age estimations. $^{7}Be$ is very sorptive. After its production in the atmosphere it immediately sticks to aerosols (e.g. dust). When it reaches the surface by precipitation it sticks to particles of the soil; up to 90% of its input stays in the topsoil

(Hohwieler 2005). However, about 10 % of the $^{7}$Be input is mobile and reaches the groundwater at some point where it may possibly be detected. $^{35}$S presents the limitation of being taken up in the sulphur-cycle of soils and plants, where it can stay up to several years (Novák et al. 2004). However, the method can work in catchments, where the soil has a very low sulphate adsorption capacity and biological influences are minimal (Sueker et al. 1999).

$^{22}$Na was detected more than 50 years ago in rainwater samples in Rio de Janeiro, Brazil (Marquez et al. 1957) by an interesting experiment. Huge water samples of 3,000 – 4,000 litres of rainwater were collected and passed through a column (area: 50 cm² height: 50 cm) filled with Amberlight IR120 resin to separate the dissolved ions of water. After regeneration of the resin and evaporating the HCl solution to dryness Ca and Mg were separated using $NH_4OH$. The anions were separated using a resin column that was eluted with 0.1M HCl and the sodium which came first was collected. After potassium came second, the column was washed with 4M HCl to determine $^{137}$Cs. The activity of $^{22}$Na was determined by the annihilation of the emitted positrons using a scintillation spectrometer. The average activity of $^{22}$Na in Rio de Janeiro was found to be 0.28 mBq/l.

A few years later, Perkins & Nielsen (1965) found $^{22}$Na in air. It was found, that the production rate varies hardly by altitude, but significantly by latitude. As $^{22}$Na is a function of the cosmic ray fluxes it increases by about one order of magnitude moving from the equator to the poles at elevations above the tropopause. Below an elevation of about 3 km the production rate varies slightly with latitude. This is also shown by Lal & Peters (1967). Their results of the dependency from both altitude and latitude for $^{7}$Be are shown in Fig. 1.1, because $^{7}$Be is also produced by spallation (see chapter 3.1.3 ), and its production rate is a function of the cosmic ray fluxes as well, having the difference of being about four times higher (Jasiulionis & Wershofen 2005). In levels close to the sea level, the production rates of $^{22}$Na show hardly any variation pointing on the geomagnetic latitudes from 90 °N to about 40 °N and the same region on the southern hemisphere. Therefore, one can to assume, that it should be possible to compare results gained from mesurements taken in these regions. By moving upwards, the production rates increase fast, which means that measurements in the mountains have to be corrected for comparison with measurements at sea level. Again, at the same altitude, even at ~7 km elevation, the production rates hardly vary moving from 90 °N to about 50 °N and the same regions on the southern hemisphere.

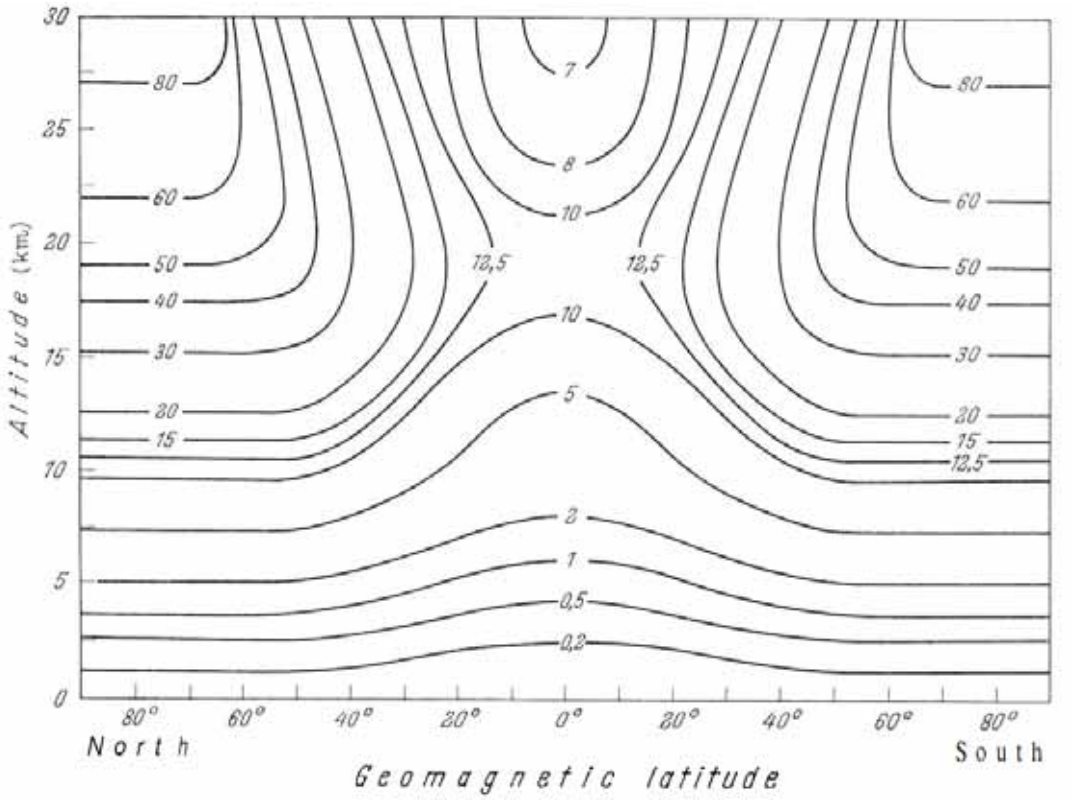


Fig. 1.1: A north - south section through the atmosphere showing surfaces of constant $^{7}$Be production rates (nuclei * min-1 * m-3 air). $^{7}$Be is produced by a spallation reaction of oxygen or nitrogen (Lal & Peters 1967).

After the 1970s only few research was done, although in this time, bomb-produced $^{22}$Na was still in the atmosphere and could have been used. In the hydrosphere, the bomb-produced $^{22}$Na disappeared in the early 1990s and since then remained on its natural levels. The fallout rates for several regions in Eurasia between the 1960s and 1980s are shown in Fig. 1.2. The very high fallout in Rome shown in the figure, occurs for unknown reasons (Fleishman 2008). The fast decreasing of the fallout rates does not contradict the evidence, that natural levels of $^{22}$Na in the hydrosphere were not reached until the 1990s.

Cigna et al. (1970) determined the $^{22}$Na concentrations in rainwater samples collected at the Casaccia Nuclear Center in Rome from 1961 to 1968 (see Fig. 1.2). The rainwater samples were collected monthly and evaporated for analysis with a sum gamma-gamma coincidence technique using two 4 x 4 in. (app. 10.16 x 10.16 cm) NaI(Tl) crystals. They showed, that the maximum of the artificial $^{22}$Na level was reached in the beginning of 1963, started to decrease and became practically constant after 1966. Furthermore, they tried to determine the natural part of the total detected $^{22}$Na, assuming that the natural component is constant. By trial and error tests, they found 0.0814 mBq/l to be the best attributable value of the natural

component. This value equates to about 666 MBq/km²/a which agrees well, in the order of magnitude, to the theoretical value (214 MBq/km²/a) reported by Lal & Peters (1962).

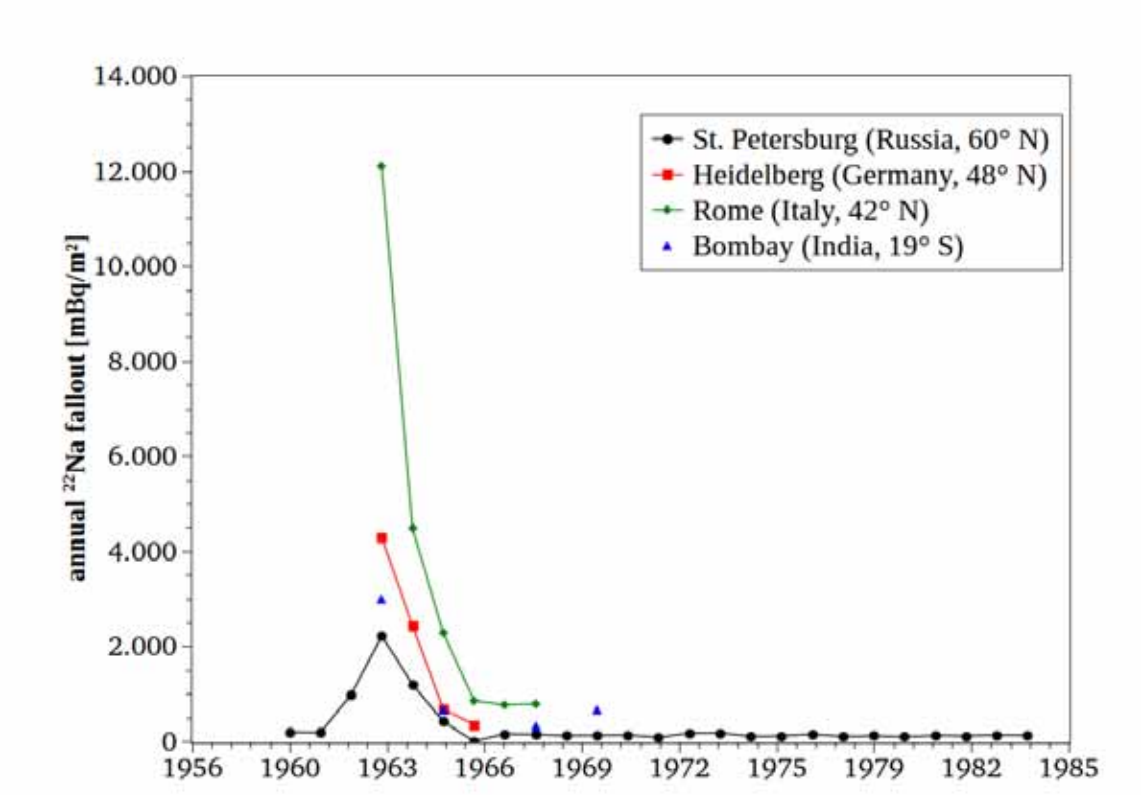


Fig. 1.2: $^{22}$Na fallout rates for four regions in Eurasia (data from Fleishman (2008)).

The deposition rates (wet and dry fallout) were also determined by Tokuyama & Igarashi (1998) at Fukui City, Japan. Rainwater samples were taken (70 – 310 l) monthly during the period of December 1991 – April 1994 using a 0.98 m² collector. $^{22}$Na was separated using a POWDEX® ion-exchange resin and measured after drying with a high-purity germanium coaxial detector. The $^{22}$Na nuclide was identified by the gamma ray peak at 1275 keV, that had the minimum detectable limit at 0.28 mBq $m^{-2}$ $d^{-1}$ using counting periods of 3 – 8 x $10^5$ seconds. Besides $^{22}$Na, $^{7}$Be was measured, as well.

The deposition rates for $^{22}$Na varied widely with a range from 0.31 to 3.1 mBq $m^{-2}$ $d^{-1}$, leading to 0.1 to 0.28 mBq $l^{-1}$ $d^{-1}$. It showed high correlation ($r^2$ = 0.94) to the deposition rates of $^{7}$Be, that ranged from 2.7 to 29 mBq $m^{-2}$ $d^{-1}$. This high correlation leads to the assumption that both radionuclides attach to aerosols and the washout mechanisms are similar. Both radionuclides showed seasonal variations having their annual peak in December ~ February. The values decreased in spring to early summer leading to the minimum concentration in June ~ August. The reason for this seasonal variation is, that the atmospheric exchange between stratospheric

and tropospheric air is higher in autumn. This is because the tropopause shows a seasonal variation in its height, being higher in summer time (Tokuyama & Igarashi 1998).

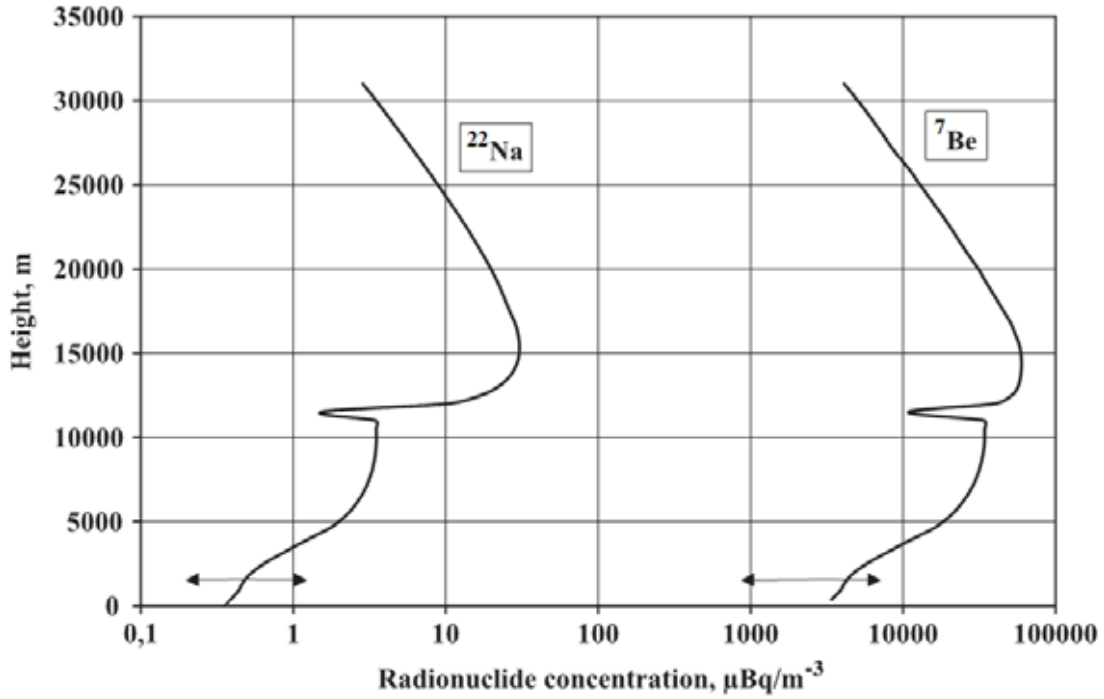


Fig. 1.3: Distribution of the mean activity concentrations of $^{7}$Be and $^{22}$Na and the range of the concentration variation in the ground-level layer, indicated by the arrows (Jasiulionis & Wershofen 2005).

This thesis was also tested and approved by Jasiulionis & Wershofen (2005). They studied the vertical transport of $^{22}$Na and $^{7}$Be in the atmosphere. By applying activity measurements of both radionuclides in ground-level air, data of the production rates and an one dimensional steady state diffusion model. To find the parameters for their model, they also used data collected in Braunschweig, Germany, from 1970 – 1976 (Kolb & Wershofen 1991) and from 1985 to 1995 (Wershofen & Arnold 1995) as their own measurements in the vicinity of the Ignalina Nuclear Power Plant, Lithuania, during 1978 to 1983 and 1995 to 1999. The results of the one dimensional steady state diffusion model are shown in Fig. 1.3. The cut at height of about 12000 m represents the tropopause. It is clear to see, that the concentration above the tropopause is significantly higher than below it. The tropopause also acts like a barrier, so that there is hardly any air exchange between the air masses below and above the tropopause. If this barrier moves downwards (like it does in winter), the air enriched with radionuclides can be exchanged with the air in lower levels and the fallout rate increases. The ground-level concentrations were mainly influenced by wet deposition.

Although there have been studies about $^{22}Na$ activities, hardly any of them were used to estimate the water-age. This was done by Sakaguchi et al. (2005), who measured the activities of $^{22}Na$ in lake and river water in Lake Biwa, Japan. They took large water samples of about 500 l, separated sodium from the other ions by a chemical procedure described in Sakaguchi et al. (2003) and used a coaxial-type pure Ge-detector to measure $^{22}Na$ activity. This detector was installed at the Ogoya Underground Laboratory at the Kanazawa University, Japan, covered by a 135 m thick rock cover, corresponding to 270 m water equivalent. The detector had an 400 ml detector volume and a 93.5 % relative efficiency. $^{22}Na$ was detected using the 1275 keV γ-ray peak. To determine the atmospheric input concentration, $^{7}Be$ was measured in rainwater samples, monthly collected from 1997 – 2002. In these samples, unfortunately, $^{22}Na$ was undetectable because the samples were too small.

The Lake Biwa System consists of two parts: the northern (surface area: 616 $km^2$, volume: 2.73 x $10^{10}$ $m^3$, and mean depth: 41 m) and the southern part (surface area: 58 $km^2$, volume: 0.2 x $10^9$ $m^3$, and mean depth: 4 m). In the northern lake water Sakaguchi et al. (2005) found concentrations ranging from 19.9 to 32.7 mBq $m^{-3}$, in the water of the southern lake 34.3 to 40.0 mBq $m^{-3}$. The riverine water contained concentrations ranging from 28.0 to 38.3 mBq $m^{-3}$ in the Ado River and from 27.4 to 34.9 mBq $m^{-3}$ in the Yasu River. Although the runoff in the rivers varied more than two orders of magnitude, the $^{22}Na$ concentrations were relative stable.

The residence time of the water in the lake was determined using a one-box model. The water in the northern part had a mean residence time of about 5.4 years, the smaller southern part had a mean residence time of about 18 days. These results were compatible to those reported for water in the lake.

# 2. Study areas

## *2.1 Dreisam River*

The catchment of the river Dreisam at the Ebnet gauging station (316 m a.s.l.) is located in the south west of the Black Forest (close to Freiburg) and has an area of ~258 km² (Fig. 2.2). Mean annual precipitation is ~1500 mm $a^{-1}$ generating an annual discharge of ~820 mm $a^{-1}$ and a groundwater discharge of about 60 mm $a^{-1}$. Evapotranspiration is ~600 mm $a^{-1}$. The permeability of topsoils in this area is large enough ($K_{sat}$ $>10_{-4}$ m $s^{-1}$), to prevent infiltration excess overland flow occurs. Total urban land use areas, producing direct runoff, are about 2 – 3 %, while water saturated areas are about 1 – 2 % of the whole area. The catchment can be divided in two areas. First, the valley “Zartener Becken”, which is the flatter part of the catchment (8 % slope), underlayed by and a 50 m deep porous aquifer. Land use is dominated by farmland, pasture land and some urban settlements. Second, the mountain region, characterized by steep hill slopes, bedrock outcrops and deep V- and U-valleys as well as plateaus. Land use here is dominated by forest (Wissmeier & Uhlenbrook 2007).

The sampling site is located next to the Ebnet gauging station, close to the mouth of the Eschbach.

## *2.2 Brugga River*

The river Brugga is located in the Black Forest in southern Germany. Its catchment is a sub-catchment of the river Dreisam and its area is ~40 km². The maximum difference in height is more than 1000 m between the exit at the gauge Oberried (434 m a.s.l.) and the peak at the Feldberg (1493 m a.s.l.) with a mean altitude of 986 m a.s.l. The mean gradient is about 17.5° while 10 % reach a gradient of over 40°. The mean discharge of the river Brugga is 1.55 m³/s (Uhlenbrook 1999).

The sampling site itself is located next to the gauge at Oberried.

## *2.3 Schauinsland*

The Schauinsland is a 1284 m (a.s.l.) high mountain in the Dreisam catchment. Mean annual precipitation is ~1750 mm (Wenninger et al. 2004). In the peak region, there are sampling stations of the Bundesamt für Strahlenschutz (BfS, Federal Authority for Radiation Protection) and the Umweltbundesamt (Federal Environmental Agency). Besides the measurement of several atmospheric micro elements like $^{85}Kr$, $^{133}Xe$ and $SF_6$, particulate matter and other meteorological data (precipitation, wind, sunshine duration, etc.) are collected by theses entities. Close to the sampling stations, about 300 m downhill is a sampling well used to collect data for this work. It is covered in a small well house where two basins are present. Water from the well flows directly in basin one. The water may flow through a bleeder into the second basin which is bigger than the first one or leave the basin through second bleeder and flow downhill (Fig. 2.1). In basin two the water stays for a while and relaxes before it is pumped into the water supply for the building of the BfS. The pumps are located at the bottom of the second basin. The samples were taken direct at the well, before the water reaches the first basin.

Fig. 2.1: Well at Schauinsland. Water flows in the first basin and may flow into the second basin (left) or leave the first one and flow downhill.

## 2.4 Hungerbrunnen

The water supplier of Freiburg, Badenova, runs three wells in the east of Freiburg, located next to the Dreisam. They are called the Hungerbrunnen (hunger well) wells, because in the past, they were often falling dry. The one, that is used for the samples of this work, is Hungerbrunnen 1 (334 m a.s.l.). It is a 30 m deep well used for the water supply of Freiburg. The water for the samples is taken before UV irradiation exposition.

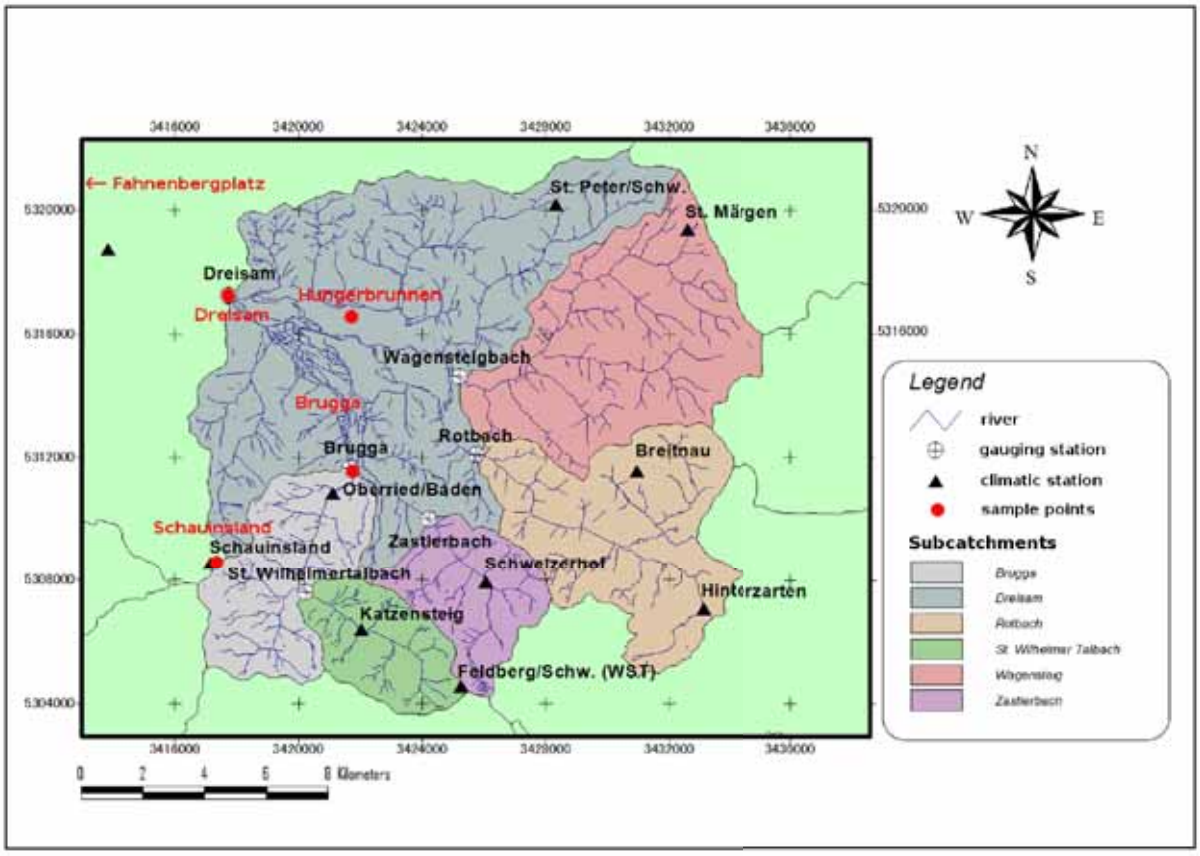


Fig. 2.2: The Dreisam catchment. Sampling points are represented by red dots (after (LUBW 2007).

# 3. Theoretical basics

## *3.1 Basic principles of sodium*

Sodium is an alkaline metal and is located in the first main group of the periodic table of the chemical elements in the third period. Elementary sodium is a soft, white metallic metal, that can be cut by a knife. With the presence of oxygen and water it oxidises fast, creating an oxidised protection layer. If no water is present, elementary sodium can be melted, even if oxygen is present. Its melting and boiling points are quite low, 97.82 °C and 881.3 °C, respectively. Elementary sodium does not exist naturally on earth. It has similar chemical characteristics as its neighbours in the first period of the periodic table: lithium and potassium. The standard electrode potential of sodium is -2.71 V. Because it has only one valence electron, it has a bigger atomic radius than its neighbour magnesium and builds compounds with halogens. The presence of only one valence electron is also the reason for its big hydration hull.

Table 3.1: Physical behaviours of sodium (after Holleman et al. (2007))

| Behaviour | value |
|---|---|
| Relative atomaric mass [-] | 22.989 |
| Electron affinity [eV] | -0.546 |
| Atomic radius [Å] | 1.91 |
| Density [g/cm³] | 0.971 |
| Melting point [°C] | 97.82 |
| Boiling point [°C] | 881.3 |
| Melting enthalpy [kJ] | 2.64 |
| Boiling enthalpy [kJ] | 99.2 |
| Specific conductivity [S/cm] | $2.38 \times 10^5$ |
| Electronegativity [-] | 0.9 |
| Hydration enthalpy [kJ] | -406 |
| Standard electrode potential [V] | -2.713 |

All compounds of sodium are ionic, covalent compounds do not exist. The most common compound is common table salt (NaCl), that is the most important mineral (halite), too. One of its most important technical compounds is sodium hydroxide (NaOH). Most of the

compounds of sodium are well dissoluble in water (Holleman et al. 2007). Whenever sodium is mentioned in this work, the ionic form ($Na^+$) is meant. The physical behaviours of sodium are given by Table 3.1.

There are five isotopes of sodium: $^{21}Na$, $^{22}Na$, $^{23}Na$, $^{24}Na$ and $^{25}Na$. Only $^{23}Na$ is stable, $^{21}Na$ and $^{25}Na$ have half-lives of a few seconds and are not useful for age-dating. $^{22}Na$ and $^{24}Na$ have half-lives of 2.602 years and about 15 hours, respectively (Holleman et al. 2007). Because the half-lives of $^{21}Na$ and $^{25}Na$ are too short to be used in hydrology, they won't be discussed here. Disintegration schemes of both $^{22}Na$ and $^{24}Na$ are shown in Fig. 3.1.

### 3.1.1 $^{22}Na$

$^{22}Na$ was produced artificially by the nuclear weapon tests in the 1960s. Because the threshold for the energy needed to produce this isotope, is about 12,8 MeV, it was probably produced only by fusion-bombs (Cigna et al. 1970). It still is produced in nuclear power plants, but the concentrations are very low and should therefore be negligible compared to the cosmogenic produced concentrations.

Cosmogenic $^{22}Na$ is produced by spallation between secondary cosmic rays and $^{40}Ar$ (Lal & Peters 1967). Its half-life is, as mentioned before, 2.602 years. It decays by the processes of electron capture (EC) or by emitting a positron ($\beta^+$-decay). The probabilities for the disintegration via $\beta^+$ is 89.84 %, while via EC it is 10.11 %. Both are of allowed nature and lead to the 1275 keV-level of $^{22}Ne$. In addition, there are two weak unique forbidden transitions ($\beta^+$ 0.056; EC 0.0010) leading to the ground state of $^{22}Ne$ (Helmer & Schönfeld 2009).

### 3.1.2 $^{24}Na$

Same as $^{22}Na$, $^{24}Na$ also was produced artificially by nuclear weapon tests in the 1960s, and still is produced in nuclear power plants. Naturally it is produced by spallation in the atmosphere as well. It decays by the emission of an electron ($\beta^-$) with a probability of 100%, leading to the 4123 keV-level $^{24}Mg$. This process is followed by two $\gamma$-rays (2754 and 1393 keV) in cascade leading to the ground state of $^{24}Mg$ (Helmer & Schönfeld 2009).

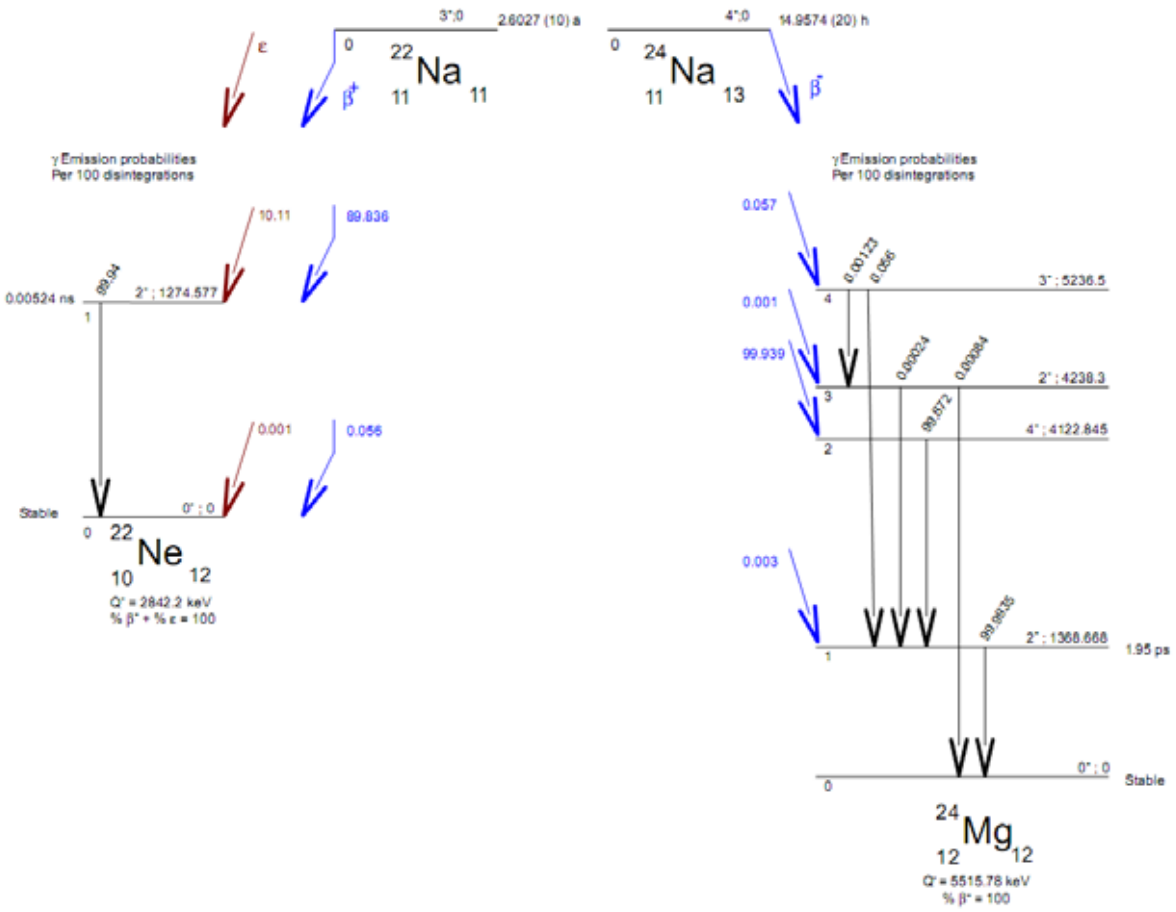


Fig. 3.1: Disintegration schemes for $^{22}$Na and $^{24}$Na (Helmer & Schönfeld 2009)

### 3.1.3 Spallation

Spallation is the process, when a nucleus of an isotope is hit by a projectile, e.g. a proton or neutron. The kinetic energy of this projectile is assigned to the nucleus. That causes the nucleus to emit one or two of its nucleons and go to an excited status, called fireball. The excessive energy is lost by emitting more neutrons, the so called spallation neutrons. If there is any energy left after this step, the nucleus decays emitting radioactive rays and goes to its ground state (ESFRI 2006). It must not be mistaken with nuclear fission (the process of joining two in one with a resulting energy emission). The spallation process is shown by Fig. 3.2.

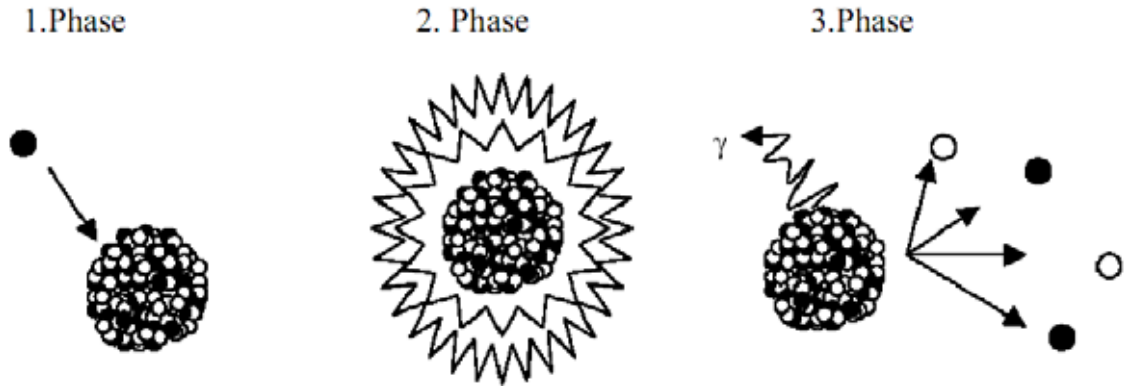


Fig. 3.2: The spallation process: 1st phase: a nucleus is hit by a projectile. 2nd phase: The nucleus is in a excited state (fireball). 3rd phase: spallation neutrons and γ-rays are emitted (Keller 1993).

## *3.2 Basics of nuclear decay*

Radioactive material can decay by several processes emitting α, β or γ-rays. An overview is given by Table 3.2.

Table 3.2: Overview over the radioactive decay modes

| **Decay** | **emitted particle/ray** | **Example** |
|---|---|---|
| **α** | 2 protons + 2 neutrons | $^{222}$Rn |
| **$\beta^-$** | electron | $^{24}$Na |
| **$\beta^+$** | positron | $^{40}$K |
| **EC** | neutrino and γ-rays | $^{22}$Na |
| **γ** | quanta | $^{137}$Cs |

### 3.2.1 α-decay

A helium nucleus is being emitted when an atom decays by this type of disintegration. The mother nuclide therefore loses two protons and two neutrons, the mass of the daughter nuclide is reduced by four u (atomic mass unit). After the particle has left the nucleus, the atom has too many electrons, it remains in an excited status. When it falls back to its ground status, γ-rays are emitted. Although the exit velocity is relatively high, about 15,000 to 20,000 km/s, the reach is quite small, only a few centimetres in air. The energy of a particle ranges from about 2 to 10 MeV, depending on which isotope decays (Harten 2009).

### 3.2.2 β-decay

The most common form of the β-decay is $\beta^-$-decay. A neutron splits up in a proton and an electron, that leaves the atom. The daughter nuclide has the same mass but one proton more than its mother nuclide, therefore it is located right next to its mother nuclide in the periodic table. Besides the $\beta^-$-decay, there is the more rare $\beta^+$-decay. Here, a proton splits up in a neutron and a positron, that leaves the atom. Once again, the mass of the daughter nuclide stays the same while it loses one proton, therefore it is located left to its mother nuclide in the periodic table. Same as in the α-decay, the atom stays in an excited status after the β-decay, sending out γ-rays when falling to its ground state. The energy of a β-particle is lower than of an α-particle. It ranges from about 20 keV to about 1 MeV, once again depending on the decaying isotope. Because of the very small mass, its reach is higher, ranging from centimetres to few metres in air (Martin & Blichert-Toft 1970).

### 3.2.3 Electron Capture (EC)

Electron capture (sometimes also called ε-decay) runs at three steps. First a core of an atom catches an electron from one of the shells, mostly from the closest shell to the core, called the K-shell. In the core this electron fusions with a proton to a neutron, producing a neutrino (subatomic particle of neutral charge) as well. The neutrino leaves the atom (second step) and the K-shell looses one electron. This lost electron is replaced by an electron of one of the outer shells. The energy gained from this process is emitted either in form of X-rays or as an Auger-electron[1] (third step).

Not always the hole energy gained from the fusion of the electron and the proton is transferred to the neutrino. Then the core stays excited, sending out γ-rays with an discrete energy spectrum when going to its ground state (Harten 2009).

### 3.2.4 γ decay

Theoretically it is incorrect to speak about γ-decay, because this occurs only after an atom decayed by α, β or EC disintegration (Harten 2009). Therefore it is more appropriate to refer as γ-rays. The energy of γ-rays must be more than 200 keV, otherwise they are called X-rays.

1 Auger-electron: physical phenomena, where the disappearing of one internal electron of the atom provokes the emission of a second electron. The second electron is called Auger-electron.

### 3.2.5 Compton backscattering effect

As mentioned, every decaying atom emits radiation at one or several defined energy levels. Radiation on higher energy levels scatters back to levels with lower energies (Weeks et al. 1997). Because $^{40}K$ emits radiation at 1461 keV (Espinosa et al. 2009), disturbing the analysis of $^{22}Na$ by its 1275 keV rays, it has to be separated from the sample in order to avoid failures in data interpretation.

## *3.3 Basics of cation exchange*

Cation exchange of sodium plays an important role on the usage of cosmic produced isotopes as tracers in hydrology. Therefore the process of cation exchange is described in this document. When dissolved cations in the soil solution moving through the soil, some of them stay there. They are getting sorbed on the negative charged anions in the soil. Whenever one cation is sorbed, another cation with the same charge or more cations with lower charges are desorbed. For example, if one aluminium-ion is sorbed on the soil, three potassium-ions or one potassium-ion and one calcium-ion can be desorbed. This process is called cation exchange. How many cations can be exchanged in the soil depends on the cation exchange capacity (Scheffer & Schachtschabel 2002). Which species of ions are absorbed and desorbed on the soil depends on the characteristics of the ions and of the soil. The most important characteristics of ions are described below.

Preliminary column experiments have shown that cation exchange can nearly be neglected for sodium (Birkholz 2007). Recovery in medium and fine sand was 93 and 80 %. Lithium shows recovery of 82 % in medium sand and 71 % in fine sand. Though, lithium is widely used as tracer in hydrology (Botter et al. 2009, Leblanc et al. 1991). The lowest recovery was observed for potassium with 29 % and 13 % for medium and fine sand, respectively, because potassium is highly exchangeable. Tracer breakthrough curves of these experiments are shown in Fig. 3.3.

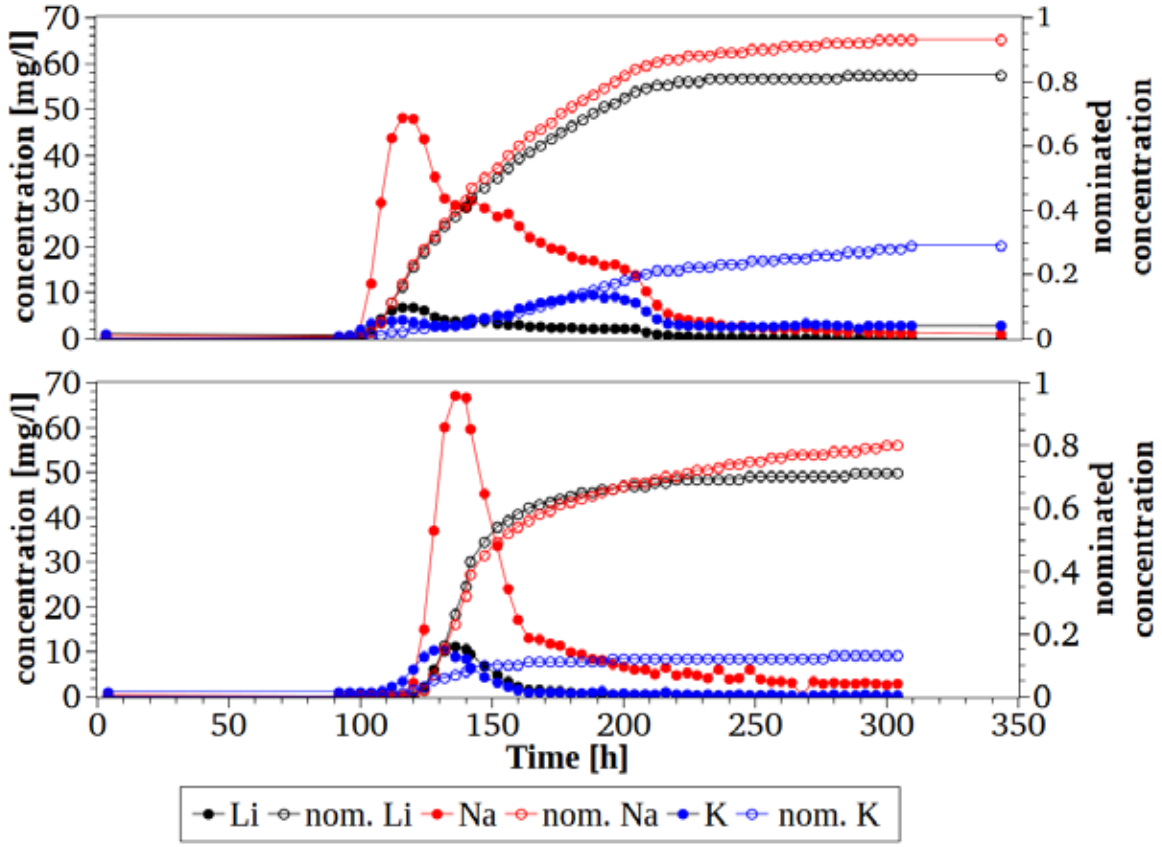


Fig. 3.3: Tracer breakthrough curve for medium sand (top) and fine sand (bottom). Data from Birkholz (2007).

### 3.3.1 Effect of steric, hydration and valence

How strong ions are attached on the soil and therefore, how easy they are influenced by exchange, depends on three effects in general: steric effect, hydration effect and valence effect. As a fourth effect, the concentration in the soil solution can be added.

#### *3.3.1.1 Steric effect*

The places, where cations lay in the soil, have spatial molecular structures. Therefore cations, that fit well in these structures, are attached better than cations, that are too big or too small to fit well. A well fitting cation is exchanged harder than a bad fitting cation. For example, potassium is attached very well in some clay minerals. The steric effect can have a greater influence on the cation exchange than the valence effect, because bivalent cations are displaced by monovalent ones (Scheffer & Schachtschabel 2002). This is shown in Fig. 3.4.

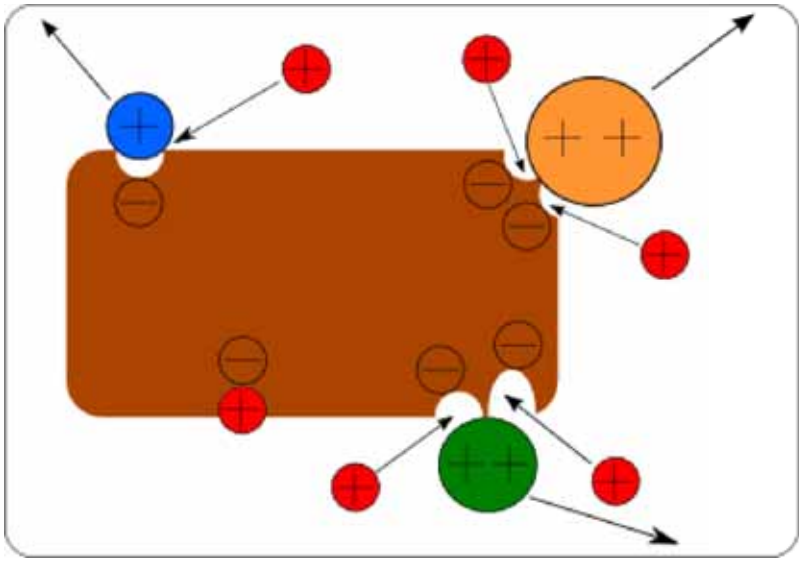

Fig. 3.4: The steric effect causes bivalent cations to be displaced by monovalent cations (red $K^+$, blue $Na^+$, green $Ca^{2+}$, orange $Mg^{2+}$).

### *3.3.1.2 Hydration effect*

Ions are polar and therefore they tend to have a hydration hull. The size of this hull depends on the valence of the ion and its mass. At constant valence and increasing mass, the polarising effect decreases. The smaller this effect is, the smaller is the hydration hull of the ion (Holleman et al. 2007). In the first period of the periodic table of the chemical elements for example, the size of the hydration hull decreases from lithium to francium while the radius of the ions increases. The bigger the hydration hull, the bigger is the effective radius of the ion and the weaker is the linkage of the ion in the soil. Although sodium is much smaller than caesium and should therefore be preferred to stick to the ion exchange places, its linkage in the soil is weaker and it is washed out. The hydration effect is indicated in Fig. 3.4: The ionic radius of sodium is smaller than of potassium and that of magnesium is smaller than that of calcium, but the pictured sizes are the other way round. Therefore, in the left corner of Fig. 3.4, sodium is replaced by potassium.

### 3.3.1.3 Valence effect

The strength of the bond is proportional to the charge of the cation. That means that bivalent cations are stronger bounded on the soil than monovalent cations but weaker than trivalent cations. The strength of the bond also depends on the size of the cation. The higher the charge of an ion, the bigger it is. These two dependencies lead to the lyotropic series, that was described first by Hofmeister (1888), and is shown in Fig. 3.5.

$$Li^+ < Na^+ < K^+ < NH_4^+ < Rb^+ < Cs^+ < Be^{2+} < Mg^{2+} < Ca^{2+} < Sr^{2+} < Ba^{2+} < Ra^{2+}$$

Fig. 3.5: Lyotropic series, after Scheffer & Schachtschabel (2002),edited.

### 3.3.1.4 Concentration effect

If one of the cation species in the soil solution has a significantly higher concentration than the others, this species will be exchanged more than the others. This means, that e.g. monovalent ions can replace bivalent ones. The steric, valence and hydration effect can be outnumbered by the concentration effect (Scheffer & Schachtschabel 2002).

## 3.4 Stable isotopes of oxygen and hydrogen

Oxygen has three stable isotopes, $^{16}O$, $^{17}O$, $^{18}O$, whereas $^{16}O$ is the most common isotope with a natural abundance of ~99.7 %, $^{17}O$ is the most rare isotope with a natural abundance of ~0.038 % (difficult to measure) and $^{18}O$ has an occurrence of 0.204%. Hydrogen has only two stable isotopes, ordinary $^{1}H$ and $^{2}H$, also called protium and deuterium (D), with an occurrence of 99.985 % and 0.015 %, respectively (Clark & Fritz 1997). $^{18}O$ and $^{2}H$ are of high interest in hydrology, because of their conservative behaviour in water (as constituents of the water molecule) and the large variability of their isotopic ratios $^{2}H/^{1}H$ and $^{18}O/^{16}O$ (Rozanski et al. 2001). Usually, they are measured in terms of their δ values (eq. 3.1). Because these δ are small numbers, they are given in ‰.

$$\delta^{2}H = \frac{\left({}^{2}H/{}^{1}H\right)_{S}}{\left({}^{2}H/{}^{1}H\right)_{Std}} - 1 \qquad \delta^{18}O = \frac{\left({}^{18}O/{}^{16}O\right)_{S}}{\left({}^{18}O/{}^{16}O\right)_{Std}} - 1 \qquad \text{(eq. 3.1)}$$

where S stands for sample and Std for reference or standard. Most used standard is VSMOW2 (Vienna Standard Mean Ocean Water 2).

δ-values in precipitation in one catchment depend on the temperature. Therefore they show seasonal variations. In small catchments, the δ-signal of river water is related to that of precipitation (Rozanski et al. 2001). This means, that the isotopic signal is transported in space and time and the origin and a proxy for age can be determined by measuring the δ-values. Other important factors influencing the signal are effects of latitude, altitude and kinetic fractionation.

## *3.5 Chemicals used in the research and their particularities*

### 3.5.1 The azeotrope of water and hydrochloric acid

When evaporating a solution of hydrochloric acid in water, it is unavoidable to produce a so called azeotrope. An azeotrope (from Greek: a = negation, zeo = boiling, tropos = direction) is an alloy of two substances that cannot be divided by distillation. The alloy has one boiling point, where both substances evaporate at a constant ratio. The vapour and the fluid have the same concentration. One of the most famous azeotropes is the solution of 95.6 % (by weight) alcohol in water. This is the technical limit for producing pure alcohol by distillation. The azeotrope of hydrochloric acid is located at 20.22 % (by weight) HCl at the standard pressure of 1013 mbar. When evaporating a solution with more than 20.22 % (by weight) HCl, the evaporation of hydrochloric acid is higher than of water until the azeotrope is reached. On contrary, when there is less HCl in the solution, water evaporates more than HCl until the azeotrope is reached. The boiling point of the azeotrope is 108.5 °C at 1013 mbar (Holleman et al. 2007). This azeotrope is produced by evaporating the eluate of the exchange resin.

### 3.5.2 Ammonium salts

Ammonium carbonate is a colourless crystal, which is well dissoluble in water (~320 g/l) but insolvable in ethanol. The chemical used is not clean ammonium carbonate, but is a 1:1 mixture composed of ammonium hydrogen carbonate ($NH_4HCO_3$) and ammonium carbamate ($CH_6N_2O_2$) (Merck 2003). When heating a solution with this mixture, ammonium carbamate reacts with water to ammonium carbonate. Ammonium carbonate itself is unstable at temperatures above 60 °C and reacts to $CO_2$, $NH_3$ and water (Holleman et al. 2007).

When adding HCl to an ammonium salt solution and evaporating to dryness, the result is ammonium chloride. Ammonium chloride ($NH_4Cl$) is a colourless crystal that sublimates at 350 °C and dissociates into HCl and $NH_3$. Its solubility in water is about 370 g/l (Holleman et al. 2007).

### 3.5.3 Tetraphenylborate (TPhB')

The TPhB' used in this research has sodium as cation. NaTPhB is a colourless crystal, which is well dissolvable in water and ethanol. TPhB' is used for gravimetric determination of potassium (Spier & Wagner 1952). The solubility in water of KTPhB is 53 mg/l (which is about 1/10 of the solubility of AgCl). Other substances as ammonium, lead, caesium and rubidium precipitate by adding TPhB' to the solution (Sarudi 1972).

# 4. Methodology

## *4.1 Materials for sampling and analysing of cosmogenic radionuclides*

### 4.1.1 Description of the first setup for the sampling machine

To take samples in the field a sampling equipment was constructed that includes a battery, a pump and a filter holder mounted in a plastic box. The system is connected with hoses to a flow meter, the water inlet and to the column containing the ion exchangers. This first machine arrangement is shown in Fig. 4.1. The pump is able to pump up to six litres per minute and can build a pressure up to three bars. It works with an energy supply from an internal battery of 12 V DC. As a measure of precaution, the machine was built to support the use of an external battery, in case the internal is discharged. If the external battery is used for energy supply, the internal one is capped from the energy cycle. This is necessary because the internal battery would be charged as well and the external one would discharge much faster then. Therefore, an power switch with three stages is used to decide whether the external power supply is switched of used to load the battery or run the pump. In addition, a power switch is installed to switch the pump on or off. This works independently from which power supply is used. Under normal conditions it is not necessary to use a external battery. The internal one has enough energy to supply the pump for taking one sample. To prevent energy overload a 6.3 A fuse is located at the box. Recharging the battery in the pumping box can be done using a standard battery recharger or by an external battery. Therefore a socket is installed and a cable with standard plug on one end and a fitting plug for connecting the internal battery on the other end can be used.

To prevent dirt contamination a filter is located outside the box and another one is located at the end of the inlet hose. Both filters have pore sizes above 45 nm. They are used to make sure, that no coarse material can get to the pump damaging it. In order to quantify the amount of water pumped, a flow monitor similar to those used in households, is installed. It can measure flow velocities up to 3 $m^3\ h^{-1}$.

The resin column is a transparent glass column of ~60 cm height and ~5 cm by diameter, which was installed on the top of the box after the flow meter and the pump. It is filled with both cation and anion exchange resin (1:1) to create the necessary anionic/cationic reactions from the pumped water. The cation resin is an Amberlite® IR-120, for the anion change an Amberlite® IRA-416 is used. The Amberlite® IR-120 is a strongly acidic cation exchanger,

the Amberlite® IRA-416 is a strongly basic anion exchanger. Both are specifically designed for water treatment and total demineralisation of water. The characteristics of both resins is shown in Table 4.1. Both resins are based on a matrix made of polystyrene cross-linked with divinylbenzene. The degree of cross-linking is in both cases, as usual, about 8%. To allow water to flow through the column without any loss of resin, a net with a pore size smaller than the grain size of the resins is installed on both sides of the column.

Table 4.1: Characteristics of the used exchanger resins (Merck 2009)

| resin | Amberlite® IR-120 | Amberlite® IRA-416 |
|---|---|---|
| type of exchanger | gel | gel |
| active group | ~ $SO_3$ | ~ $N^+(CH_3)_2(CH_2OH)$ |
| exchanged ion | $H^+$ | $Cl^-$ |
| exchange capacity [mval/ml] | > 1.7 | > 1.35 |
| soaking [%] | 7 | 15 |
| maximum working temperature [°C] | 120 | 80 |
| pH range | 0 – 14 | 0 – 14 |
| grain size [mm] | 0.3 – 1.2 | 0.3 – 1.2 |
| Moisture [%] | 45 – 55 | 40 |
| bulk density [g/l] | ~ 800 | 700 |
| regeneration agent | HCl or $H_2SO_4$ or NaCl | NaCl or HCl |

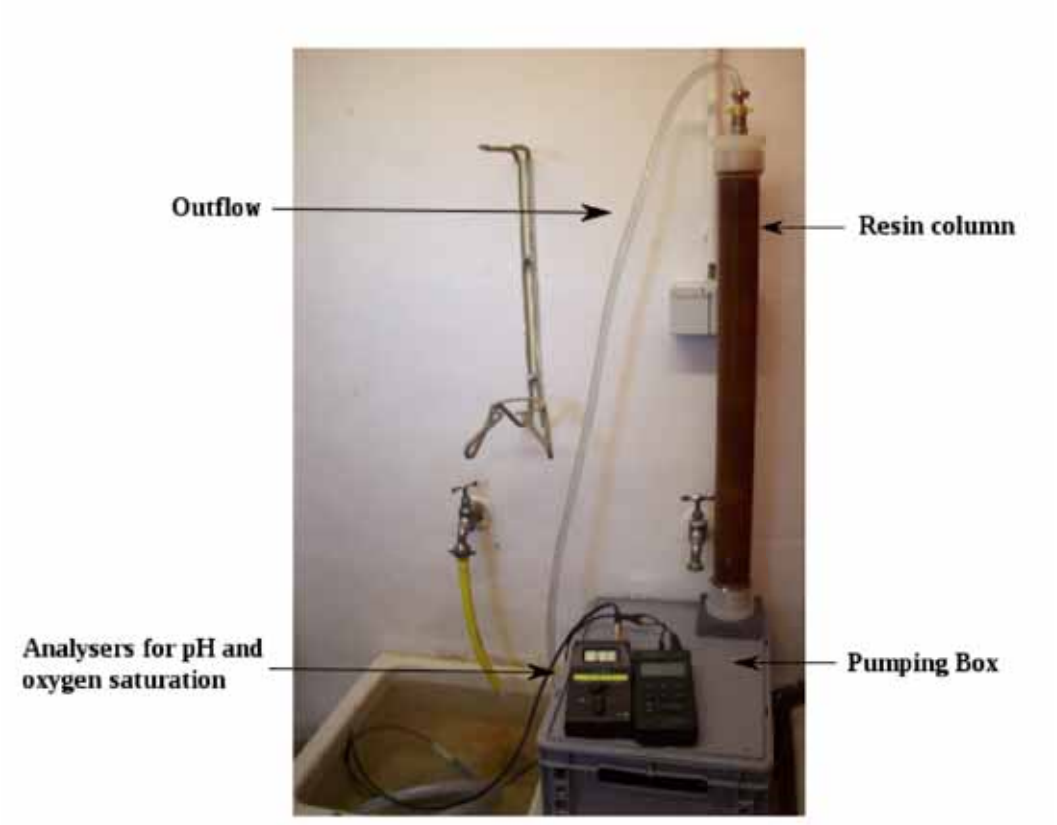


Fig. 4.1: First setup of the sampling machine.

### 4.1.2 Changes in the setup

After the first test with the machine was done, some modifications were made in order to improve the use and installation of the machine in the field. The final setup used for all samples excluding the first one, is shown in detail in Fig. 4.2. The modifications made include:

- The pumping rate of the old arrangement was not adjustable. Therefore an Y-pipe was installed for use as a bypass in order to reduce column inlet flow. To adjust the flow through the bypass, a flow valve was installed.

- The resin column was installed separately at a tripod and connected to the pump box with hoses. This modification was needed because in the old arrangement the column as installed at the top of the box-lid making it difficult to open the box during sampling. The current arrangement allows the user to easily open the lid of the pumping box to dry the box if water has found its way into the box or to change the pump fuse, if needed. Advantageous is also that the tripod can be safety installed even on rough surfaces, since the column is made of glass, it is safer in that way.

- The flow meter was located under the tripod, before the column, assuring that only water flowing through the exchangers is considered.

- The water filter was located inside the box making the box more handy.


Fig. 4.2: The sampling machine. Left: Sampling machine while taking a sample. Right top: Inside view of the pumping box. Right bottom: Front view of the pumping box.

### 4.1.3 Sample collection

Mounting the equipment in general is easy, only a few things must be considered. The hoses must not be interchanged, even if the plugs do fit on every slot. The riverine hose has, as mentioned, a filter located at the riverine end. The bypass hose has only one plug, the other end is without any connection. Same for the outfow hose, whereas this one has a transparent part of about 10 cm length to check if any air is getting pumped. The connection hose has the same connections on both ends, therefore it does not matter, which end is connected to the box.

Before mounting the resin column the pump should have been run as long until water comes out at the tripod. Now the breech located at the bottom side of the column can be unscrewed. Due to depression no water should flow out of the resin. Before unscrewing the breech located at the upper side of the column the pump should run again, whereas the bypass should be halfway opened. To mount the outflow hose the bypass flow can be adjusted that the resin is not falling dry, but the flow is not too fast to mount the hose. If the resin did fall dry, it is recommended to close the bypass for some time until most of the entrapped air is exhausted. In general, bypass flow should be adjusted so the flow velocity through the resin is about two

litres per minute. The faster water flows through the resin, the worse this can work. If flow velocity is adjusted to about two litres sampling needs three to four hours.

### 4.1.4 Sample preparation

After the column has been taken to the laboratory the resin has to be eluted with ~2 litres of 4M hydrochloric acid (HCl) for minimum three hours. To provide better results sodium was separated from the alkali and alkaline earth metals (mainly calcium, magnesium and potassium) with a posterior procedure mentioned later. The chemical separation of potassium is done in several steps, first, this was done using a chemical separation method published by Sakaguchi et al. (2003). The exchanger resin is eluted with two litres of 4M HCl, the solution is evaporated to dryness, dissolved again in 2M HCl, heated, stirred and filtered. Evaporation was done by a heater combined with a magnetic stirrer. The solution rose to the boiling temperature of the azeotrope of HCl and water of 108.5 °C (see chapter 3.5). The pH of the solution is adjusted to 8 – 9 using ammonium hydroxide ($NH_4OH$). By adding 2.5M ammonium carbonate ($(NH_4)_2CO_3$) instead of 6M (according to Jander & Blasius (1989)) and ethanol calcium and magnesium precipitated (in form of their carbonates) and were centrifuged. Ammonium carbonate and ethanol must not be mixed before adding to the solution but both chemicals have to be added separately, because ammonium carbonate is insoluble in ethanol. By bringing the pH to above 7 beryllium is precipitated as well in form of $Be(OH)_2$ (Patnaik 2002). The solution is adjusted to pH 7 using HCl and evaporated to dryness at 500 °C for 12 hours. By dissolving the minerals in 0.1M HCl and adding sodium tetraphenylborate, $Na[B(C_6O_5)_4]$ (TPhB'), potassium precipitated in form of the potassium tetraphenylborate (Wittig et al. 1949). The solution was evaporated to dryness again and then analysed by gamma-spectroscopy. This procedure is shown in Fig. A.1 in the appendix.

As the mentioned procedure is quite long this procedure was modified after the first attempt in order to accelerate the process and the chemical separation in particular. According to several scientific publications (e.g. Spier & Wagner (1952), Flaschka & Barnard (1960)) the separation of potassium via TPhB' works quantitative even if the solution contains a big surplus of calcium, magnesium and sodium. According to this the exchange resin is eluted, the solution is evaporated to dryness and weighted. Now the residue is brought back to solution by adding 0.1M HCl and NaTPhB is added to precipitate potassium. The precipitate of KTPhB is separated by filtering (45 nm pore size). The quantity of the precipitation is checked by adding NaTPhB again. If no precipitate is observed, the solution is evaporated to dryness, if any precipitate is observed, it is filtered again and a new check is done until no precipitate is observed. This procedure is shown in Fig. 4.3.

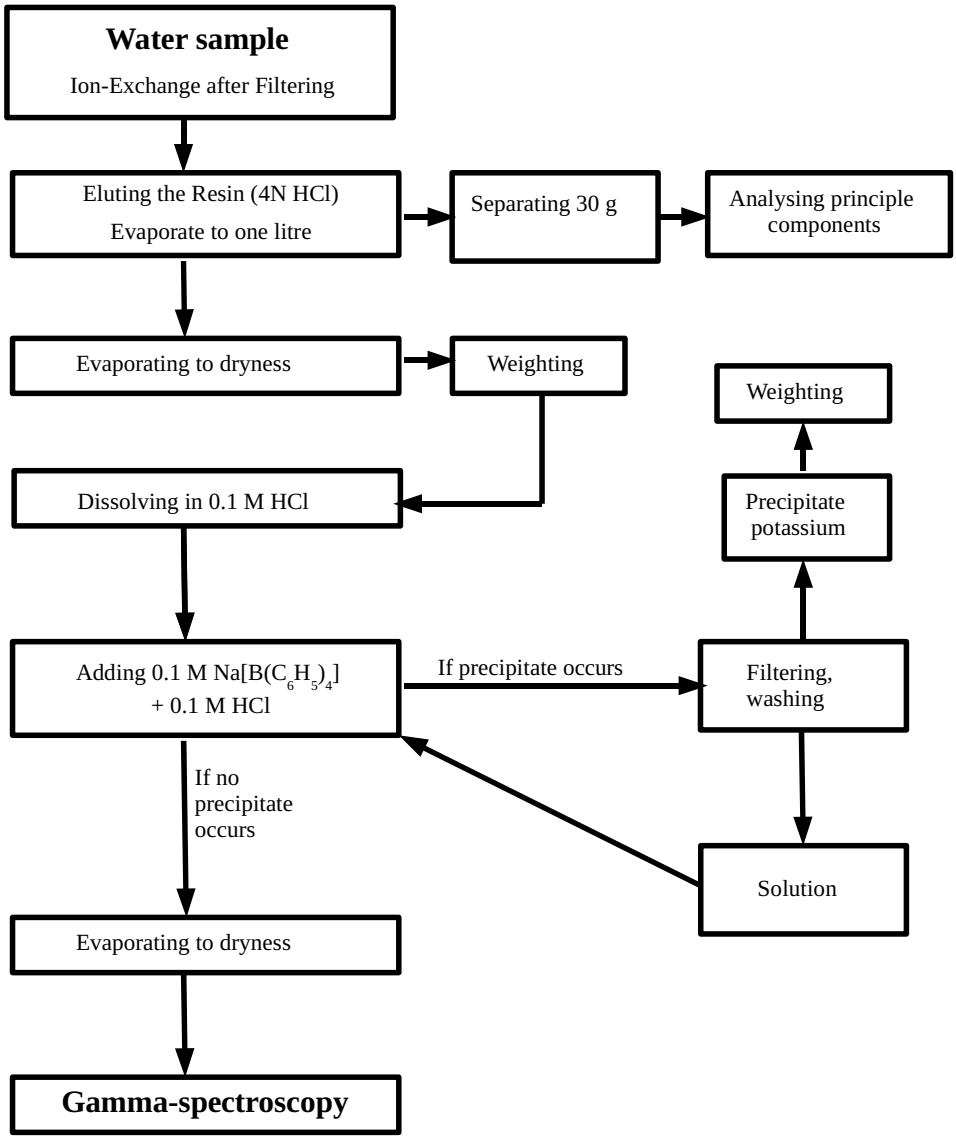


Fig. 4.3: Modified chemical separation of potassium

### 4.1.5 Measurements

In general, there are two kinds of detectors used to measure γ-rays – scintillation and semiconductor detectors. Semiconductor detectors mostly use germanium crystals, whereas NaI(Tl) crystals are used in scintillation detectors. Both detectors have advantages and disadvantages. Although the HPGe detector gives less counts in the same time than the NaI(Tl) detector a single isotope can be analysed much better because the peaks are sharper. This means, for the usage of a NaI(Tl) detector the sample must be free of disturbing contaminations and background radiations have to be eliminated or reduced as good as possible, whereas a HPGe detector gives good results even without total elimination of the

radiation background. A comparison of the spectra of both a HPGe and a NaI(Tl) detector is shown by Fig. 4.4. Both detectors are described in the following:

#### *4.1.5.1 NaI(Tl) detector*

A NaI(Tl) scintillation detector can be used to detect both electrons and γ-quanta. The size of the crystals varies, often a size of 100 x 100 mm or 200 x 200 mm is used. The material used is sodium iodide doped with thallium. A particle causes a flash inside the scintillation material that can be detected by a photomultiplier (Demtröder 2005). Both electrons and γ-quanta have a typical energy depending on the nucleus they were emitted from. By detecting the energy spectrum at a high resolution it is possible to get information of the type of isotope that produced the radiation.

#### *4.1.5.2 Germanium detector*

Another possibility to detect γ-rays is to use a semiconductor detector. Tension causes a lack of charge carriers the p/n-junction. When a particle is absorbed in the environment of this depleted p/n-junction, it causes many electron-hole pairs. These electron-hole pairs can be divided in the electric field and detected at the electrodes. The most common material used is germanium or silicon. The n- and p-part can be doped with phosphorous or antimony (as a donor) and boron or aluminium (as an acceptor), respectively. A semiconductor detector works in analogy to an ionisation chamber (Demtröder 2005). Similar to using a NaI(Tl) detector the energy spectrum can be detected at a high resolution, and therefore it is possible to identify the isotopes causing the radiation.

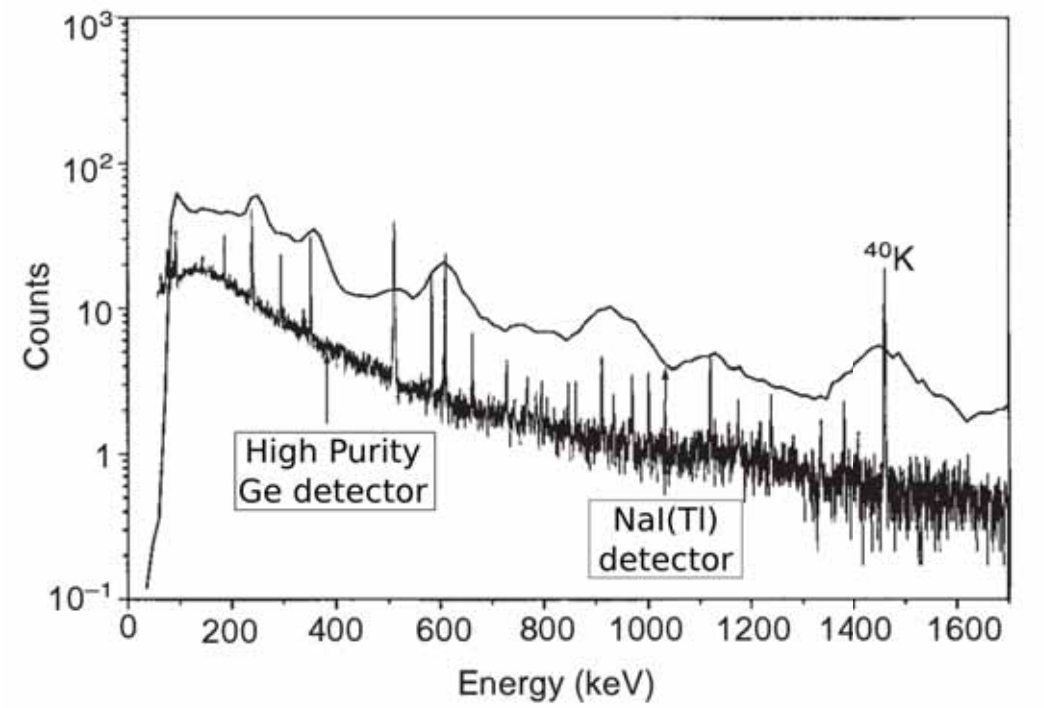


Fig. 4.4: Comparison of the spectra of a High Purity Germanium detector (lower spectrum) and a NaI(Tl) detector (Boschung (1998), edited).

Independent on the detector used there is the possibility to use a coincidence setup where two crystals are placed in front of each other (coincidence). When a positron stops in a medium (NaI(Tl)- or Ge-crystal) it annihilates with an electron and emits two γ-ray peaks at 511 keV simultaneously. The technique used to measure this annihilation peak is called PALS (Positron Annihilations Lifetime Spectroscopy). If PALS is combined with γ-spectroscopy, it can be used to detect the decay of an isotope. For $^{22}$Na, for example, this means that the γ-ray peak at 1275 keV and the 511 keV annihilation peak must be detected. Therefore several measurement regimes are possible. When detecting the 1275 keV γ-ray peak, $^{40}$K, which emits γ-rays at 1460 keV (Samat & Green 1997), interferences with $^{22}$Na. Measurements at 1786 keV (1275 + 511 keV) are disturbed by the 1810 keV γ-rays emitted by $^{26}$Al. When detecting only the energy of 511 keV, $^{106}$Ru, that emits γ-rays at 513 keV, can cause contributions. Best results are given when detecting all three energy levels (Nevinskii et al. 2004). Unfortunately, in this work no coincidence measurements could be made.

### 4.1.6 The Ge-detector at the BfS

The BfS (Bundesamt für Strahlenschutz – Federal Office for Radiation Protection) runs four HPGe-detectors. Two of them are Low-Level-Detectors, which means that the electric is located outside of the detector. The electronic of the other two detectors is located inside. All detectors are covered by a lead layer to minimize background radiation. Two of them (the oldest two ones) are covered in an old, nearly $^{210}$Pb-free, self-made lead layer. The newer ones are covered with an 80 mm thick standard lead outside and a 20 mm thick nearly $^{210}$Pb-free inside layer. The efficiencies of the detectors vary between 70 and 30 % (compared to a defined NaI(Tl) detector). To prevent thermal noise that would produce leakage flow, the detectors are cooled down to the temperature of liquid nitrogen (77 K). Depending on the activities of the samples and the efficiency needed counting times vary from one to three days per sample. All detectors can analyse samples of about one litre of liquid, nested in a so called Marinelli- can. This is a can in form of a ring that contains the sample. The can is placed on the detector and encloses it providing a good efficiency. Another possibility is to compress dust from air filters or the dried residue of a wet sample in a tablet and place it on the detector.

The detector used in this work is detector 5 (Fig. 4.5), one of the old ones with efficiency of 30%. All samples were dried before analysis because dried samples have a defined geometry and therefore, are easier to calibrate than wet samples in a Marinelli-can.


Fig. 4.5: Detector 5 used for the measurements at the BfS

## *4.2 Materials for sampling and analyses of radon*

Activities of radon ($^{222}$Rn) provide information about changes in processes influencing the residence time of groundwater. However, $^{222}$Rn cannot be used for age-dating directly. To analyse radon in a water sample a defined volume of water is necessary. In this work 40 ml bottles were used. The bottles have to be filled completely with water avoiding any air bubbles inside. The water should be collected underneath the surface of the water to reduce degasification possibilities.

### 4.2.1 Measurements

Due to the short half-life of the $^{222}$Rn-isotope of about 3.8 days, the samples have to be analysed shortly after sampling. For analysing an $\alpha$-counter, e.g. a Geiger-counter, is necessary. The $\alpha$-counter used in this research is a RAD7 from Durridge Co. In principle it is a classical Geiger-counter but its detector is calibrated for detection of $^{222}$Rn decay. Therefore it uses a detector that has an energy resolution of about 0.05 MeV. The detector allows the user to use several tests and protocols according to the type of detection required. A protocol defines the procedure how the RAD7 measures the actual sample. There are several predefined protocols and options to configure a user protocoll. An overview is given by Table 4.2. Cycle defines the duration of one test cycle (hours and minutes), recycle gives the repetition of the cycle. Mode sets up whether sniff, auto, normal, WAT-40 or WAT-250 mode is used. The sniff mode gives rapid response to changing radon levles using the $^{218}$Po (polonium) peak. The radon concentration is calculated by that peak alone. Normal mode also counts $^{214}$Po. This gives higher statistical precision. If using auto mode, the RAD7 changes to normal mode after three hours of continious measuring. WAT-40 and WAT-250 modes are used to calculate the concentrations of the 40 ml and 250 ml sampling bottles coming with the RAD7. The pump can be set to on, off, grab and auto. On and off does not need to be explained. Grab initiates a five minute grab sequence at the beginning of the test, followed by a five minute equillibrium delay. This means, at the start of the test the pump runs for five minutes, then five minutes nothing happens and then the first cycle starts. If the pump is set to auto, the pump runs for four minutes at the start of a new test and then one of five minutes until the end of the cycle. If the humidity of the air in the sampling cell is above 10 %, the pump stays turned on to allow the air to dry (RAD7Manual 2000).

If not mentioned, the water samples were analysed using the WAT-40 protocol. All samples where given in pCi/l and converted in µBq/m³ (1 pCi/l = 37 µBq/m³).

Table 4.2: Overview over the predefined protocols in the RAD7 detector

| **Protocol** | **Cycle** | **Recycle** | **Mode** | **Thoron** | **Pump** |
|---|---|---|---|---|---|
| Sniff | 00:05 | 00 | Sniff | Off | Auto |
| 1-day | 00:30 | 48 | Auto | Off | Auto |
| 2-day | 01:00 | 48 | Auto | Off | Auto |
| Weeks | 02:00 | 00 | Auto | Off | Auto |
| User | xxx | xxx | xxx | xxx | xxx |
| Grab | 00:05 | 04 | Sniff | Off | Grab |
| WAT-40 | 00:05 | 04 | WAT-40 | Off | Grab |
| WAT-250 | 00:05 | 04 | WAT-250 | Off | Grab |
| Thoron | 00:05 | 00 | Sniff | On | Auto |

Before sampling, the humidity of the air needs to be reduced. This is done by pumping air trough a column filled with drying gravel. This also flushes the detector chamber and makes sure, that no old radioactive material is being detected. Therefore, the system has to be purged for minimum 10 minutes without closing the air cycle and afterwards until the relative humidity has has reached a value below 7 %. The setup for the RAD7 is shown in Fig. 4.6.

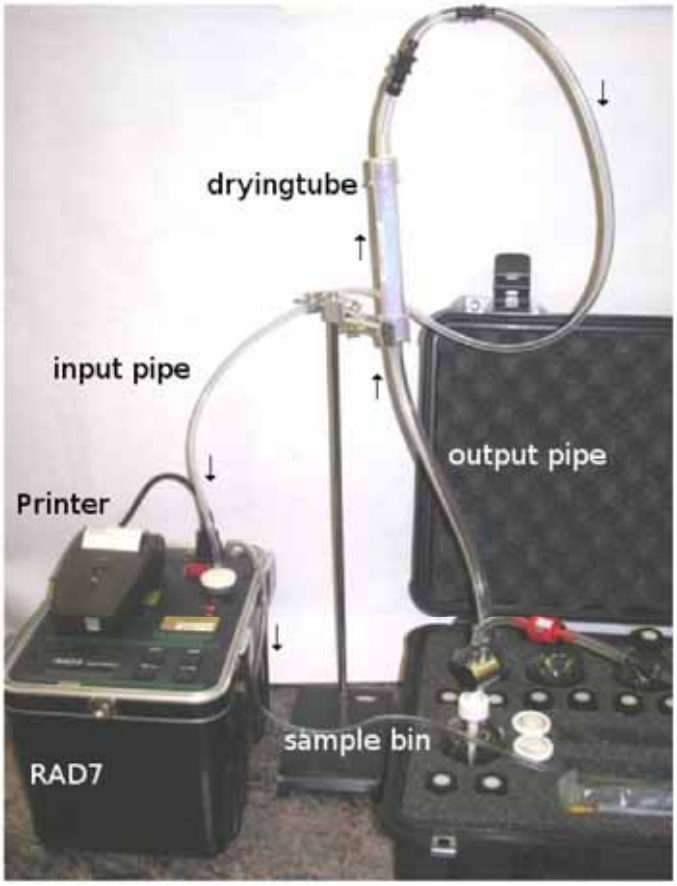


Fig. 4.6: Setup for the RAD7 sampling a water sample. Arrows mark the flow direction of air in the system. Edited from (RAD7Manual 2000).

## *4.3 In situ measurements*

For the field parameters (pH, water temperature, electric conductivity and oxygen saturation) a multimeter (one machine, measuring all these data) was used. Similar to activities of $^{222}Rn$ in situ parameters are useful to provide information about changes in residence time of water. These parameters were taken at the sampling points after a minimum of five minutes of levelling off in the water. Oxygen saturation was taken in absolute and relative units, mg/l and %, respectively. If either the relative or absolute oxygen saturation was not possible to measure in the field, it was calculated using eq. 4.1 which is also used in SWAT (Soil and Water Assessment Tool (Neitsch et al. 2005)). Here $Ox_{sat}$ is the equilibrium saturation oxygen concentration at the pressure of 1013 mBar in mg / l and K is the water temperature in Kelvin. For temperature the unit °C was used and electric conductivity was taken in µS/cm at 25 °C. Other parameters taken in the field were the type of the water sample (e.g. groundwater, riverine water), clearness of the water, its smell and the current weather during sampling.

If a multimeter was not available, the parameters were measured using a pH-meter (model WTW pH 330), an oxygen-probe (model Oxi 330) and a probe for electric conductivity (WTW LF-92). The pH-meter and the oxygen-probe have to be calibrated before usage. This was done by the automatic calibration function of each instrument. For the pH-meter, this means that a two point calibration with the technical standards pH 4.01 and 7.00 was used.

$$Ox_{sat} = \exp\left[-139.34410 + \frac{1.575701\times10^{5}}{T} - \frac{6.642308\times10^{7}}{(T)^{2}} + \frac{1.243800\times10^{10}}{(T)^{3}} - \frac{8.621949\times10^{11}}{(T)^{4}}\right] \quad \text{(Eq. 4.1)}$$

## *4.4 Laboratory measurements*

In the laboratory all water samples were analysed measuring stable isotopes ($^{18}O$ and $^{2}H$) and hydrochemical parameters (main components). Stable isotopes were measured using Wavelength-Scanned Cavity Ring Down Spectroscopy (WS-CRDS). The instrument used in this work is a *Picarro* 1102i. This method is developed for continuous measuring of polyatomic gases. It uses the effect that nearly every small gas has a unique near-infrared absorption spectrum by exposing the gas to a laser beam. At sub-atmospheric pressure this consists of a series of well resolved, sharp lines, each at a characteristic wavelength that represents a particular element (or isotope). Because the wavelengths of gases are known the concentration of any species can be determined by measuring the strength of this absorption (Brand et al. 2009).

The main components of the water samples were analysed using both anion and cation chromatography. The technique is based on ion exchange and therefore will not be discussed in detail here. To analyse the samples it is necessary to make sure that there are no contaminations in water. Therefore, the samples were filtered using a 45 nm filter which was washed with sample water first. Afterwards, 5 ml of the filtered water were put into a bin from where the samples were taken to the analyser. This was done for anions and cations and for each sample separately.

## *4.5 Age dating of water*

If the input of a cosmogenic radionuclides is known (atmospheric history of the substance), it is possible to date the age of a sample with known actual radioactive activity. Age dating is done by using equation 4.2 according to:

$$N(t) = N_0 \cdot e^{-\lambda t} \quad \text{with} \quad \lambda = \frac{\ln(2)}{T_{1/2}} \qquad \text{(Eq. 4.2)}$$

here N(t) = actual number of nuclides
N0 = number of nuclides at time 0
λ = decay constant
t = time

By transformation and logarithmic calculus of equation 4.2 equation 4.3 follows:

$$t = \frac{\ln\left(N_{(t)} / N_{(0)}\right)}{\lambda} \qquad \text{(Eq. 4.3)}$$

# 5. Results

## *5.1 In situ measurements*

Besides the activities of $^{222}Rn$ and the determination of the principal components in the samples (showed afterwards) field parameters measured were electric conductivity, temperature, oxygen concentration and pH-value. All these data provide relative informations about changes in residence time.

### 5.1.1 Rivers

Field parameters for the rivers Dreisam and Brugga are shown in Table 5.5 and their graphs are shown in Fig. 5.1 and Fig. 5.2, respectively.

Because most of the data were obtained by the regular data collection available done weekly by the Institute of Hydrology (called the Dreisam and Brugga tour), there is no oxygen saturation data available. pH-values, in both rivers, are quite stable, ranging from 7.96 to 6.49 in samples of the river Dreisam and from 7.26 to 6.39 in the river Brugga. Temperatures of the river Dreisam fall from 18.3 degrees in August to 1.1 degrees in December, whereas the temperatures of the river Brugga in general are lower, ranging from 15.5 degrees in August to 1.4 degrees in December. Values of electric conductivities are higher in the river Dreisam than in Brugga, though they show similar behaviour with a minimum in late November and a slope to higher values in January.

Table 5.1: Field parameters of the rivers Dreisam and Brugga

| Date | Dreisam | | | Brugga | | |
|---|---|---|---|---|---|---|
| | pH | Temperature [°C] | Electric conductivity [µS/cm 25°C] | pH | Temperature [°C] | Electric conductivity [µS/cm 25°C] |
| 07.08.2009 | 7.82 | 16.8 | 130.0 | 7.10 | 13.8 | 103.0 |
| 14.08.2009 | 7.47 | 16.9 | 130.5 | 6.90 | 14.1 | 106.9 |
| 21.08.2009 | 7.45 | 18.3 | 129.4 | 7.01 | 15.5 | 110.6 |
| 28.08.2009 | 7.62 | 17.0 | 130.6 | 7.26 | 14.9 | 111.8 |
| 04.09.2009 | 7.18 | 15.0 | 116.3 | 6.98 | 13.2 | 101.4 |
| 11.09.2009 | 7.96 | 18.1 | 128.1 | 7.06 | 12.9 | 112.1 |
| 18.09.2009 | 7.37 | 13.1 | 131.6 | 6.95 | 12.0 | 110.5 |
| 24.09.2009 | 7.51 | 13.2 | 132.1 | 7.02 | 12.6 | 112.9 |
| 02.10.2009 | 7.34 | 11.5 | 131.4 | 7.03 | 11.1 | 113.9 |
| 09.10.2009 | 7.14 | 13.7 | 130.8 | 6.87 | 12.2 | 104.3 |
| 16.10.2009 | 7.19 | 4.4 | 125.8 | 7.10 | 4.9 | 105.3 |
| 22.10.2009 | 6.97 | 8.8 | 118.5 | 6.70 | 8.4 | 101.1 |
| 30.10.2009 | 7.14 | 8.4 | 124.5 | 6.47 | 7.5 | 106.6 |
| 07.11.2009 | 7.06 | 7.8 | 111.8 | 6.88 | 7.1 | 88.1 |
| 14.11.2009 | 7.05 | 9.2 | 116.5 | 6.82 | 8.5 | 88.9 |
| 24.11.2009 | 7.05 | 8.4 | 110.2 | 6.85 | 7.3 | 85.7 |
| 27.11.2009 | 6.75 | 6.7 | 104.6 | 6.39 | 6.3 | 80.4 |
| 04.12.2009 | 6.77 | 5.4 | 111.5 | 6.49 | 4.5 | 90.5 |
| 11.12.2009 | 6.90 | 6.5 | 107.6 | 6.65 | 5.4 | 82.8 |
| 18.12.2009 | 6.95 | 1.1 | 107.3 | 6.83 | 1.4 | 86.7 |
| 22.12.2009 | 6.99 | 2.0 | 161.6 | 7.07 | 2.9 | 145.3 |
| 31.12.2009 | 6.49 | 6.4 | 104.6 | 6.50 | 5.5 | 78.6 |
| 08.01.2010 | 6.52 | 2.6 | 115.0 | 6.78 | 2.3 | 93.7 |
| 15.01.2010 | 6.69 | 3.2 | 130.9 | 7.12 | 2.8 | 105.0 |
| 22.01.2010 | 6.59 | 4.8 | 129.7 | 6.80 | 4.0 | 107.9 |
| 29.01.2010 | 6.73 | 2.1 | 169.7 | 7.00 | 1.6 | 126.2 |

Oxygen saturation is not available because it is not measured on the weekly Dreisam and Brugga tour.

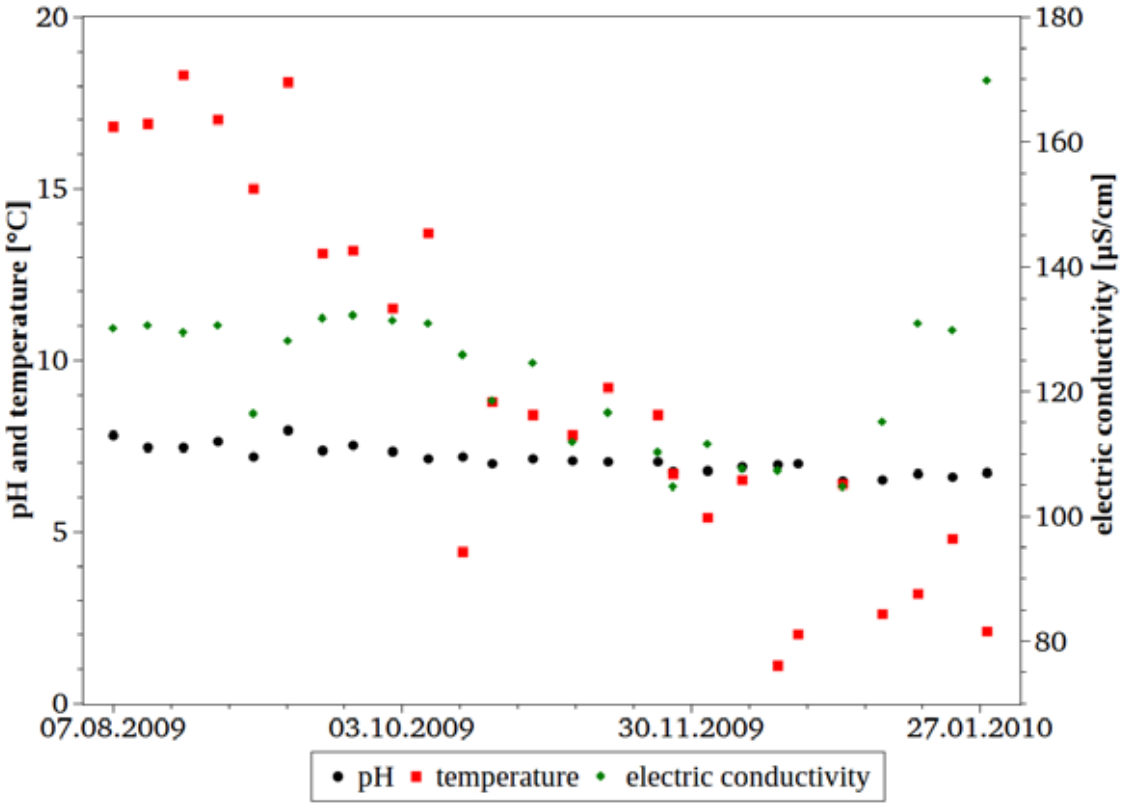


Fig. 5.1: Field parameters of the river Dreisam.

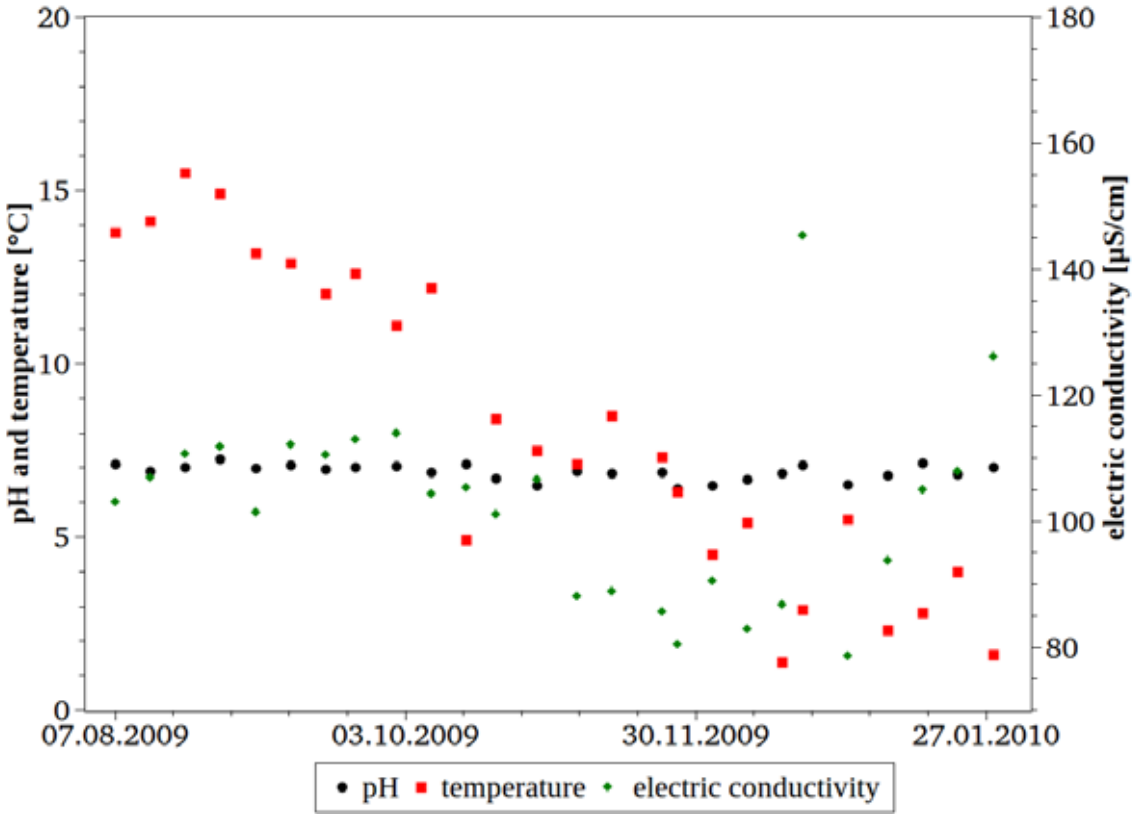


Fig. 5.2: Field parameters of the river Brugga.

### 5.1.2 Groundwater

Field parameters from the wells for groundwater sampling locations (Schauinsland and Hungerbrunnen) are shown in Table 5.2 and Table 5.3, respectively. Their respective graphs are shown in Fig. 5.1 and Fig. 5.2.

pH values have to be seen with an accuracy of approximately ±0.5 for Schauinsland because it is hard to measure pH in water with low mineralisation. Also for Hungerbrunnen, pH-values vary less probably because this water shows higher mineralisation. Under such conditions pH-values on both sampling locations are considered relatively stable. Electric conductivity varies low over time. Temperatures vary approximately ±3 °C at the Schauinsland well but only about ±1.5 °C at Hungerbrunnen. At both sampling points temperature was measured using the temperature probe from the oxygen probe. Relative oxygen saturation also varies more at Schauinsland than at Hungerbrunnen. It was measured in beakers filled with water from each sampling point. Because it was not possible to measure oxygen saturation in a passage bin, the values have to be considered carefully.

Electric conductivity and pH were also taken from water after the exchange resin during the $^{22}$Na measurements. Mean values of these parameters per sample are given by Table 5.4.

Table 5.2: Field parameters of Schauinsland sampling point

| Date | pH | Temperature [°C] | Oxygen saturation [%] | Electric conductivity [µS/cm, 25°C] |
|---|---|---|---|---|
| 13.08.09 | 6.52 | 9.6 | 89.50 | 56.4 |
| 24.09.09 | 5.42 | 6.9 | - | 53.1 |
| 08.10.09 | 6.70 | 7.6 | 63.55 | 59.4 |
| 15.10.09 | 6.00 | 5.8 | 46.36 | 57.2 |
| 19.10.09 | 5.99 | 5.8 | 46.36 | 56.2 |
| 04.11.09 | 5.70 | 7.1 | 58.63 | 62.8 |
| 11.11.09 | 5.85 | 6.5 | 52.89 | 61.0 |
| 19.11.09 | 6.08 | 8.9 | 74.48 | 61.0 |
| 01.12.09 | 6.58 | 6.3 | 51.01 | 54.0 |
| 22.01.10 | 6.25 | 6.2 | 50.04 | 52.2 |

On October, 24$^{th}$, no oxygen probe was installed.

Table 5.3: Field parameters of Hungerbrunnen sampling point

| Date | pH | Temperature [°C] | Oxygen saturation [%] | Electric conductivity [µS/cm, 25°C] |
|---|---|---|---|---|
| 15.10.09 | 6.00 | 10.6 | 73.30 | 159.1 |
| 19.10.09 | 6.07 | 10.4 | 88.14 | 159.1 |
| 04.11.09 | 5.85 | 11.2 | 93.88 | 156.8 |
| 14.12.09 | 6.22 | 10.6 | 95.24 | 153.3 |
| 14.01.10 | 5.66 | 10.4 | 93.02 | 157.2 |
| 21.01.10 | 6.40 | 9.7 | 85.31 | 159.5 |

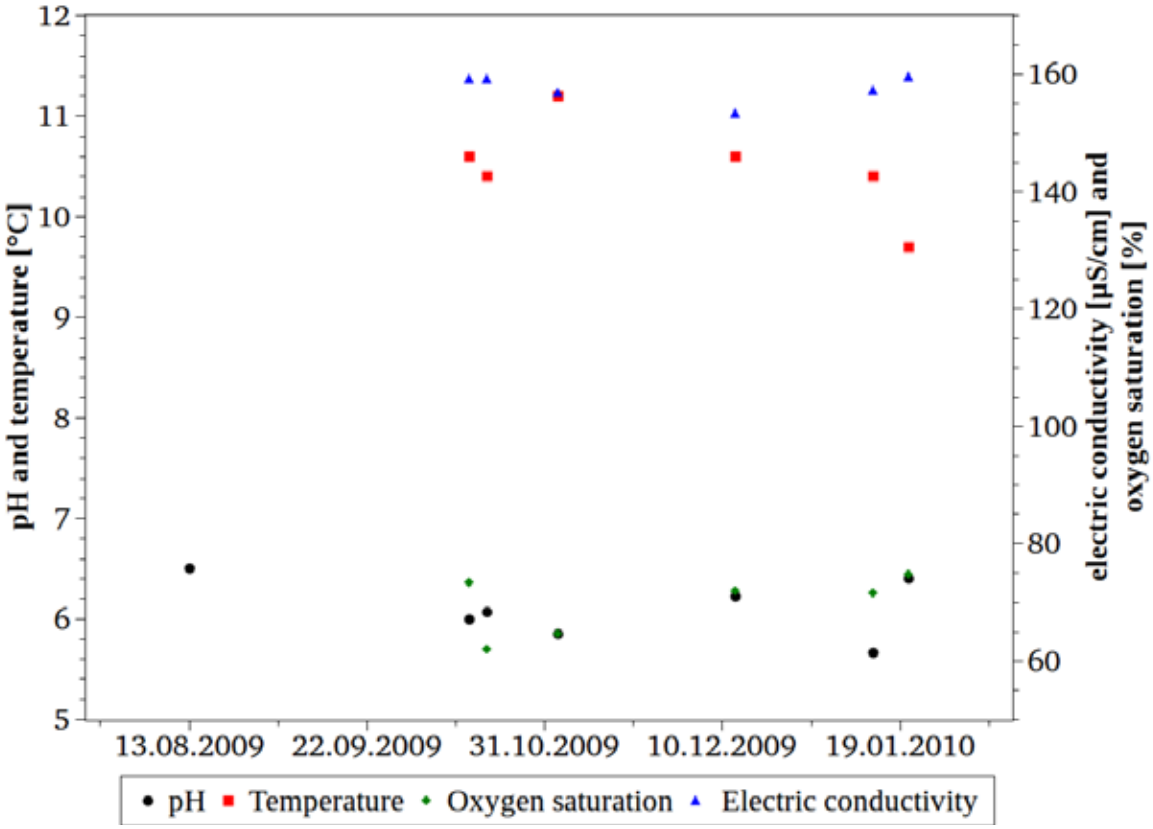


Fig. 5.3: Field parameters of Hungerbrunnen.

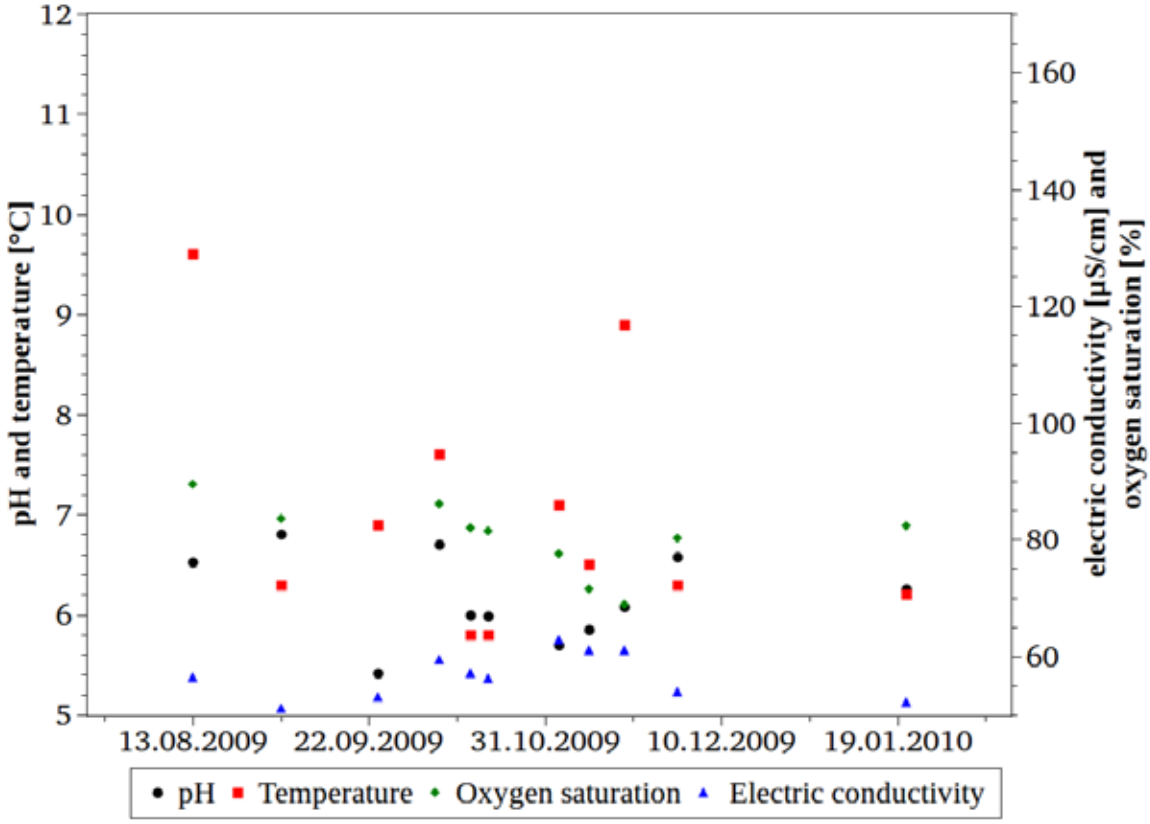


Fig. 5.4: Field parameters of Schauinsland.

Table 5.4: Mean values of pH and electric conductivity before and after pumping water through the exchange resin

| Sample | pH | Electric conductivity [µS/cm] | pH* | Electric conductivity [µS/cm]* |
|---|---|---|---|---|
| Schauinsland I | 3.5 | 115 | 5.8 | 60 |
| Schauinsland II | 3.3 | 117 | 5.2 | 54 |
| Brugga | 3.1 | 230 | 6.7 | 89 |
| Hungerbrunnen | 2.9 | 386 | 5.7 | 157 |
| Snow | 3.4 | 80 | 6.3 | 32 |
| Dreisam | 2.8 | 450 | 6.2 | 172 |

* Mean value of water before flowing through the exchange resin

## *5.2 Chemical parameters*

Part of every sample was a sample for analysing the principle components of the sampled water. The results for the rivers, Dreisam and Brugga, at different dates are shown in Fig. 5.5 and Fig. 5.6. These data were obtained from the mentioned Dreisam-Tour. The results from the other sampling sites, Schauinsland and Hungerbrunnen, are shown in Fig. 5.7 and Fig. 5.8.

For cations-analysis, in most cases, calcium shows the highest concentrations, followed by sodium. Potassium and magnesium show low concentrations. Characteristics of the anions differ from rivers to groundwater samples. Rivers show highest concentrations in chloride, followed by sulphate and nitrate. Nitrate shows higher concentrations than chloride in samples of Hungerbrunnen. Sulphate shows the lowest concentrations. In samples from Schauinsland there is no clear difference for the occurrence. Differences in concentrations of the anions in general are smaller than of the cations. It should be noted that no carbonates and bicarbonates were measured.

Silicate concentrations have been measured only in samples of Hungerbrunnen and Schauinsland as shown in Fig. 5.9. Samples from Schauinsland, in general, present higher concentrations than samples from Hungerbrunnen. The difference is about 3 – 5 mg/l, whereas both series show similar behaviour showing a minimum on October, 15$^{th}$. This minimum is stronger distinct in the Schauinsland series showing a slight trend to lower concentrations in winter.

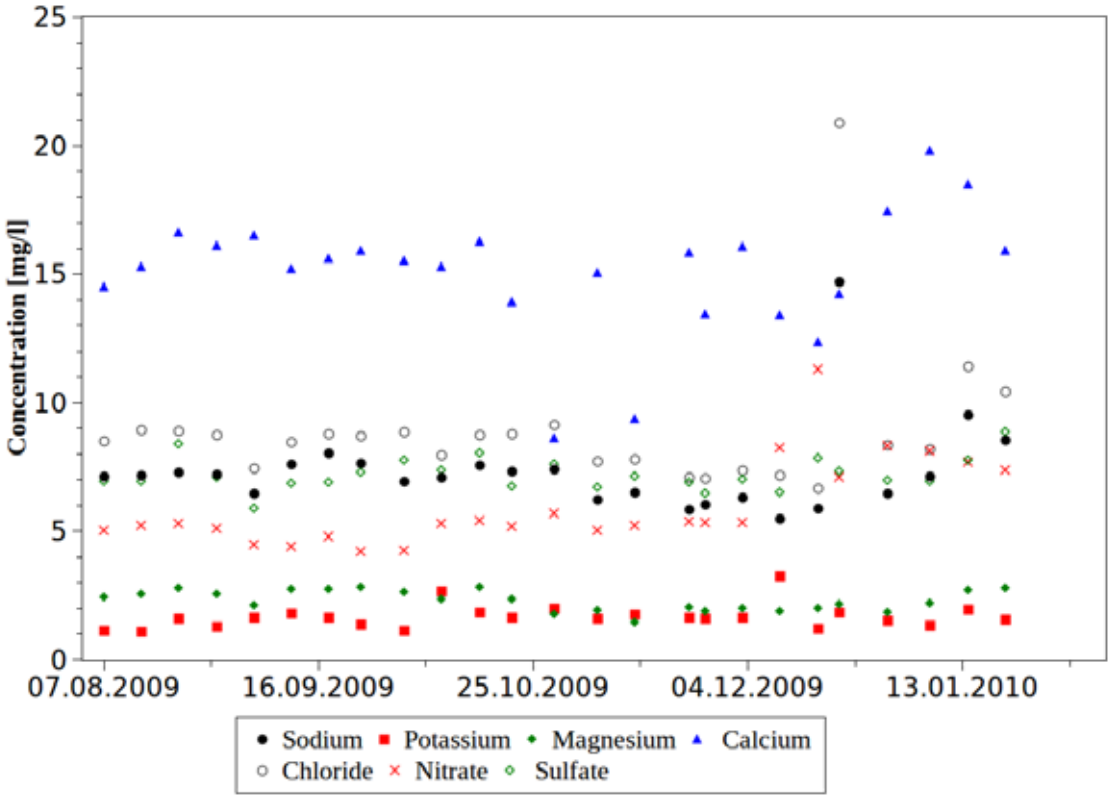


Fig. 5.5: Principal components of the river Dreisam.

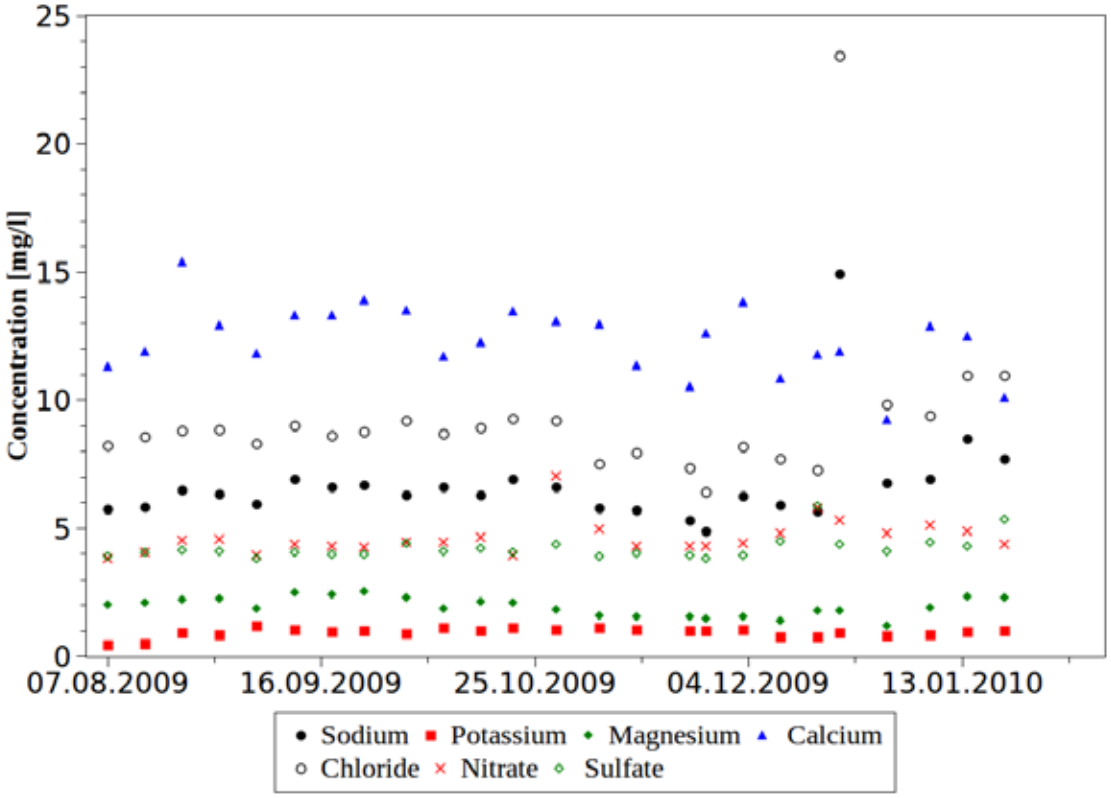


Fig. 5.6: Principal components of the river Brugga.

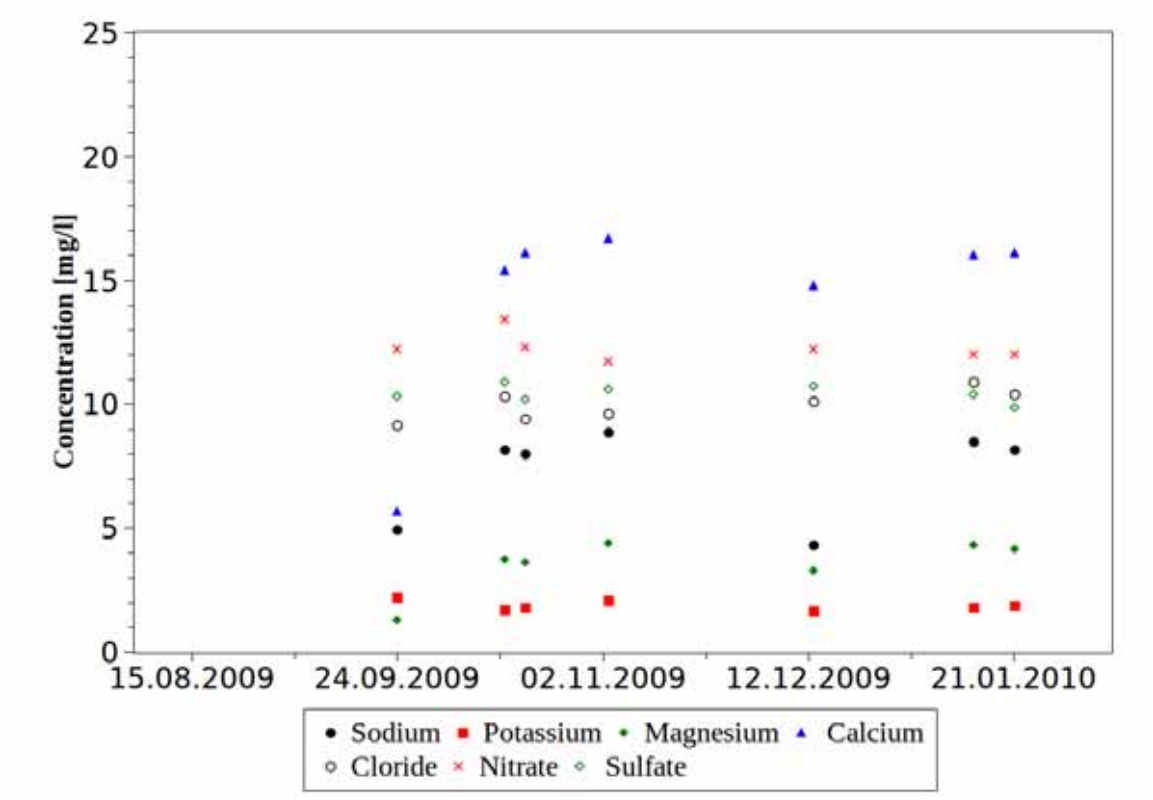


Fig. 5.7: Principal components of water from Hungerbrunnen.

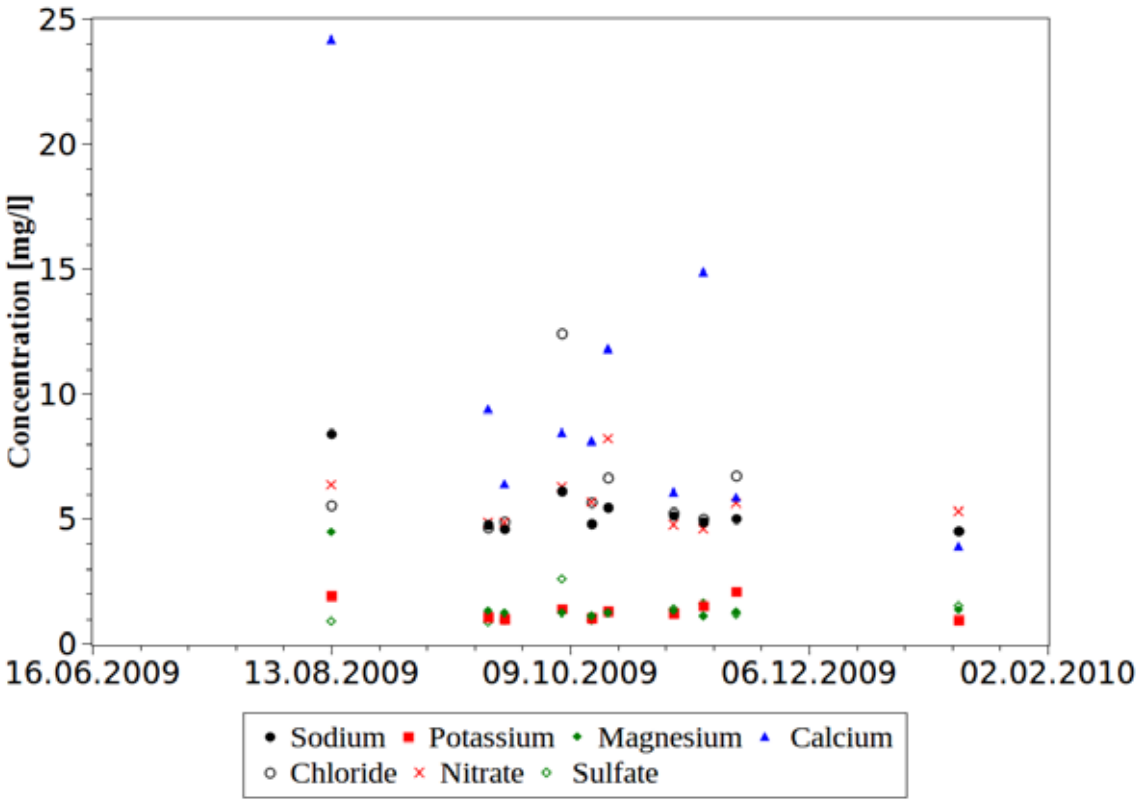


Fig. 5.8: Principal components of water from Schauinsland.

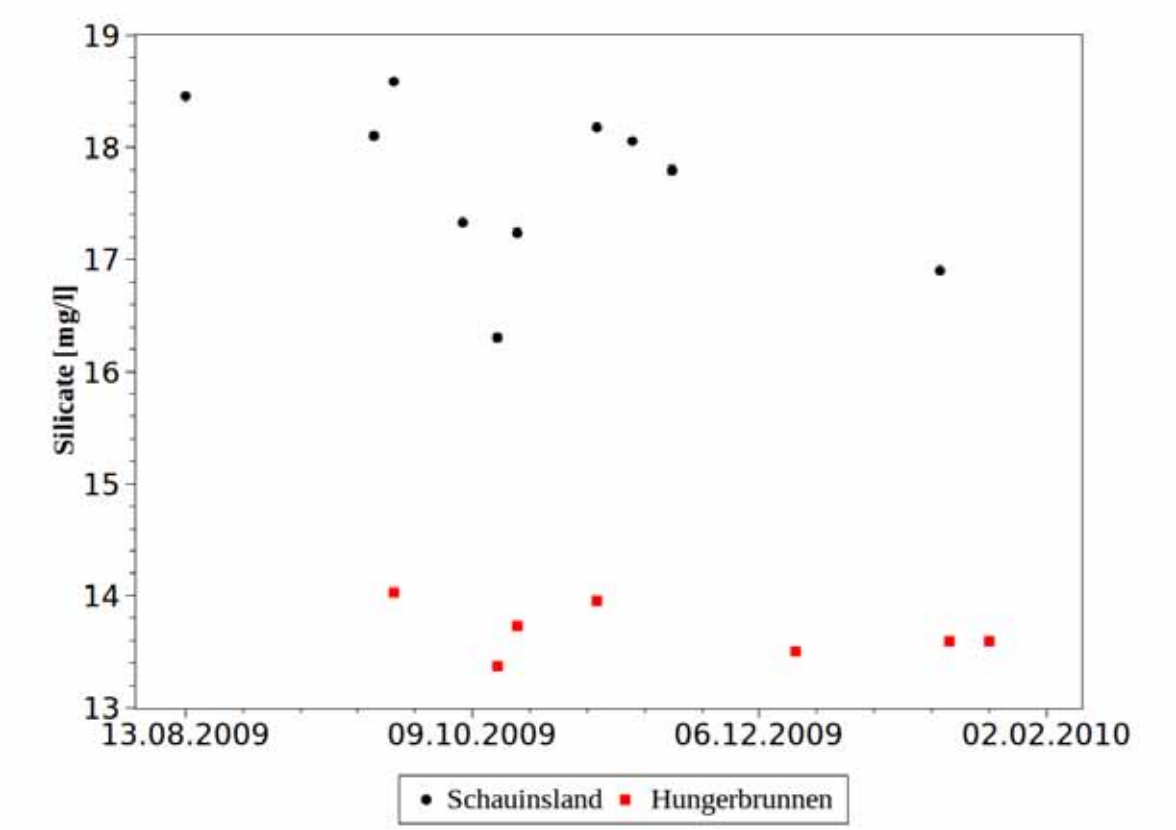


Fig. 5.9: Silicate concentrations of water from Schauinsland and Hungerbrunnen.

## *5.3 Radon ($^{222}$Rn)*

Activities of radon in water samples measured by the RAD7 are shown in Table 5.1 and in Fig. 5.19. Radon activities are quite constant, whereas samples from Schauinsland show higher activities than samples from Hungerbrunnen. There is a little depression noticeable in September in waters from Schauinsland which was not observed in Hungerbrunnen samples. Only water from the river Dreisam taken on 4$^{th}$ of February 2010 shows more than the double of the activity than the sample taken in late summer (taken on 2$^{nd}$ of September). The river Brugga shows constant radon activities. Errors are computed by the RAD7 and ranging from about 5 – 10 %.

Table 5.5: Activity of radon in water samples

| Date | Sampling point | Radon activity [µBq/m³] | Error [µBq/m³] |
|---|---|---|---|
| 13.08.09 | Brugga | 403 | 251 |
| | Schauinsland | 84400 | 6430 |
| 02.09.09 | Dreisam | 608 | 218 |
| | Brugga | 605 | 407 |
| | Schauinsland | 77200 | 3840 |
| 24.09.09 | Hungerbrunnen | 26000 | 1290 |
| | Schauinsland | 91300 | 4810 |
| 08.10.09 | Schauinsland | 89900 | 5100 |
| 15.10.09 | Schauinsland | 105000 | 10800 |
| | Hungerbrunnen | 31400 | 2250 |
| 19.10.09 | Hungerbrunnen | 33300 | 2330 |
| | Schauinsland | 83100 | 4210 |
| 04.11.09 | Schauinsland | 80100 | 4620 |
| | Hungerbrunnen | 38400 | 3920 |
| 11.11.09 | Schauinsland | 91400 | 4580 |
| 19.11.09 | Schauinsland | 94600 | 4730 |
| 01.12.09 | Schauinsland | 81500 | 4070 |
| 10.12.09 | Brugga | 402 | 251 |
| 14.12.09 | Hungerbrunnen | 26500 | 1810 |
| | Hungerbrunnen | 32200 | 2730 |
| 22.01.10 | Hungerbrunnen | 24600 | 2440 |
| | Schauinsland | 71000 | 3550 |
| 04.02.10 | Dreisam | 1409 | 407 |
| Mean | Schauinsland | 86318 | 5158 |
| | Hungerbrunnen | 30343 | 2396 |
| | Dreisam | 1009 | 313 |
| | Brugga | 470 | 303 |

Errors are computed by the RAD7 (equation not available in the manual).

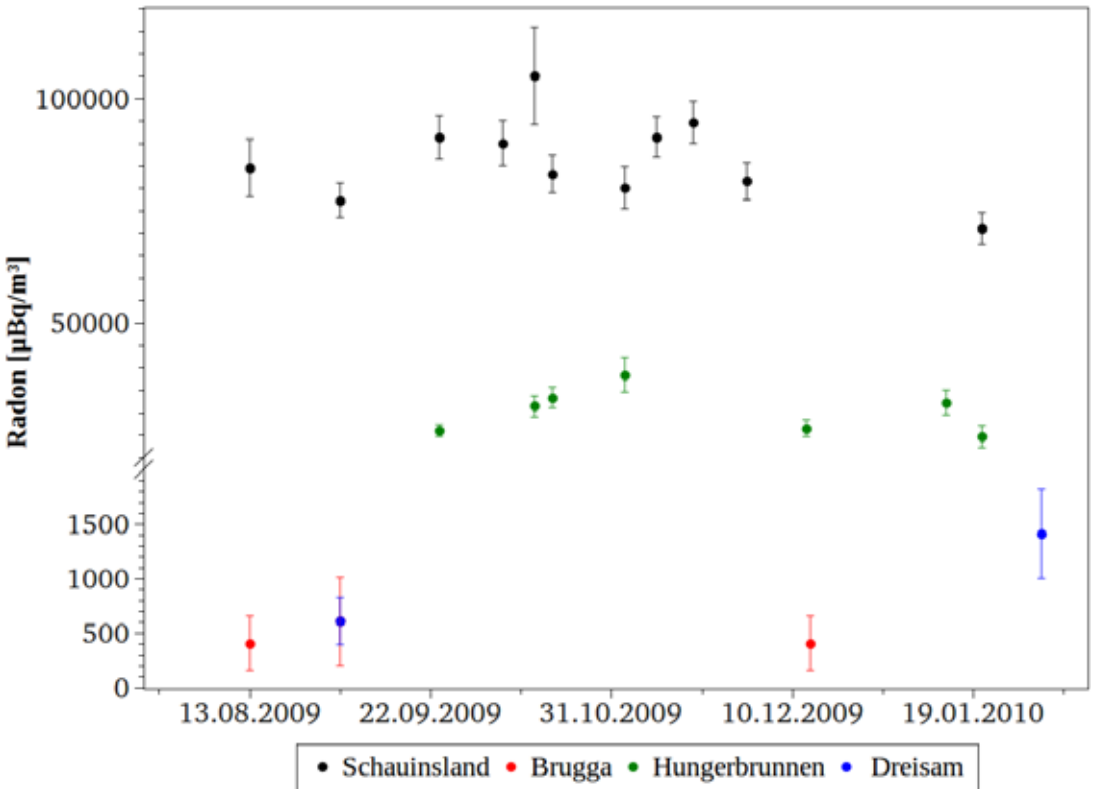


Fig. 5.10: Activity of radon in water samples.

Error bars are based on values computed by the RAD7. The break of the axis reaches from 2 000 to 20 000 µBq/m³.

## *5.4 Stable isotopes*

Stable isotopes of oxygen and hydrogen, $^{18}O$ and deuterium ($^{2}H$), were determined from each sample. For samples taken on the weekly Dreisam tour only $^{18}O$ data was available. Measurement was done via Wavelength-Scanned Cavity Ring Down Spectroscopy for all samples where both $^{2}H$ and $^{18}O$ data is available and via mass spectrometry for the other samples. Delta notations of $^{18}O$ for the four sampling points are shown in Fig. 5.11. Samples from the rivers show a minimum in December and some peaks in early autumn. Water samples from the river Brugga in general are slightly lighter than samples from the river Dreisam showing similar behaviour through the time scale. Similar are the samples from Schauinsland as the ones from Hungerbrunnen which do not show any clear trend, whereas the riverine samples are slightly heavier in winter than in late summer. Much more lighter are water samples from Schauinsland, whereas samples from Hungerbrunnen in general are the heaviest ones. Fig. 5.4 presents the isotope signatures. All signatures are in line with the

Global Meteoric Water Line (GMWL). Precipitation differs extreme from the other samples, being much lighter.

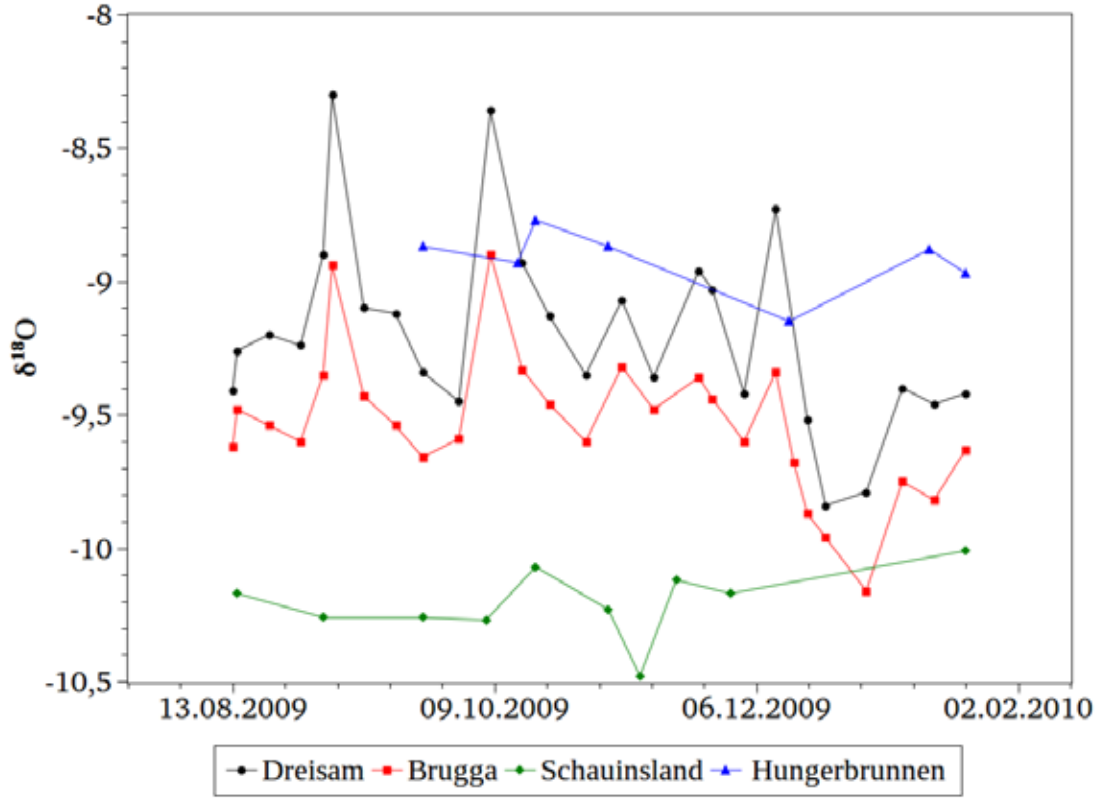


Fig. 5.11: Delta notations of $^{18}O$ in Dreisam, Brugga, Hungerbrunnen and Schauinsland.

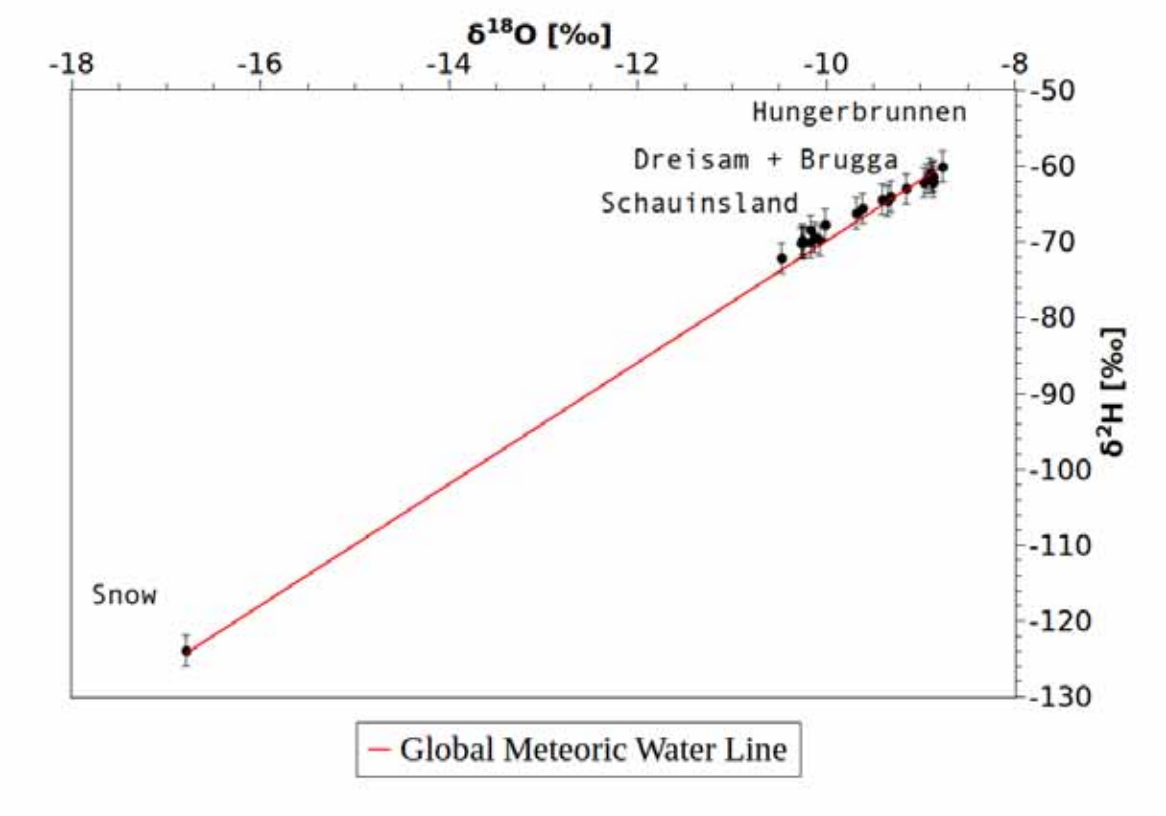


Fig. 5.12: Isotope signatures of samples from rivers, groundwater and precipitation.

## *5.5 Cosmogenic radionuclides*

### 5.5.1 Efficiency of the ion exchange resin

In order to date the age of sampled water using an exchange resin, it is essential to know the efficiency of the exchange resin used. To provide this information regarding $^{7}$Be, a 10 litre aliquot of precipitation water gained from snow previously collected, was evaporated to dryness. The residue was analysed via gamma spectroscopy. This sample had an activity of 2.5 Bq ($^{7}$Be) which is more than double of the radiation the sample taken from the same water, when using the exchange resin, if the activities are equated in Bq/l (0.12 Bq/l vs. 0.25 Bq/l).

General information about the efficiency of the resin is gained by analysing the eluate of this resin. This was done for every sample. Due to the high concentrations of chloride in the eluate (due to the hydrochloric acid), it is impossible to analyse the eluate via ionchromatography. Therefore, it was analysed via AAS (atomic absorption spectroscopy). At high concentrations of chloride this technique is very inaccurate. Not even the errors made can be assigned exactly. This is the reason why efficiencies of more than 100 % are being reached. Results of

these analyses are shown in Fig. 5.3, where the efficiencies for sodium and potassium are plotted in percentages. Efficiencies of potassium are in the range of 30 to 100 %, whereas sodium reaches 50 to 150 %.

As described already, pH and electric conductivity were measured in water after passing the exchange resin. This was done at a high resolution of about 15 minutes – as long as it takes until the pH probe is equilibrated. Due to the availability of only one pH probe, this was only possible for precipitation at this resolution, because precipitation was stored in one huge bucket having constant pH and electric conductivity values. For other samples the pH probe must equilibrate alternately for ground- or riverine water and for sewage which means that a maximum resolution of about 30 minutes is possible. The results of these high resolution measurements are shown in Fig. 5.18. pH values hardly vary, whereas electric conductivity decreases from 92.3 to 78.5 µS/cm.

If the concentration of cations and pH values of sampled water are known, based on the exchange of cations against protium ions ($H^+$), a theoretical pH value can be calculated. Table 5.6 gives the theoretical pH and measured pH values of the taken samples. Concentrations for the sample at Dreisam are mean values of the sampled period. Because for the actual sample, there is no information of principal components.

Table 5.6: Equated and measured pH values for water passing the exchange resin

| **Sample** | **pH equated** | **pH measured** | **difference** |
|---|---|---|---|
| Schauinsland I | 3.17 | 3.5 | 0.33 |
| Schauinsland II | 3.15 | 3.3 | 0.15 |
| Brugga | 3.17 | 3.1 | -0.07 |
| Hungerbrunnen | 2.79 | 2.9 | 0.11 |
| Snow | 3.67 | 3.4 | -0.27 |
| Dreisam | 2.95 | 2.8 | -0.15 |

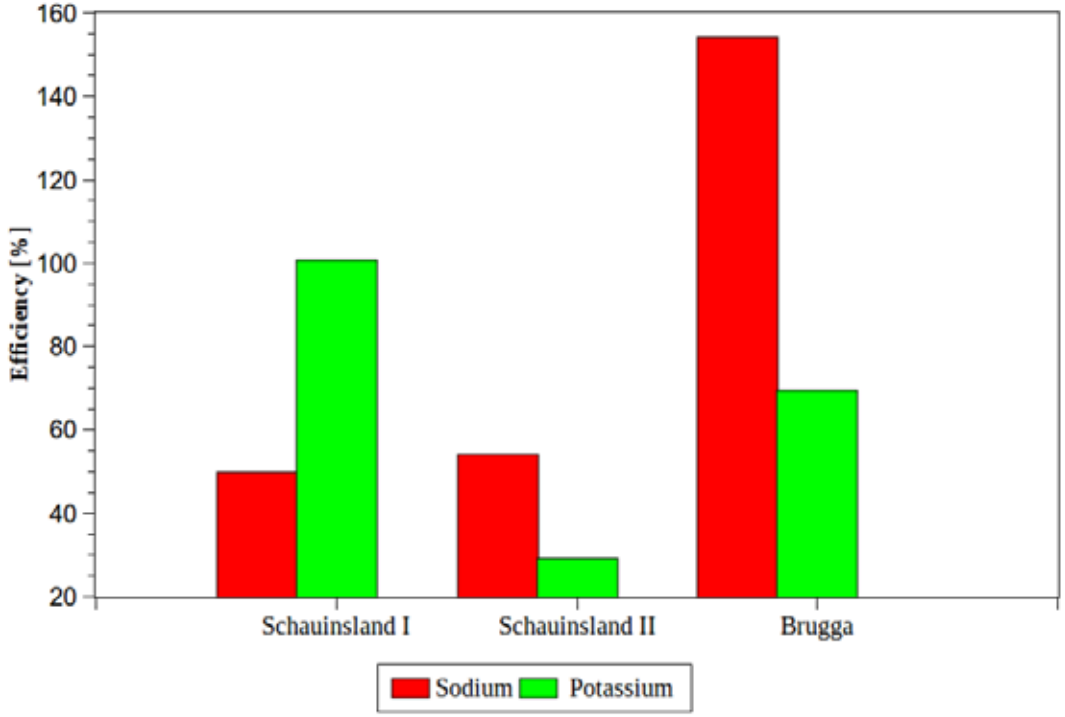


Fig. 5.13: Efficiencies of the ion exchange resin. Values are afflicted with huge errors.

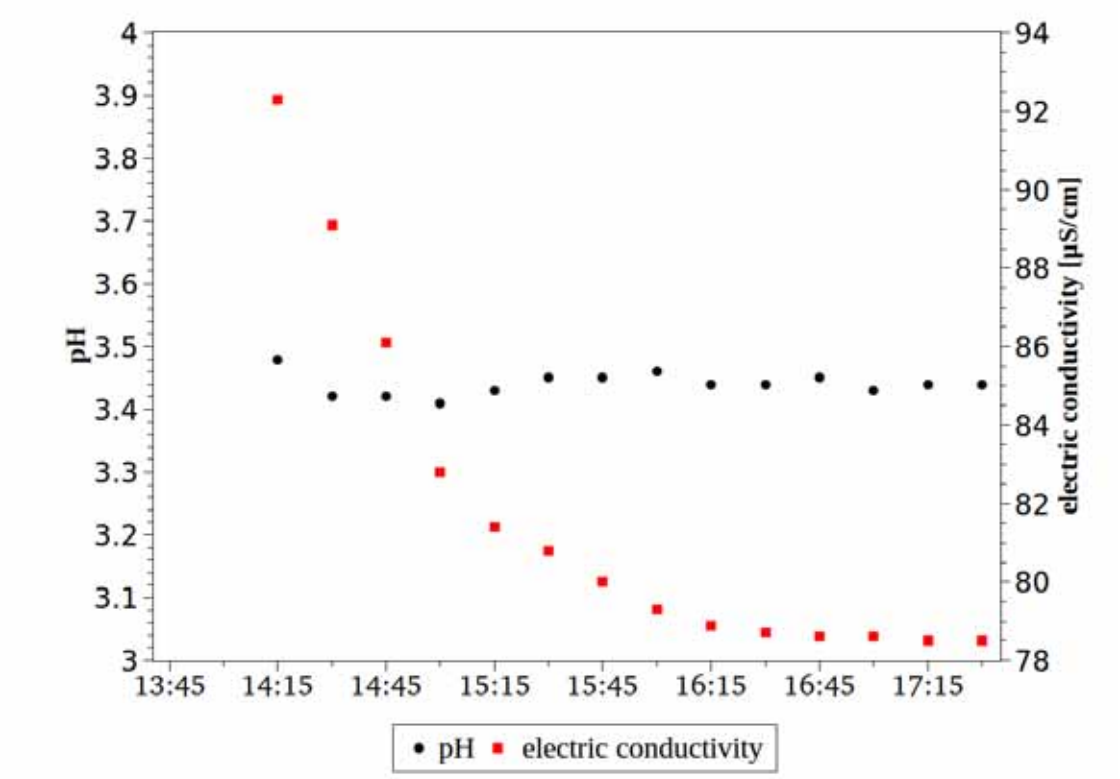


Fig. 5.14: Measurement of pH and electric conductivity at a high resolution in water after passing the exchange resin.

### 5.5.2 Sample at Schauinsland

The first run of the sampling campaigns was done at the Schauinsland, not in the well house, but in the living house about 200 m uphill on November, 24th. A direct pipe leads from the well house to the living house where an approximately 50 litres basin is installed to make sure there is enough pressure on the pipes inside the house. When the pressure in this basin falls below a defined level, the pumps in the well house begin to pump. Before sampling, water flew at maximum speed for about 15 min to make sure that the water in the basin was replaced and that the pipes inside the house where flushed with fresh water.

Just after the start of sampling several problems were noticed. First of that the top-fitting of the ion exchanger column was not water-proof. That was because of some ion exchange resin particles stuck between the fitting and the luting of the plastic screw of the column. Next problem was the safety-fuse which broke several times due to overcharge; after fixing that with a 5 A fuse (instead of a 4 A previous used), the system worked well but pumped air though the exchanger resin first for a while. Then, the system worked in the desired way pumping about 5 litres per minute through the exchange resin.

Back in the laboratory the resin was eluted with about 2.5 litres of 4 M HCl for about three hours. After filling the solution in a plastic basin it was left through the weekend for natural evaporation to a volume of ~1.37 litres (Fig. 5.15, picture a). Then the solution was weighted and filled in two plastic basins to enlarge the surface and accelerate the evaporation process. After natural evaporation for another 24 hours the solution was weighted again. At a volume of 1.16 litres and a weight of 1247.6 g 30 g of the solution were separated to determinate the efficiency of the ion exchange resin. One millilitre of these 30 g was neutralized by adding 2.4 ml ammoniac and completed up to 100 ml with distilled water. The rest of the solution was stirred and heated up to ~45 °C for about 4 hours Then the temperature was raised to ~80 °C for another 4 hours (Fig. 5.15, picture b). The remaining 800 ml where filled in a higher glass beaker and brought to a temperature of 105 °C. A slight boiling process could be observed. The solution was dried to complete dryness and dissolved with 10 ml distilled water. This solution was filled in a small dish used from the BfS for the gamma-spectroscopy analysis and dried to complete dryness again in an oven at 60 degrees for about 16 hours (Fig. 5.15, picture c).

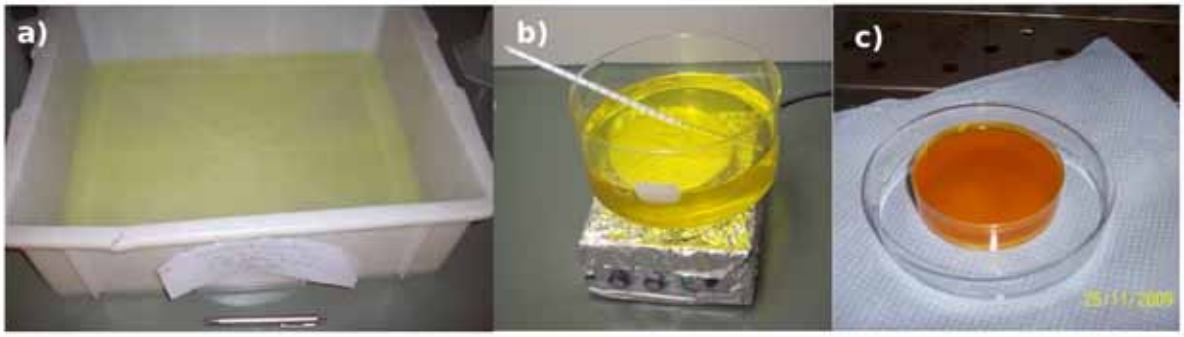


Fig. 5.15: Evaporation process of the first $^{22}$Na sample. a) The eluate is evaporating naturally in a plastic basin. b) Heating and stirring of the eluate to accelerate the evaporation process. c) Sample (still wet) in a small dish for gamma-spectroscopy analysis at the BfS.

The results of the first gamma spectroscopy analysis are shown in Fig. 5.16. The analysis was done before the chemical separation of potassium. Analysis duration was 320000 seconds. $^{22}$Na could not be detected in this sample. The detector had an efficiency of 30 %. The detection limits were 17.5 mBq for $^{22}$Na, 395.2 mBq for $^{40}$K, 13.0 mBq for $^{137}$Cs and 503.5 mBq for $^{210}$Pb.

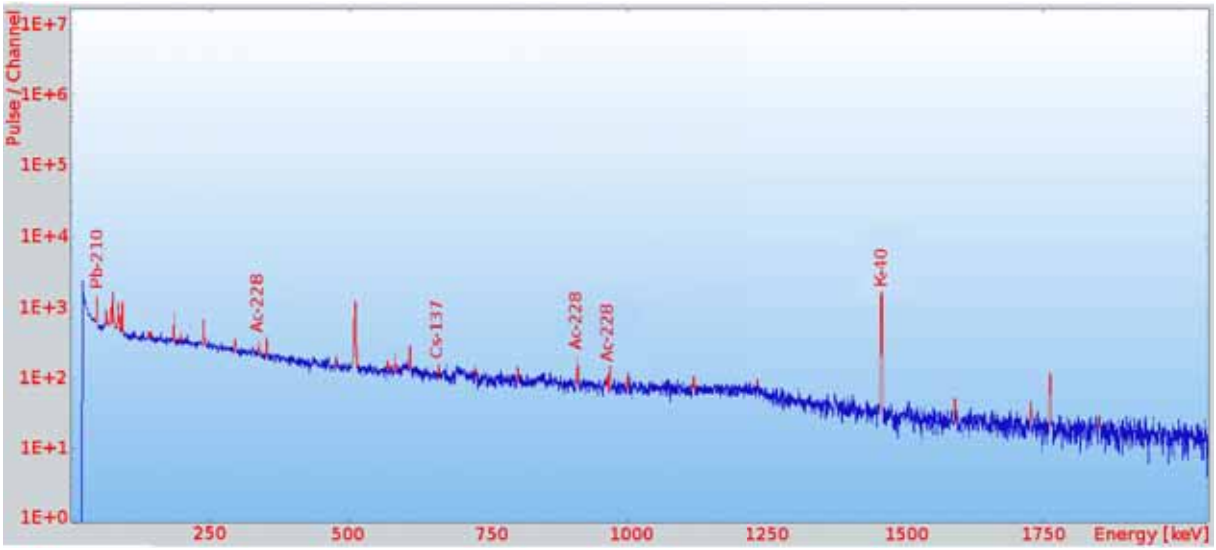


Fig. 5.16: Results of the gamma spectroscopy of the first sample before separation of potassium.

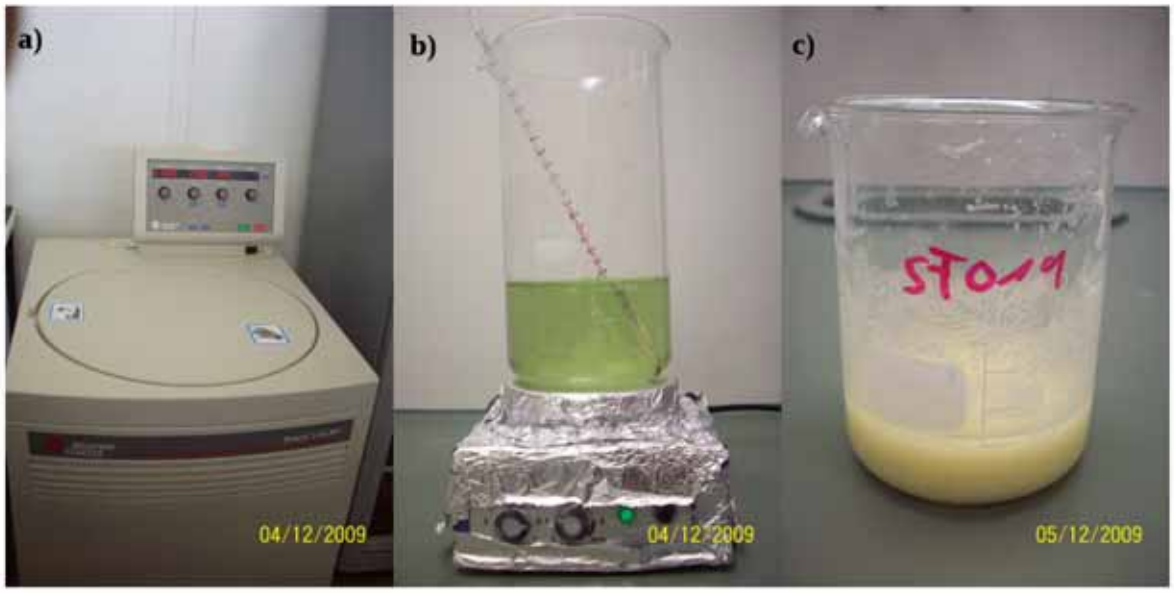


Fig. 5.17: Separation of Calcium and Magnesium. a) The centrifuge at the institute of biochemistry. b) Ammonium carbonate is being destroyed by heating. c) The "solution" is evaporated to approx. 100 ml.

After gamma-spectrometry (Fig. 5.16) the residue was brought back to solution by adding 200 ml 2M HCl and adjusted to a pH of approximately 8 by adding $NH_3$ (25%). By adding 160 ml ammonium carbonate and 160 ml ethanol (99%, denatured) calcium and magnesium carbonates were precipitated and centrifuged. This was done in the Institute of Biochemistry at the University of Freiburg. The centrifuge used one litre cups, was cooled down to 10 °C and ran at 2500 G for 15 minutes (Fig. 5.17, a). The precipitate was washed with the same ingredients as before and centrifuged for another 15 minutes. The solution was heated to 70 °C for about an hour to evaporate ammonium hydroxide generated from ammonium carbonate at temperatures above 60 °C (Holleman et al. 2007). After cooling down, the pH was adjusted to 7 using HCl. The solution was evaporated at 80 – 90 °C to a volume of approximately 100 ml and then evaporated to dryness in a drying chamber at 100 °C. Subsequently it was heated at 500 °C for 12 hours. This was done to vaporize ammonium chloride, that was produced by adding HCl to the ammonium carbonate solution to adjust the pH to 7. Both drying and vaporizing processes were done in the Institute for Inorganic Chemistry at the University of Freiburg.

After evaporating the sample was dissolved in 300 ml 0.1M HCl again and 50 ml of the Kalibor solution (0.1M HCl and 0.1M $Na[B(C_6H_5)_4]$, proportion 1:1) were added. A colourless precipitate could be observed. The $K[B(C_6H_5)_4]$ containing solution was filtered using a 45 nm filter after letting the solution stand for about 20 minutes. The filtrate was dried at 120 °C for

about an hour and weighted. To check the integrity of the precipitation another 50 ml of the Kalibor solution was added to the filtered solution. This was done repeatedly until no precipitation was observed, which occurred at the third attempt. The solution was evaporated to dryness (to 7.2 g) and analysed via gamma spectroscopy.

The residue was dissolved again and the alkaline earths were separated. The filtrate of the potassium separation had a weight of 1.7 g, whereas the residue of the separation of calcium and magnesium had a weight of 4.4 g. The sample was analysed on the same detector again for 242000 seconds. Once again $^{22}$Na could not be detected. Neither could $^{40}$K, $^{137}$Cs or $^{210}$Pb which were in the sample before the separation. The detection limits were 18.6 mBq for $^{22}$Na, 453.8 mBq for $^{40}$K, 15.5 mBq for $^{137}$Cs and 554.0 mBq for $^{210}$Pb.

### 5.5.3 Sample at the Schauinsland well house

After the first run of the sampling machine, the mentioned modifications were done resolving the mentioned problems. The machine worked well then and the sample was more adequate taken. The sample was taken at the Schauinsland as well, not in the living house but in the well house where the samples for $^{222}$Rn activities, chemical parameters and in situ measurements were taken, too. Date of sampling was December, 1$^{st}$. This sample was evaporated to dryness in the laboratory, but without doing any chemical separation procedures. Its weight was 9.7 g after evaporating to dryness. Similar as the previous measurements $^{22}$Na could not be detected. The sample was analysed on the same detector for 173500 seconds which leaded to a detection limit of 23.2 mBq for $^{22}$Na. The only radionuclide detected in this sample was $^{40}$K with an activity of 7.1 Bq (detection limit of 532.0 mBq).

### 5.5.4 Sample from the river Brugga

This sample was taken from the Brugga sampling site. Sampling started at December, 10$^{th}$, sadly after ~100 litres were pumped through the exchange column the sampling construct stopped to work. The reason was that the fuse did break several times again. After replacing the fuse by a 6.3 A one (instead of the 5 A fuse, that was still installed), the pump worked again in laboratory conditions. In the field on December, 14$^{th}$, the pump refused to work again; the reason is unclear. There was a little stone stuck between the chassis and the membrane of the pump causing the membrane to be unmoveable. But after fixing that, the pump did not work, yet. Just after opening the chassis and closing it again (nothing was changed) the pump

worked smoothly again. Sampling could continu on December, 15th. The exchange resin was not eluted between the two sampling days so that on the second sampling day only 400 litres were pumped through the column to complete the 500 l required.

The resin was eluted as described before. After evaporating to nearly dryness and adjusting the pH to about 7 ($NH_3$) the residue was heated with a Bunsen burner to vaporize ammonia chloride until no more smoke was observed. This replaced the step in the oven at 500°C. After cooling down the procedure was continued with adding TPhB'.

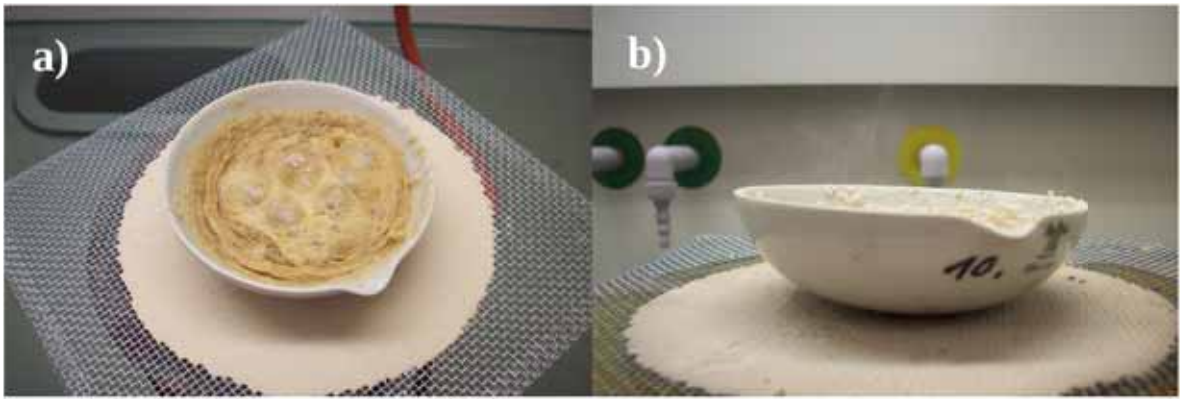


Fig. 5.18: Evaporating the residue to dryness (a) and vaporizing ammonia chloride. The smoke (hard to be seen) is NH4Cl.

The filtrate of the potassium separation had a weight of 5.29 g. The sample was analysed for 416000 seconds leading to a detection limit of 14.9 mBq for $^{22}$Na, 102.3 mBq for $^{7}$Be and 347.8 mBq for $^{40}$K. Also in this sample $^{22}$Na could not be detected. Detected radionuclides were $^{40}$K and $^{7}$Be with a activity of 2.13 Bq and 0.83 Bq, respectively.

### 5.5.5 Sample at Hungerbrunnen

It was taken at the Hungerbrunnen well house on January, 14th. After taking the sample to the laboratory and after evaporating to dryness the sample had a weight of 26.5 g. When trying to dissolve the dry sample again not everything was observed to be dissolved again, therefore the solution was heated to approximately 60 °C and TPhB' was added to provoke the precipitation. The precipitate of KTPhB had a weight of 7.95 g. Detection time of 276000 seconds leaded to a detection limit of 17.5 mBq for $^{22}$Na and 116.3 mBq for $^{7}$Be. $^{7}$Be could be detected with a activity of 0.11 Bq, whereas $^{22}$Na could not be detected. Neither could $^{40}$K, showing an adequate chemical reaction in the precipitation process.

### 5.5.6 Rainwater Sample

Snow was collected, melted and the water was used for the fourth sample. The snow was collected right at the site of the Fahnenbergplatz, where the Institute of Hydrology is located. It was taken only from the surface of the snow layer to make sure that there was no contamination from material of the ground in the sample. Further, it was made sure that there was no de-icing salt strewn at this location. The snow was carried in a barrow and filled in a huge bucket located in the cellar to induce melting by exposing the bucket to heat from the room to accelerate the melting process. After the snow was completely melted the water was sampled in the same way as in the sampling campaigns.

After eluting the exchanger resin the solution contained foreign particulate (e.g. dirt). Therefore, the solution was filtered, using the same filters as used to separate the precipitate of KTPhB, twice before evaporating to dryness. The residue had a weight of 11.7 g before potassium was separated. The precipitate of KTPhB had a weight of 1.48 g.

In this sample $^{22}$Na could be detected with an activity of 0.019 Bq almost on the limit of detection. Other detected radionuclides were $^{7}$Be and $^{210}$Pb with activities of 61.4 Bq and 1.3 Bq, respectively. Counting time was 363000 seconds leading to detection limits of 127.3 mBq for $^{7}$Be, 15.1 mBq for $^{22}$Na and 535.1 mBq for $^{210}$Pb. To find $^{22}$Na in this sample was very interesting and showed that the procedure is working.

### 5.5.7 Sample from the river Dreisam

On February, 5$^{th}$, the sample was taken at the Dreisam sampling point, next to the gauge at Ebnet. The solution was observed to contain foreign particulate after the resin was eluted. The origin could be a cloud of sediment observed in the middle of the sampling process, same that was coming out of the Eschbach. The solution was filtered before evaporating it to dryness. After evaporating, the sample had a weight of 25.1 g, whereas the weight of the precipitate of KTPhB was 5.81 g.

After a detection time of 325000 seconds $^{7}$Be and $^{210}$Pb could be detected with activities of 6.82 Bq and 0.45 Bq, respectively, whereas the detection limits were 409.2 mBq for $^{7}$Be and 148.7 mBq for $^{210}$Pb. A third radionuclide detected is $^{243}$Am (americum) with an activity of 0.05 Bq and a detection limit of 5.19 mBq. Americum is an exclusive artificial produced metal (Seaborg 1964) without any stable isotope. The half-life of $^{243}$Am is 7370 years (Wade & Wolf 1967).

### 5.5.8 Measurement verification

To verify the measurements done and to get more sensitive detection limits all samples were analysed not only by the BfS, but by the GSF (National Research Center for Environment and Health), in Munich, Germany, as well. Samples were analysed using a borehole HPGe detector, having the advantage, that as the sample is nested inside the detection crystal the detection is more sensitive. Detected radionuclides are given in Table 5.7. Reference date of the first four samples is February, 8$^{th}$, correction was done using eq. 4.2. This correction is needed to compare the results from both laboratories because of the time lack between the analysis and the decaying process. Unfortunately, results of measurements from samples from precipitation and from the river Dreisam could not be considered because they were not achieved in time.

Table 5.7: Results from gamma spectroscopies at GSF (Munich)

| | **raw data** | | **error** | | **corrected data** | |
|---|---|---|---|---|---|---|
| **Sample** | **22Na** | **7Be** | **22Na** | **7Be** | **22Na** | **7Be** |
| Schauinsland I | < 0.0083 | < 0.062 | - | - | < 0.0088 | < 0.182 |
| Schauinsland II | < 0.0064 | < 0.034 | - | - | < 0.0067 | < 0.086 |
| Brugga | < 0.0097 | 0.270 | - | 0.027 | < 0.0101 | 0.589 |
| Hungerbrunnen | < 0.0057 | 0.110 | - | 0.028 | < 0.0058 | 0.152 |
| Precipitation | - | - | - | - | - | - |
| Dreisam | - | - | - | - | - | - |

## *5.6 Age-dating*

For age-dating of water, both $^{7}$Be and $^{22}$Na were used. For both radionuclides there is input data available in the literature. This input data is about 1 – 2 Bq/l for $^{7}$Be (Knies et al. 1994) and about 0.1 – 0.3 mBq/l for $^{22}$Na (Tokuyama & Igarashi 1998).

In general, there are two possibilities of water age-dating. First, the measured data can be applied directly (activity per sample divided by the litres pumped) and second by considering the efficiency where the obtained activities have to be divided by the water that flew through the exchanger resin multiplied by its efficiency (eq. 5.1). Efficiency relating to $^{7}$Be and $^{22}$Na differ, being 50 % and 70 %, respectively (see chapter 6.5.1).

$$A_{eff} = \frac{A_s}{V \cdot E} \qquad \text{(Eq. 5.1)}$$

with

$A_{eff}$ = effective activity per litre [Bq/l]
$A_s$ = measured activity in a sample [Bq]
V = volume of water, flew through the exchange resin [l]
E = efficiency of the exchange resin (0...1) [-]

Both possibilities mentioned lead to two other alternatives – relating to literature data or to data obtained by analysis of precipitation, setting rainwater to the age of zero. According to Tokuyama & Igarashi (1998), either $^{7}$Be or $^{22}$Na show annual peaks in December to February. Therefore, literature input data is assumed to be 2 Bq/l for $^{7}$Be and to 0,28 mBq/l for $^{22}$Na. Due to the high sorption of $^{7}$Be in soils, input is set to 0.2 Bq/l. However, $^{7}$Be in snow is not influenced by sorption processes. If considering the efficiency and relating to obtained data, the efficiency of the precipitation analysis also needs to be considered. Relating the information to obtained data in both cases leads to the same values because the ratio between $N_{(0)}$ and $N_{(t)}$ in eq. 4.3 remains constant, whether both values are divided by the efficiency or not. Table 5.8 and Table 5.9 give the estimated water ages using $^{7}$Be and $^{22}$Na, respectively, measured by BfS, while Table 5.10 and Table 5.11 give the estimated water ages using both radionuclides measured by GSF.

Table 5.8: Age-dating using $^{7}$Be activities, measured by BfS

| | | | | **age [d] related to** | | |
|---|---|---|---|---|---|---|
| **Sample** | **activity [mBq]** | **activity [mBq/l]** | **effective activity [mBq/l]** | **literature** | **literature (effective)** | **obtained data** |
| Brugga | 830 | 1.660 | 3.320 | 360.29 | 308.17 | 323.61 |
| Hungerbrunnen | 110 | 0.220 | 0.440 | 512.25 | 460.13 | 475.57 |
| Snow* | 61400 | 122.800 | 245.600 | 209.82 | 157.70 | 0 |
| Dreisam | 6820 | 13.640 | 27.280 | 201.92 | 149.80 | 165.24 |
| Schauinsland | < 62 | < 0.12 | < 0.25 | > 555.36 | > 503.24 | > 518.69 |
| Schauinsland II | < 34 | < 0.07 | < 0.14 | > 600.54 | > 548.42 | > 563.86 |

* sorption is not considered

Table 5.9: Age-dating using $^{22}Na$ activities, measured by BfS

| | | | | age [d] related to | | |
|---|---|---|---|---|---|---|
| **Sample** | **activity [mBq]** | **activity [mBq/l]** | **effective activity [mBq/l]** | **literature** | **literature (effective)** | **obtained data** |
| Brugga | < 14.93 | < 0.030 | < 0.04 | > 3066.81 | > 2578.11 | > 340.36 |
| Hungerbrunnen | < 17.52 | < 0.04 | < 0.05 | > 2847.62 | > 2358.92 | > 121.17 |
| Snow | 19.14 | 0.04 | 0.06 | 2726.45 | 2237.75 | 0 |
| Dreisam | < 33.13 | < 0.07 | < 0.10 | > 1974.69 | > 1485.99 | 0 |
| Schauinsland | < 18.63 | < 0.04 | < 0.05 | > 2763.46 | > 2274.75 | > 37 |
| Schauinsland II | < 23.29 | < 0.05 | < 0.07 | > 2457.56 | > 1968.86 | 0 |

Table 5.10: Age-dating using $^{7}Be$ activities, measured by GSF

| | | | | age [d] related to | |
|---|---|---|---|---|---|
| **Sample** | **activity [mBq]** | **activity [mBq/l]** | **effective activity [mBq/l]** | **literature** | **literature (effective)** |
| Brugga | 589 | 1.178 | 2.356 | 386.08 | 333.96 |
| Hungerbrunnen | 152 | 0.304 | 0.608 | 487.93 | 435.81 |
| Schauinsland | < 18.2 | < 0.036 | < 0.073 | > 474.38 | > 422.27 |
| Schauinsland II | < 8.6 | < 0.017 | < 0.034 | > 530.75 | > 478.63 |

Table 5.11: Age-dating using $^{22}Na$ activities, measured by GSF

| | | | | age [d] related to | |
|---|---|---|---|---|---|
| **Sample** | **activity [mBq]** | **activity [mBq/l]** | **effective activity [mBq/l]** | **literature** | **literature (effective)** |
| Brugga | < 10.1 | < 0.020 | < 0.029 | > 3602.33 | > 3113.62 |
| Hungerbrunnen | < 5.8 | < 0.012 | < 0.017 | > 4362.33 | > 3873.62 |
| Schauinsland | < 8.81 | < 0.018 | < 0.025 | > 3789.55 | > 3300.85 |
| Schauinsland II | < 6.74 | < 0.013 | < 0.019 | > 4156.53 | > 3667.82 |

Because no data from precipitation and from the river Dreisam measured by GSF are available, no age related to obtained data can be estimated.

## *5.7 Summary of the results*

Results of the data gained from measurements of field parameters (temperature, electric conductivity, pH-value and oxygen saturation) do not show any obvious or important trend in the focused time, besides temperatures drops during late summer to winter. Electric conductivities in groundwater samples show a minimum in December but increase again in January to previous observed levels. Riverine samples do not show this particularity. Also principal components, neither in groundwater nor in riverine water, show any remarkable trend. In most cases calcium has the highest observed concentrations, followed by chloride. It should be noted that no carbonates were measured. Determinations of silicate were only made in groundwater samples where the samples from Schauinsland trend to show slightly lower concentrations in winter time. Both series show the same behaviours with minimum values in October and rising again.

Radon activities in all cases are relative stable, in order of their errors, over time. Of course, in groundwater samples activities are much higher than in riverine samples, whereas Schauinsland samples have more than double the activities of Hungerbrunnen.

Measurements of stable isotopes, $^{2}H$ and $^{18}O$, were made for groundwater samples and when a sample for the determination of cosmogenic radionuclides was taken. For weekly samples of the two rivers only $^{18}O$ data is available. Focused on $^{18}O$ groundwater samples do not show any trend of importance, whereas riverine water was lighter in December but rose again in January. In general, groundwater shows less variation than riverine water. The signatures of all samples are in line, in order of their errors, with the global meteoric water line. Samples from Hungerbrunnen are the heaviest, followed by the rivers Dreisam and Brugga. Schauinsland are the lightest, only precipitation water gained from melted snow is even much more lighter.

$^{22}Na$ was detectable in melted snow only with an activity of 0.019 Bq. All samples, except of the first one that had to be repeated, were taken under the same conditions. Water from Schauinsland contained only $^{40}K$ which is not possible to use for water age-dating. In all other samples $^{7}Be$ could be detected, whereas precipitation showed the highest activity of 61.4 Bq, followed by water from the river Dreisam (6.82 Bq), Brugga (0.83 Bq) and Hungerbrunnen (0.11 Bq). These results have been verified at the GSF in Munich. Though the detector used provided more sensitive detection limits, $^{7}Be$ activities differ only slightly from activities found between the GSF and the BfS as follows: Brugga: 0.589 Bq, Hungerbrunnen: 0.152 Bq.

All activities, given in Bq per sample, are shown in Fig. 5.12, where filled dots represent measurements from BfS and rings measurements from GSF.

Application of $^{7}$Be activities to age-dating leads to different ages, whether the efficiency of the resin is considered or activities are related to literature or obtained data. Ages in days are: Brugga: 308.17 – 386.08; Dreisam: 149.5 – 201.92; Hungerbrunnen: 435.81 – 512.25; Snow: 0 – 209.82 days. According to the detection limit of $^{7}$Be, water from Schauinsland is older than 422.27 days. Due to the long half-life and the low measured activity with simultaneous large errors, applying $^{22}$Na data to determine water age leads to high variabilities of water ages. Because $^{22}$Na could be determined in precipitation only, it is not possible to date other samples but to give minimum ages namely: Brugga: 340.36; Dreisam: 0; Hungerbrunnen: 121.17; snow: 0 days. For these estimations, the age of snow was set to zero. Because of the higher detection limit from the measurements of Dreisam than of snow, the minimum age of water from Dreisam is estimated to be as old as snow. These results are shown in Fig. 5.20 for ages estimated using $^{7}$Be and in Fig. 5.21 for ages estimated using $^{22}$Na.

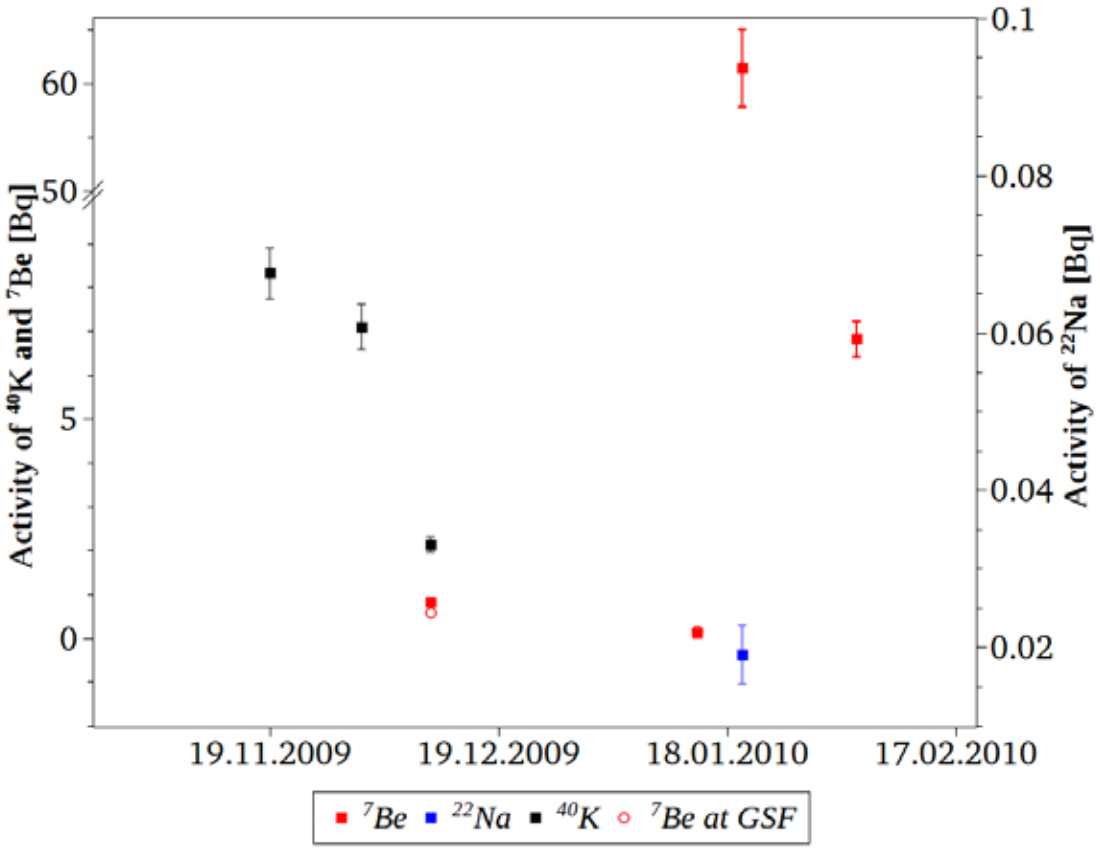


Fig. 5.19: Radionuclides detected by the BfS (dots) and GSF (rings), errors are computed by the detector software.

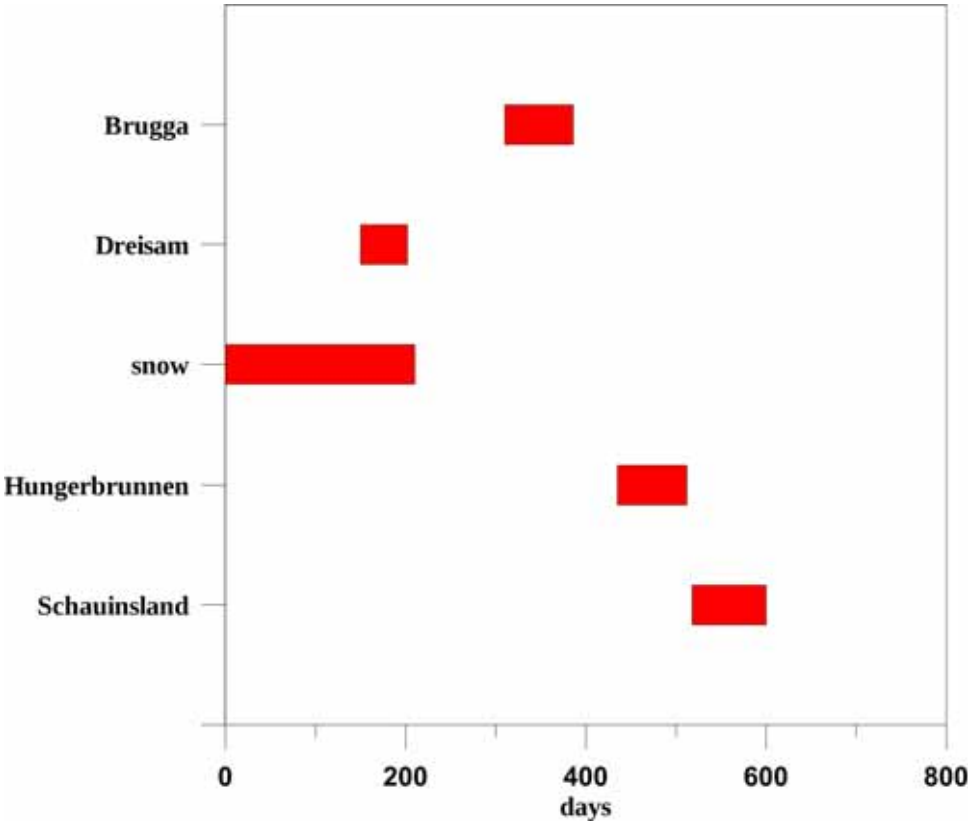


Fig. 5.20: Range of estimated ages using $^{7}$Be (data both from BfS and GSF).

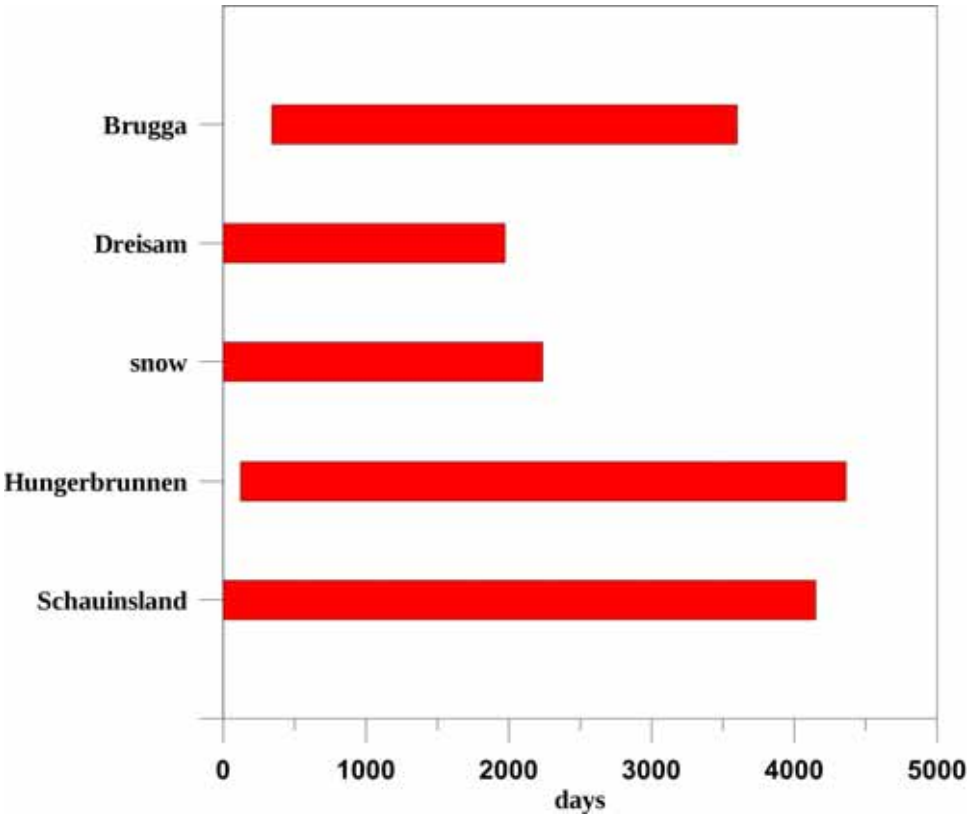


Fig. 5.21: Range of estimated ages using $^{22}$Na (data both from BfS and GSF).

# 6. Discussion

## *6.1 In situ parameters*

### 6.1.1 Rivers

Temperatures of riverine water samples, as expected, dropped from late summer to winter, whereas pH-values do not show significant variations. Electric conductivity in both rivers shows a minimum in December before rising again later. This minimum could be a sign that during this time the influence of fast components is greater than in times when electric conductivities are higher. In December wide areas of the catchments were covered in snow and soils were frozen making it hard for runoff to infiltrate and get enriched with minerals. In the same period de-icing salt was distributed. At the end of this cold period snow melted, de-icing salt was transported to rivers and electric conductivity rose to even higher values than before. Also water temperatures rose again from this time.

### 6.1.2 Groundwater

The behaviour mentioned in 6.1.1 cannot be observed in groundwater samples. Temperatures are relatively constant in samples from Hungerbrunnen (9.7 – 11.2 °C) and vary only slightly in sample from Schauinsland (5.8 – 9.6 °C). Because the mean annual temperature for Freiburg is 10.8 °C (DWD 2007), water from Hungerbrunnen should be a mixture of waters with an age of more than one year without great influences of fast runoff components. This is also represented by the observed constant values of electric conductivity ranging from 153.3 to 159.5 µS/cm. According to the Umweltbundesamt (2010) the annual mean temperature for the last 10 years is 6.2 °C. Therefore, influences of fast runoff components with residence times less than a year are possible due to the higher variability in temperature values. Electric conductivity is much lower in samples from Schauinsland. This could be a hint for shorter residence times. Still the geology has to be considered: Hungerbrunnen is located in the Zartener Becken and therefore in alluvial bedrock, whereas Schauinsland consists of granite and gneiss which is much less soluble.

## 6.2 Main chemical components

In general, all samples show similar chemical composition with calcium as the most dominant cation and chloride as the most dominant anion. The extreme high values for sodium and chloride in riverine water on December, 31$^{st}$, can be linked to de-icing salt. The generally higher values of sodium and chloride in January match well to the higher values of electric conductivity in this time and, as it should be assumed, can be linked to de-icing salt as well. Principal components in water from Hungerbrunnen and riverine water are similar showing similar concentrations and reduced variations, leading to the assumption that no dominant runoff component was changing at this time. Hungerbrunnen shows higher concentrations of nitrate, probably due to fertilisation processes in this area. Greater variances occur in samples from Schauinsland. Whereas calcium is the most dominant ion in most of the cases, nitrate, chloride and sodium occur in alternating concentrations. These variations are another hint to suppose short residence times as well. Pointing to the concentrations of silicate in groundwater samples this hint can be solidified although Schauinsland samples show higher concentrations of silicate than samples from Hungerbrunnen but also higher variations. As mentioned before, the geology of Schauinsland consists mainly of granite and gneiss containing higher silicate concentrations than the alluvial bedrock where Hungerbrunnen is located. It may be possible, that there is a fast runoff component reducing the silicate concentrations because of shorter contact times with the bedrock that is initiated by other factors, e.g. by rainfall.

## 6.3 Radon

The hypothesis of the existence of a fast runoff component at the Schauinsland well can be solidified by pointing on the measured $^{222}$Rn activities. The little depression in September matches well to the depression in silicate concentrations in this time. The activity of $^{222}$Rn in water is a function of contact time with the bedrock as well.

Radon activities must not be compared between sample points but only within the series. Higher activities in Schauinsland water, on that account, do not mean longer residence times because of the high concentration of uranium ($^{238}$U and $^{234}$U) in granite. Absolute information cannot be gained from radon (Hoehn & Gunten 1989), but generally less variation means less change of contact time and therefore less change on the water-age.

Radon activities in samples of the river Brugga have low variation, whereas the sample taken from Dreisam at February, 2$^{nd}$, shows more than double of activity than the sample taken on

February, 9th. This phenomenon would be explained by base flow characteristics of the second sample though both sampling dates the river showed similar runoff volumes. Another reason might be the different sampling location, though being in the same area, was done in different measurement points. The second sample was taken right at the Ebnet gauging station, whereas the first one was taken about 200 metres upstream. If groundwater infiltrates into the river in the direct vicinity of the second sampling point, this would explain the difference in radon activities. Due to the fast degassing of radon in surface waters, this information is difficult to use for age-dating.

## *6.4 Stable isotopes*

### 6.4.1 Rivers

Both rivers show similar behaviour on the time scale with slightly lighter water in winter. The minimum in January (see Fig. 5.11) can be linked to heavy snowfall at this time. Due to the effect of temperature, snow is much lighter than water from other samples, since they represent a more or less well mixed mixture of older and younger rainwater precipitated in warm and cold times (see Fig. 5.4). This also might be the reason for the two peaks in late summer and early autumn. Due to high temperatures, rainfall was heavier at these times. The generally lighter values of the river Brugga may be correlated to its smaller catchment with a higher proportion of it located at high altitude in comparison to the Dreisam catchment, where proportionally more area is located at lower altitudes. In addition, due to its bigger catchment size, water of the Dreisam may have a higher proportion of well mixed (old and young) waters, in general responsible for heavier water in the stream, though both rivers show similar behaviour about their response time. In contrast, the maximum difference between lightest and heaviest water samples is higher for Dreisam samples than for Brugga samples, with 1.53 ‰ and 1.26 ‰, respectively. The higher this value, the less mixed components (older and younger) are in the water sample. It is important to mention that the mouth of the Brugga is located upstream from the sampling location of the river Dreisam. Therefore, water at this point contains components from the Brugga river water as well.

### 6.4.2 Groundwater

In general, groundwater shows less variation in $\delta^{18}O$ because of the well mixed water in the aquifer at the sampling point (Fig. 5.11). Maximum difference between lightest and heaviest water samples is higher for Schauinsland samples than for Hungerbrunnen samples with 4.46 ‰ and 2.93 ‰, respectively. Therefore, Schauinsland water should be less well mixed with different waters. Reasons for that could be that it has shorter residence times, resulting in worse mixed runoff components, or that there are other dominant flow processes in the catchment. If piston flow was the dominant process at Schauinsland, this could explain the higher variability. The cut on November, 11$^{th}$, favours the idea of short residence times. The week before this sample was taken, the peak region of Schauinsland was covered in snow, that lasted only a few days. Due to the temperature effect, this melting water should be isotropically lighter than rainwater. If this is the reason for that cut, there are fast flow components at Schauinsland. It is worth to mentio, that the peak region was covered in snow at the date when the last sample was taken, too, but, due to constant temperatures below zero over a long period of time snow was not melting and therefore was not isotropically detectable in runoff.

The difference between Hungerbrunnen and Schauinsland can be traced back to the effect of temperature as well as to the effect of the precipitation volume. The difference for $\delta^{18}O$ values is about 1.3 ‰ and about 8 ‰ for $\delta^{2}H$ values (Fig. 5.4), which agrees well with annual precipitation data (~950 mm in Freiburg (Matzarakis & Mayer 2000) and ~1750 mm at the Schauinsland (Wenninger et al. 2004)).

## *6.5 Cosmogenic radionuclides*

### 6.5.1 Efficiency of the ion exchange resin

It was found that the efficiency of the exchange resin is ~50% for beryllium. Only one sample was used to determine that value. In order to use this procedure for age-dating more precise information is required. Reasons for the mentioned efficiency, besides from characteristics of the sampling procedure (discussed below) are of chemical nature. What compounds are built by beryllium and how well they are exchanged by the resin? The answer of this question cannot be given in this thesis. Further work is needed to get more information for applying this method for age-dating.

Pointing on sodium efficiencies are even more blurry. The efficiency may vary at each sample depending on several factors. One is the water flow velocity. The faster the water flows, the shorter is the contact time with the resin and the worse is the efficiency of the resin. Normally, flow velocity is set to about 2 litres per minute, but at the first run there was no bypass installed, so the velocity was about 5 litres per minute. Nevertheless, it is not clear if 2 litres per minute is an adequate pump flow. This velocity is chosen because it was mentioned in the literature from previous experiments by Sakaguchi et al. (2005) as well.

Another possibility, which might be negligible, is the amount of resin in the column. This varies little at each filling, when the column is being prepared for a measure campaign. During sampling, at the bottom end of the column, where the water was entering the system, a zone was observed where the resin was not as dense as in the rest of the column. This zone was between 1 and 3 centimetres in height. Compared to the entire length of the column this should have a negligible effect, but it could also be important to be mentioned.

Another reason for a varying efficiency might be the elution of the resin. It is possible that the elution using 4M HCl for minimum 2 hours is not complete. That would have effect on the sample taken before and the ions being eluted as well as on the sample taking with the eluted exchanger resin because if not all exchanger places are free, the capacity of the resin is reduced. Looking at Fig. 5.18, it is possible to notice that the capacity of the resin is high enough for the complete amount of dissolved ions to be exchanged. This can be proven by the electric conductivity, which drops about 12 µS/cm to lower levels. But this loss is rather small achieved until stable state is reached. Also pH value does not serious changes over the time. Generally, at all samples calculated and measured pH-values match well (Table 5.6). The higher difference occurring at the first sample campaign made at the Schauinsland can be traced back to the high pumping velocity of this sample.

Whereas an aliquot of the eluate was separated for every sample taken, due to lack of time, only three samples could be analysed. In addition, these samples were analysed via AAS producing large errors (see Fig. 5.3). Water passed through the resin was taken and evaporated, but due the lack of time could not be analysed. Providing this information, much precise conclusions about the efficiency could have been made. Efficiency of sodium is assumed to be about 70 % because this is the mean value of the previous determined efficiency, if no efficiencies higher than 100 % are allowed.

### 6.5.2 Discussion of the procedure

The original chemical separation procedure published by Sakaguchi et al. (2003) (see Fig. A.1 in the appendix) has two main disadvantages. First one is the time needed for sampling and post treatment of the sample which takes at minimum four days. It has to be evaporated to dryness, dissolved again and calcium and magnesium have to be separated. By adding $(NH_4)_2CO_3$ to the solution containing HCl $NH_4Cl$ is produced. For further work this needs to be eliminated in a muffle furnace at 500 °C for 12 hours because ammonia is precipitate by TPhB'. In the case of this thesis this was even more problematic because the Institute of Hydrology neither owns a centrifuge nor a muffle furnace. The second disadvantage is linked to this first one. By precipitating calcium and magnesium, also beryllium gets precipitated in form of $Be(OH)_2$. If the activity of $^{7}Be$ of a sample is of interest, it has to be measured before this separation which takes a minimum of one extra day.

By not separating calcium and magnesium the time needed from sampling to analysing could be reduced to three days – including the measurement of the activity of $^{7}Be$ – whereas most of the time is needed to evaporate the solutions, especially for the last step in the compartment drier because the Petri dish used is only made for temperatures below 80 °C. However, if the sampled water is highly mineralised, it might present the disadvantage not to separate calcium and magnesium, due to the total mass of the residue and the limiting size of the Petri dish. If, in that case, analysing an aliquot, detection limits are higher, but the procedure is faster.

### 6.5.3 Detected radionuclides

In the first sample $^{210}Pb$, $^{137}Cs$, $^{40}K$ and the peaks of $^{228}Ac$ could be detected. After the chemical separation was done none of those isotopes could be detected any more. This means that the separation of $^{40}K$ worked well. Due to the chemical separation of potassium, neither $^{210}Pb$ nor $^{137}Cs$ could be detected in this sample. Potassium is precipitated using TPhB'. This compound does not only precipitate potassium but also lead, caesium and ammonia. Also in the other samples no $^{40}K$ was detected excluding two cases, the second sample from Schauinsland and the sample taken from Brugga. The reason for the occurrence of $^{40}K$ in the sample from Brugga is, that ammonia was added to adjust the pH, which is totally unnecessary and prevents a quantitative separation of potassium if it was not quantitative vaporized. Potassium was not separated from the second sample taken on Schauinsland on purpose, because of the idea to show differences in analysing samples with and without separating potassium. Unfortunately, neither in the first (separated) nor in the second sample

$^{22}$Na could be detected. Neither could $^{7}$Be, which was detectable in other samples, like in water from Hungerbrunnen, which is of groundwater source, too. For the first sample this could have several reasons: the pumping rate was too high, leading to a bad efficiency of the exchange resin (see chapter 6.6) and that sampling was not done at the well house, where all other samples where taken, but in the living house uphill. Although the basins in the well house were flushed a few days before and the pipes leading to the house were new and consisted of synthetics influences cannot certainly be eliminated. Sampling was repeated a few days later with the final setup of the sampling machine, though. In this second sample neither $^{22}$Na nor $^{7}$Be could be detected. Another reason might be that the water was simply too old to detect $^{7}$Be. But another (more plausible) reason is that $^{7}$Be is not that mobile in soils of the Schauinsland-catchment, as it is in soils of the catchment of Hungerbrunnen. It is not clear which compounds of beryllium are highly mobile in soils, yet. Veselý & Majer (1994) found that the concentrations of beryllium are about 100 times higher in acidic waters than in waters with pH-values of 7 – 8. But as well water from Schauinsland as from Hungerbrunnen did show pH-values in the slightly acidic array. Furthermore, this study could show that the concentration of beryllium is low if free fluoride is missing in water. This leads to the assumption that beryllium forms highly mobile compounds with fluoride. Also DOC (Dissolved Organic Carbon) might be able to build highly mobile compounds with beryllium (Fricke & Schützdeller 1923). Unfortunately, neither fluoride nor DOC concentrations have been measured in samples for this work. If higher concentrations of these compounds can be found in water from Hungerbrunnen, than in water from Schauinsland, this would explain why no $^{7}$Be could be detected.

In fact, in non of the samples, excluding the one from precipitation, $^{22}$Na was found leading to the question about the reasons for this. As already discussed, the efficiency of the procedure could be too bad to collect as much $^{22}$Na as needed for an adequate detection. Errors leading to a loss during the chemical separation can be nearly neglected if the working procedure is carefully done. After decanting the solution, the previously used bin should be washed three times at least with distilled water to make sure decanting is quantitative. The limiting factor on efficiency therefore is sampling including, as already discussed, the resin, pumping velocity etc. It is possible that the amount of $^{22}$Na collected could be enlarged by increasing the sample size or by using other sampling techniques (e.g. semipermeable membrane technologies). Other possibilities, including the use of more sensitive detectors, make it possible to detect less amounts of $^{22}$Na. Possibly, the reason why this radionuclide was not detectable is not the efficiency of the resin but cation exchange processes in soils. Even if Birkholz (2007) could show by column experiments, that more than 90 % of sodium can be recovered, there could be processes in soils reducing the amount of $^{22}$Na without influencing the total mass balance; there may be cation exchange processes with sodium stored in the soil, increasing the residence time without influencing the mass balance, but changing the isotope

signature. If the residence time of water in an aquifer, e.g. the Zartener Becken, where Hungerbrunnen is located, is shorter than the residence time of sodium, this could explain why $^{22}$Na was not detectable in water samples.

## *6.6 Age dating*

Different procedures are possible to estimate the water age. In general, the high difference of the input value for $^{22}$Na in literature to the observed one leads to a far too high age for snow. Therefore, if $^{22}$Na (and $^{7}$Be) is used for age-dating, the input has to be determined. It could be considered for dating other waters. Due to the low detected activity of this radionuclide in precipitation and the huge differences of detection limits, in some cases being even higher than the observed activity, calculated ages are affected with large errors leading even to negative ages. To avoid this it is recommended to use either the enrichment of $^{22}$Na – via higher sample volumes and/or better efficiencies – or detection limits have to be advanced. Nevertheless, age-dating with this technique might be possible.

The use of $^{7}$Be for age-dating leads to more accurate results because of the short half-life of this radionuclide. Detection errors lead to smaller variations in ages. Due to the high uncertainty of sorption processes in soils and bedrock, these ages are afflicted by errors, as well.

If the activity of snow is used as input, ages calculated by $^{22}$Na and $^{7}$Be match better if literature values are used. An advantage of this method is that the systematic error of the efficiency is negligible and ages should be more realistic considered because precipitation is set to its true age of zero. In fact, relative ages of the sample match well with reported ages. Dreisam water is younger than water of Brugga, which has a higher part of baseflow. This is younger than water from Hungerbrunnen (see Fig. 5.19). Compared to absolute ages determined in preliminary researches, e.g. (Adolph 2009).

# 7. Conclusions

Natural $^{22}Na$ levels are too low to be detected with simple sampling. A method for the enrichment of this radionuclide, presented by Sakaguchi et al. (2003), could be established. Due to improvements of the chemical separation of potassium (needed to obtain better results of $^{22}Na$ analysis), it was possible to accelerate the process and to detect as well $^{22}Na$ as $^{7}Be$, which was precipitated in the original chemical separation. Efficiencies of this method are about 70% for $^{22}Na$ and 50% for $^{7}Be$. Due to large errors in the analysis technique more research is needed to verify the efficiency for $^{22}Na$ and in different conditions. A recommended approach is to analyse both sampled water and deionised water and compare the results.

Values presented in the literature for both radionuclides are higher than the detected ones, whereas the difference is slightly higher for $^{7}Be$ (0.25 Bq/l detected vs. 1 – 2 Bq/l in literature (Knies et al. 1994)), than for $^{22}Na$ (0.038 mBq/l detected vs. 0.1 – 0.3 mBq/l in literature (Tokuyama & Igarashi 1998)). In fact, relative differences of $^{7}Be$ are comparable with those of $^{22}Na$ (4 – 8 times vs. 2.6 – 7.9 times, respectively) indicating that fallout rates of cosmogenic radionuclides in general at the observed time were smaller than the values found in literature. In order to apply both $^{7}Be$ and $^{22}Na$ to age-dating better results are obtained if the activity of precipitation is determined and taken as input function to estimate residence times.

On one hand, probably sorption processes are the reason why $^{7}Be$ could not detected in water from Schauinsland even if fluctuations of temperature and $\delta^{18}O$ – values indicate that this water is influenced by fast runoff components. On the other hand, $^{7}Be$ was detectable in Hungerbrunnen showing less of these fluctuations and indicating higher residence times. As $^{7}Be$ is liable to sorption processes in soils and bedrock, Hohwieler (2005) could show in column experiments that only about 10 % of the input is mobile in soils. However, it is unknown which compounds of beryllium are mobile. While You et al. (1989) found that organic matter has little effect on beryllium mobility, the work of Veselý et al. (1989) indicates that beryllium is strongly bound to natural organics (e.g. fulvic substances). Besides that high fluoride concentrations and low pH values lead to the highly mobile compounds $BeF_3^-$ and $BeF_2$. To obtain more accurate activities of $^{7}Be$ and more precise residence times more research is needed to determine the exact influence of DOC and fluoride concentrations in water on the mobility of beryllium.

$^{22}$Na was neither detectable in groundwater nor in riverine water samples. Results from age-dating using observed $^{7}$Be levels in precipitation for input indicate that other processes than the radioactive decay are responsible for such measurement difficulty. According to Birkholz (2007) sodium is hardly affected by sorption processes, however, there might be exchange processes with ('new') sodium and ('old') sodium stored in the soil, without influencing the mass balance of the substance. This would lead to a different sodium-age than the water-age, similar to processes observed on $^{35}$S (Novák et al. 2004).

It could be shown in this work that it is possible to detect $^{7}$Be and $^{22}$Na in rainwater samples, whereas $^{7}$Be is detectable in groundwater and riverine water samples. Also $^{7}$Be seems to be a useful indicator for short residence times (weeks up to two years). However, to produce more reliable data the mobility factors such like concentrations of DOC and fluoride have to be quantified more accurately. $^{22}$Na shows also a potential to be applied to determine residence times of water. But again, better enrichment and/or better analysing techniques are necessary. Using both radionuclides at the same time, the information could provide better understanding of rainfall-runoff processes, e.g. the old water paradox (Kirchner 2003).

# 8. Outlook

It could be shown in this work that both $^{7}Be$ and $^{22}Na$ is detectable in precipitation using an enrichment method, however, $^{22}Na$ cannot be detected in groundwater and riverine water. To apply this radionuclide for age-dating more research is required. A few suggestions for further works are given in the following.

In general, it is possible that there is a loss of efficiency in the procedure of the chemical separation, especially if decanting the solution. To avoid this and even accelerate the separation ionic chromatography could be used to separate sodium from potassium. This procedure is presented by Holzapfel et al. (1962). Certainly, it has to be checked if beryllium ends in the fraction of sodium, potassium or a different one.

To provide better detection limits two approaches are possible: first, improved analysing techniques, e.g. coincidence measurements, can be used, second, the enrichment can be improved. An adequate approach could be to take even larger water samples, whereas the size of these samples is limited by the capacity of the exchange resin. Moreover, there are other enrichment techniques available, such as reverse osmosis using semipermeable membranes. Of course, best results should be provided if both techniques are tested and compared.

In addition, samples can be taken from young water with well known age. This age must not have been determined using CFCs or $SF_6$ because these tracers only date the last contact of water with atmosphere, whereas cosmogenic radionuclides date the age of water from time of formation of precipitation. Besides that, time series could be sampled, e.g. during snowmelt or storm events, where surface runoff processes should be dominant.

Unlike $^{22}Na$, $^{7}Be$ could be detected in groundwater and riverine water although beryllium was supposed to be highly sorptive and, therefore, not expected to be found. Factors influencing the mobility of beryllium are not clearly identified and quantified. These are the conditions for using it to estimate water-ages. Preliminary column experiments of Hohwieler (2005) should be repeated, using defined concentrations of fluoride and DOC which are supposed to have great influence on the mobility of $^{7}Be$.

# 9. References

Adolph, G. (2009): *Kombination von Isotopenmethoden und Grundwassermodellen in der Altlastenbearbeitung*. *Freiburger Schriften zur Hydrologie* **28**, Institut für Hydrologie der Universität Freiburg im Breisgau, pp. 206.

Birkholz, A. (2007): *Bewertung von verfahren der Sickerwasser- und Transportdiagnose von Schadstoffen*. Albert-Ludwigs-Universität, Freiburg im Breisgau, 134 pp.

Boschung, M. (1998): *The high purity germanium detector whole-body monitor at PSI*. Radiation Protection Dosimetry **79**, pp. 481 - 484.

Botter, G.; Milan, E.; Bertuzzo, E.; Zanardo, S.; Marani, M. & Rinaldo, A. (2009): *Inferences from catchment-scale tracer circulation experiments*. Journal of Hydrology **369**, pp. 368-380.

Brand, W. A.; Geilmann, H.; Crosson, E. R. & Rella, C. W. (2009): Cavity ring-down spectroscopy versus high-temperature conversion isotope ratio mass spectrometry; a case study on $\delta^{2}H$ and $\delta^{18}O$ of pure water samples and alcohol/water mixtures. Rapid Communications in Mass Spectrometry **23**, pp. 1879 - 1884.

Cigna, A. A.; Clemente, G. F. & Giorcelli, F. G. (1970): *Cosmogenic and Artificial Na-22 Levels in Rainwater.* Health Physics **18**, pp. 379 - 382.

Clark, I. & Fritz, P. (1997): *Environmental Isotopes in Hydrogeology*, 1. edition, CRC Press, Boca Raton, 352 pp.

Demtröder, W. (2005): *Experimentalphysik 4*, 2. edition, Springer Verlag, Berlin, Heidelberg, New York, 517 pp.

DWD (2007): *Mittelwerte der Temperaturen für den Zeitraum 1961 - 1990*. www.dwd.de, (22.02.2010).

ESFRI (2006): *European Roadmap for Research Infrastructures – Report 2006*, 1. edition, European Communities, Brussels, 84 pp.

Espinosa, G.; Hernández-Ibinarriaga, I. & Golzarri, J.-I. (2009): *An analysis of the potassium concentrations of soft drinks by HPGe gamma spectrometry.* Journal of Radioanalytical and Nuclear Chemistry **282**, pp. 401-404.

Flaschka, H. & Barnard, A. J. (1960): *Tetraphenyl boron (TPB) as an analytical reagent*. Advances in analytical chemistry and instrumentation **1**, pp. 1 - 117.

Fleishman, D. G. (2008): *Cosmogenic $^{22}Na$ as an index of the residence time of water in freshwater basins: a review.* Journal of Environmental Radioactivity **99**, pp. 1203 - 1215.

Fricke, R. & Schützdeller, H. (1923): *Untersuchungen über Hydrate in wäßriger Lösung. I. Mitteilung. Das Berylliumion*. Zeitschrift für anorganische und allgemeine Chemie **131**, pp. 130 - 139.

Gooddy, D. C.; Darling, W. G.; Abesser, C. & Lapworth, D. J. (2006): *Using chlorofluorocarbons (CFCs) and sulphur hexafluoride ($SF_6$) to characterise groundwater movement and residence time in a lowland Chalk catchment*. Journal of Hydrology **330**, pp. 44 - 52.

Harten, U. (2009): *Physik - Einführung für Ingenieure und Naturwissenschaftler,* 4. edition, Springer Verlag, Berlin, Heidelberg, 441 pp.

Helmer, R. G. & Schönfeld, E. (2009): *Table de Radionucléides*, BNM-LNHB.

Hoehn, E. & Gunten, H. R. V. (1989): *Radon in Groundwater: A Tool to Assess Infiltration From Surface Waters to Aquifers*. Water Resources Research **25**, pp. 1795 - 1803.

Hofmeister, F. (1888): *Zur Lehre von der Wirkung der Salze*. Archiv für Experimentelle Pathologie und Pharmakologie **24**, pp. 247 - 260.

Hohwieler, N. (2005): *Beryllium-7 als neuer Tracer in der hydrologischen Prozessforschung - eine Machbarkeitsstudie*. Albert-Ludwigs-Universität, Freiburg im Breisgau, 109 pp.

Holleman, A. F.; Wiberg, N. & Wiberg, E. (2007): *Lehrbuch der Anorganischen Chemie*, 102. edition, deGruyter, Berlin, 2149 pp.

Holzapfel, H.; Ehrhardt, H. & Tischer, W. (1962): *Beitrag zur Trennung der Alkaliionen am Kationenaustauscher.* Journal für praktische Chemie **18**, pp. 62 - 71.

Hong, Y.-L. & Kim, G. (2005): *Measurement of Cosmogenic $^{35}S$ Activity in Rainwater and Lake Water.* Analytical Chemistry **77**, pp. 3390 - 3393.

Jander, G. & Blasius, E. (1989): *Lehrbuch der analytischen und präparativen anorganischen Chemie*, 13. edition, S. Hirzel Verlag, Stuttgart, 554 pp.

Jasiulionis, R. & Wershofen, H. (2005): *A study of the vertical diffusion of the cosmogenic radionuclides, $^{7}Be$ and $^{22}Na$ in the atmosphere*. Journal of Environmental Radioactivity **79**, pp. 157 - 169.

Keller, C. (1993): *Grundlagen der Radiochemie*, 3. edition, Otto Salle Verlag, Frankfurt am Main, 202 pp.

Kirchner, J. W. (2003): *A double paradox in catchment hydrology and geochemistry.* Hydrological Processes **17**, pp. 871 - 874.

Knies, D.; Elmore, D.; Sharma, P.; Vogt, S.; Li, R.; Lipschutz, M.; Petty, G.; Farrell, J.; Monaghan, M.; Fritz, S. & Agee, E. (1994): *$^{7}Be$, $^{10}Be$ and $^{36}Cl$ in precipitation*. Nuclear Instruments and Methods in Physics B **92**, pp. 340 - 344.

Kolb, W. & Wershofen, H. (1991): *Radionuclide concentration in ground-level air in 1990 in North Germany and North Norway*, 1. edition, Physikalisch-Technische Bundesanstalt, Braunschweig, 20 pp.

Lal, D. & Peters, B. (1967): *Cosmic Ray Produced Radioactivity on the Earth*. In: Flügge, S. (Ed.), *Handbuch der Physik* **46**, Springer Verlag, Berlin, Heidelberg, New York, pp. 551 - 612.

Lal, D. & Peters, B. (1962): *Cosmic ray produced isotopes and their application to problems in geophysics*. In: Wilson, J. & Wouthuysen, S. (Ed.), *Progress in Elementary Particle and Cosmic Ray Physics* **6**, North Holland, Amsterdam, pp. 1 - 74.

Leblanc, D. R.; Garabedian, S. P. & Hess, K. M. (1991): *Large scale natural gradient tracer test in sand and gravel, Cape Cod, 1. experimental design and observed tracer movement*. Water Resources Research **25**, pp. 779 - 910.

LUBW (2007): *WABOA - Wasser und Bodenatlas Baden-Württemberg*, 3. edition, Landesamt für Umwelt, Messungen und Naturschutz Baden-Württemberg, Stuttgart, 70 pp.

Marquez, L.; Costa, N. L. & Almeida, I. G. (1957): *The formation of $^{22}$Na from atmospheric argon by cosmic rays*. Il nuovo cimento **6**, pp. 1292-1295.

Martin, M. & Blichert-Toft, P. (1970): *Radioactive atoms: Auger-Electron, α-, β-, γ-, and X-Ray Data*. Atomic Data and Nuclear Data Tables **8**, pp. 1 -198.

Matzarakis, A. & Mayer, H. (2000): *Jährliche Variabilität von Lufttemperatur und Niederschlag in Freiburg*. Berichte des Meteorologischen Institutes der Unversität Freiburg **5**, pp. 201 - 226.

Merck (2003): *Sicherheitsdatenblatt Ammoniumcarbonat reinst Ph Franc, E 503*, Merck KGaA, Darmstadt, 5 pp.

Merck (2009): *Ionenaustauscher und Adsorberharze*, Merck KGaA, Darmstadt, 16 pp.

Neitsch, S. L.; Arnold, J. G.; Kiniry, J. R. & Williams, J. R. (2005): *Soil And Water Assessment Tool Theoretical Documentation*, 1. edition, Grassland, Soil and Water Research Laboratory, USDA-ARS, Temple, 494 pp.

Nevinskii, I. O.; Tsvetkova, T. V. & Zheleznyak, G. S. (2004): *Low-Background Measurements of $^{22}$Na in Natural Waters of Krasnodar Krai*. Atomic Energy **96**, pp. 57-60.

Nimz, G. J. (1998): *Lithogenic and Cosmogenic Tracers in Catchment Hydrology.* In: Kendall, C. & McDonnell, J. J. (Ed.), *Isotope Tracers in Catchment Hydrology*, Elsevier, Amsterdam, pp. 247 - 290.

Novák, M.; Michel, R.; Přechová, E. & Štěpánová, M. (2004): *The Missing Flux in a $^{35}$S Budget for the Soils of a Small Polluted Catchment*. Water, Air & Soil Pollution: Focus **4**, pp. 517 -529.

Patnaik, P. (2002): *Handbook Of Inorganic Chemicals*, 1. edition, McGraw-Hill Professional Publishing, New York, 1086 pp.

Perkins, R. W. & Nielsen, J. M. (1965): *Sodium-22 and Ceasium-134 in foods, man and air.* Nature **205**, pp. 866 - 867.

RAD7Manual (2000): *RAD7 Radon Detector Owner's Manual*, 6.0.1. edition, Durridge Company Inc., Bedford, 77 pp.

Rozanski, K.; Froehlich, K. & Mook, W. G. (2001): *Surface Water.* In: Mook, W. (Ed.), *Environmental isotopes in the hydrological cycle* **III**, UNESCO, Paris, pp. 1 - 121.

Sakaguchi, A.; Ohstuka, Y.; Yokota, K.; Sasaki, K.; Komura, K. & Yamamoto, M. (2005): *Cosmogenic radionuclide $^{22}$Na in the Lake Biwa system (Japan): residence time, transport and application to the hydrology.* Earth and Planetary Science Letters **231**, pp. 307 - 316.

Sakaguchi, A.; Yamamoto, M.; Ohstuka, Y.; Sasaki, K.; Yokota, K. & Komura, K. (2003): *Low-level measurement of the cosmogenic $^{22}$Na radionuclide in fresh water by ultra low-background gamma-ray spectrometry after simple radiochemical separation*. Journal of Radioanalytical and Nuclear Chemistry **258**, pp. 101 - 105.

Samat, S. B. & Green, S. (1997): *A comparison of measurement sensitivity of two different gamma-ray analysis systems for $^{137}$Cs and $^{40}$K*. Applied Radiation and Isotopes **48**, pp. 379 - 381.

Sarudi, I. (1972): *Kaliumbestimmung durch Chemiluminescenztitartion*. Fresenius' Journal of Analytical Chemistry **260**, pp. 114-116.

Scheffer, F. & Schachtschabel, P. (2002): *Lehrbuch der Bodenkunde*, 15. edition, Spektrum Akademischer Verlag, Heidelberg, Berlin, 593 pp.

Seaborg, G. T. (1964): *Element 95 and Method of Producing said Element*. Patent No. 3156523, by the United States Atomic Energy Commission, Chicago, 6 pp.

Solomon, D. K.; Poreda, R. J.; Schiff, S. L. & Cherry, J. A. (1992): *Tritium and helium-3 as groundwater age tracers in the Borden aquifer.* Water Resources Research **28**, pp. 741-755.

Spier, H. W. & Wagner, G. (1952): *Tetraphenylborat als kaliumblockierendes Anion*. Journal of Molecular Medicine **30**, pp. 757-759.

Sueker, J. K.; Turk, J. T. & Michel, R. L. (1999): *Use of cosmogenic $^{35}$S for comparing ages of water from three alpine-subalpine basins in the Colorado Front Range*. Geomorphology **27**, pp. 61 - 74.

Tokuyama, H. & Igarashi, S. (1998): *Seasonal variation in the environmental background level of cosmic-ray-produced $^{22}$Na at Fukui City, Japan*. Journal of Environmental Radioactivity **38**, pp. 147 - 161.

Uhlenbrook, S. (1999): *Untersuchung und Modellierung der Abflußbildung in einem mesoskaligen Einzugsgebiet. Freiburger Schriften zur Hydrologie* **10**, Institut für Hydrologie der Universität Freiburg im Breisgau, pp. 218.

Umweltbundesamt (2010): *Luft und Luftreinhaltung Berichte: Jahresmitteltabellen*. www.umweltbundesamt.de, (26.01.2010).

Veselý, J.; Beneš, P. & Ševči, K. (1989): *Occurrence and speciation of beryllium in acidified freshwaters*. Water research **23**, pp. 711 - 717.

Veselý, J. & Majer, V. (1994): *The Effect of pH and atmospheric Deposition on Concentrations of Trace Elements in Acidified Freshwaters: A statistical Approach*. Water, Air and Soil Pollution **88**, pp. 227 - 246.

Wade, W. Z. & Wolf, T. (1967): *Preparation and some properties of americium metal*. Journal of Inorganic and Nuclear Chemistry **29**, pp. 2577 - 2587.

Weeks, K. J.; Litvinenko, V. N. & Madey, J. M. J. (1997): *The Compton backscattering process and radiotherapy.* Medical Physics **24**, pp. 417 - 423.

Wenninger, J.; Uhlenbrook, S.; Tilch, N. & Leibundgut, C. (2004): *Experimental evidence of fast groundwater responses in a hillslope/floodplain area in the Black Forest Mountains, Germany.* Hydrological Processes **18**, pp. 3305-3322.

Wershofen, H. & Arnold, D. (1995): *Radionuclides in Ground-Level Air in Braunschweig - Report of the PTB Trace Survey Station for 1993 and 1994*, 1. edition, Physikalisch-Technische Bundesanstalt, Braunschweig, 31 pp.

Wissmeier, L. & Uhlenbrook, S. (2007): *Distributed, high-resolution modelling of $^{18}$O signals in a meso-scale catchment*. Journal of Hydrology **332**, pp. 497 - 510.

Wittig, G.; Keicher, G.; Rückert, A. & Raff, P. (1949): *Über Bor-alkalimetall-organische Komplexverbindungen*. Justus Liebigs Annalen der Chemie **563**, pp. 110 - 126.

Wogman, N. A.; Thomas, C. W.; Cooper, J. A.; Engelmann, R. J. & Perkins, R. W. (1968): *Cosmic Ray-Produced Radionuclides as Tracers of Atmospheric Precipitation Processes*. Science **159**, pp. 189 - 192.

You, C.-F.; Lee, T. & Li, Y.-H. (1989): *The partition of Be between soil and water.* Chemical Geology **77**, pp. 105 - 118.

# A) Appendix

Table A.1: Field parameters for sample at Schauinsland on November, 11th 2009

| Samples taken before pumping through the exchange resin. | | | | | |
|---|---|---|---|---|---|
| **Measuring** | **Time** | **pH** | **Temperature [°C]** | **Oxygen saturation [%]** | **Electric conductivity [µS/cm. 25°C]** |
| 1 | 12:00 | 6.35 | 8.9 | 70.94 | |
| 2 | 12:10 | 6.08 | 8.9 | 68.28 | 61.0 |
| 3 | 12:20 | 5.91 | 8.6 | 66.76 | 60.2 |
| 4 | 12:30 | 5.68 | 8.4 | 66.76 | 59.9 |
| 5 | 12:40 | 5.52 | 8.4 | 76.36 | 59.6 |
| 6 | 13:00 | 5.43 | 8.2 | 80.47 | 59.6 |
| Samples taken after pumping through the exchange resin. | | | | | |
| 1 | 13:10:00 | 3.5 | - | - | 115 |

Table A.2: Field parameters for sample at Schauinsland on December, 1st 2009

| Samples taken before pumping through the exchange resin. | | | | | |
|---|---|---|---|---|---|
| **Measuring** | **Time** | **pH** | **Temperature [°C]** | **Oxygen saturation [%]** | **Electric conductivity [µS/cm. 25°C]** |
| 1 | 12:30:00 | 6.58 | 6.3 | 80.13 | 54.0 |
| 2 | 12:50:00 | 5.09 | 6.3 | 79.33 | 54.0 |
| 3 | 13:10:00 | 5.07 | 6.2 | 79.93 | 54.0 |
| 4 | 13:20:00 | 4.98 | 6.2 | 79.93 | 54.0 |
| 5 | 13:30:00 | 4.92 | 6.2 | 70.74 | 54.0 |
| 6 | 14:00:00 | 5.05 | 6.2 | 79.93 | 54.0 |
| 7 | 14:20:00 | 5.03 | 6.2 | 79.93 | 53.9 |
| 8 | 14:40:00 | 5.06 | 6.2 | 79.12 | 53.9 |
| Samples taken after pumping through the exchange resin. | | | | | |
| 1 | 12:40:00 | 3.51 | - | - | - |
| 2 | 13:10:00 | 3.30 | - | - | 119.6 |
| 3 | 13:25:00 | 3.40 | - | - | 111.7 |
| 4 | 13:40:00 | 3.25 | - | - | 121.9 |
| 5 | 14:05:00 | 3.23 | - | - | 114.2 |
| 6 | 14:30:00 | 3.29 | - | - | 115.4 |
| 7 | 14:50:00 | 3.20 | - | - | 116.5 |

Table A.3: Field parameters for sample at Brugga on December, 10th and 15th 2009

| Samples taken before pumping through the exchange resin. | | | | | |
|---|---|---|---|---|---|
| **Measuring** | **Time** | **pH** | **Temperature [°C]** | **Oxygen saturation [%]** | **Electric conductivity [µS/cm. 25°C]** |
| 1 | 11:00:00 | 6.74 | 6.6 | 88.08 | 83.2 |
| 2 | 11:30:00 | 6.49 | 6.7 | 87.49 | 79.9 |
| 3 | 09:30:00 | 6.85 | 1.8 | 92.05 | 91.5 |
| 4 | 10:00:00 | 6.67 | 1.7 | 91.08 | 91.8 |
| 5 | 10:30:00 | 6.60 | 1.7 | 87.77 | 96.9 |
| 6 | 11:00:00 | 6.61 | 1.8 | 90.11 | 91.3 |
| 7 | 11:30:00 | 6.75 | 1.8 | 90.83 | 88.3 |
| 8 | 12:30:00 | 7.00 | 1.8 | 90.11 | 88.8 |
| Samples taken after pumping through the exchange resin. | | | | | |
| 1 | 11:00:00 | 3.09 | - | - | 200 |
| 2 | 09:30:00 | 3.18 | - | - | 238 |
| 3 | 10:00:00 | 3.16 | - | - | 224 |
| 4 | 10:30:00 | 3.10 | - | - | 246 |
| 5 | 11:00:00 | 3.12 | - | - | 238 |
| 6 | 11:30:00 | 3.10 | - | - | 229 |
| 7 | 12:30:00 | 3.27 | - | - | 234 |

Table A.4: Field parameters for sample at Hungerbrunnen on January, 14th 2010

| Samples taken before pumping through the exchange resin. | | | | | |
|---|---|---|---|---|---|
| **Measuring** | **Time** | **pH** | **Temperature [°C]** | **Oxygen saturation [%]** | **Electric conductivity [µS/cm. 25°C]** |
| 1 | 11:00:00 | 5.66 | 10.4 | 71.54 | 157.2 |
| 2 | 12:00:00 | 5.65 | 10.4 | 76.91 | 157.5 |
| 3 | 13:00:00 | 5.63 | 10.4 | 71.54 | 157.6 |
| 4 | 14:00:00 | 5.71 | 10.3 | 75.83 | 157.5 |
| 5 | 15:00:00 | 5.62 | 10.4 | 76.01 | 157.3 |
| Samples taken after pumping through the exchange resin. | | | | | |
| 1 | 12:00:00 | 2.95 | - | - | 418 |
| 2 | 12:30:00 | 2.89 | - | - | 360 |
| 3 | 13:30:00 | 2.90 | - | - | 385 |
| 4 | 14:30:00 | 3.00 | - | - | 380 |

Table A.5: Field parameters for sample from snow, collected from January, 11th to 15th 2010

| Sample taken before pumping through the exchange resin | | | | | |
|---|---|---|---|---|---|
| **Measuring** | **Time** | **pH** | **Temperature [°C]** | **Oxygen saturation [%]** | **Electric conductivity [µS/cm. 25°C]** |
| 1 | 14:00:00 | 6.28 | 17.8 | - | 32.5 |
| Samples taken after pumping through the exchange resin. | | | | | |
| 1 | 14:20:00 | 3.48 | - | - | 92.3 |
| 2 | 14:35:00 | 3.42 | - | - | 89.1 |
| 3 | 14:50:00 | 3.42 | - | - | 86.1 |
| 4 | 15:00:00 | 3.41 | - | - | 82.8 |
| 5 | 15:15:00 | 3.43 | - | - | 81.4 |
| 6 | 15:30:00 | 3.45 | - | - | 80.8 |
| 7 | 15:45:00 | 3.45 | - | - | 80.0 |
| 8 | 16:00:00 | 3.46 | - | - | 79.3 |
| 9 | 16:15:00 | 3.44 | - | - | 78.9 |
| 10 | 16:30:00 | 3.44 | - | - | 78.7 |
| 11 | 16:45:00 | 3.45 | - | - | 78.6 |
| 12 | 17:00:00 | 3.43 | - | - | 78.6 |
| 13 | 17:15:00 | 3.44 | - | - | 78.5 |
| 14 | 17:30:00 | 3.44 | - | - | 78.5 |

Table A.6: Field parameters for sample at Dreisam on February, 4th 2010

| Samples taken before pumping through the exchange resin. | | | | | |
|---|---|---|---|---|---|
| **Measuring** | **Time** | **pH** | **Temperature [°C]** | **Oxygen saturation [%]** | **Electric conductivity [µS/cm. 25°C]** |
| 1 | 11:30:00 | 7,26 | 2,9 | 102,24 | 174,5 |
| 2 | 12:00:00 | 5,72 | 3,1 | 102,05 | 173,3 |
| 3 | 12:30:00 | 5,82 | 3,4 | 102,12 | 172,6 |
| 4 | 13:00:00 | 5,93 | 3,7 | 101,34 | 171,0 |
| 5 | 14:00:00 | 6,23 | 4,2 | 101,23 | 169,4 |
| 6 | 14:45:00 | 6,08 | 4,4 | 100,99 | 168,8 |
| Samples taken after pumping through the exchange resin. | | | | | |
| 1 | 11:45:00 | 2.95 | - | - | 472 |
| 2 | 12:00:00 | 2.75 | - | - | 457 |
| 3 | 12:45:00 | 2.64 | - | - | 444 |
| 4 | 13:30:00 | 2.76 | - | - | 451 |
| 5 | 14:30:00 | 2.99 | - | - | 429 |

Table A.7: Principle components in riverine samples

| | Brugga | | | | | | | Dreisam | | | | | | |
|---|---|---|---|---|---|---|---|---|---|---|---|---|---|---|
| **Date** | **Cl** | **NO3** | **SO4** | **Na** | **K** | **Mg** | **Ca** | **Cl** | **NO3** | **SO4** | **Na** | **K** | **Mg** | **Ca** |
| 07.08.09 | 8.21 | 3.79 | 3.88 | 5.74 | 0.44 | 1.99 | 11.30 | 8.51 | 5.02 | 6.93 | 7.13 | 1.13 | 2.43 | 14.53 |
| 14.08.09 | 8.54 | 4.05 | 4.04 | 5.81 | 0.47 | 2.09 | 11.88 | 8.95 | 5.20 | 6.94 | 7.18 | 1.09 | 2.55 | 15.26 |
| 21.08.09 | 8.81 | 4.52 | 4.13 | 6.46 | 0.89 | 2.21 | 15.35 | 8.90 | 5.28 | 8.38 | 7.28 | 1.60 | 2.77 | 16.56 |
| 28.08.09 | 8.85 | 4.56 | 4.09 | 6.30 | 0.83 | 2.23 | 12.94 | 8.73 | 5.08 | 7.09 | 7.22 | 1.29 | 2.55 | 16.06 |
| 04.09.09 | 8.30 | 3.92 | 3.79 | 5.92 | 1.16 | 1.86 | 11.80 | 7.45 | 4.48 | 5.87 | 6.47 | 1.63 | 2.13 | 16.50 |
| 11.09.09 | 8.97 | 4.37 | 4.03 | 6.90 | 1.04 | 2.46 | 13.32 | 8.45 | 4.40 | 6.84 | 7.62 | 1.81 | 2.74 | 15.19 |
| 18.09.09 | 8.61 | 4.27 | 3.95 | 6.59 | 0.96 | 2.40 | 13.34 | 8.76 | 4.79 | 6.90 | 8.05 | 1.66 | 2.74 | 15.56 |
| 24.09.09 | 8.76 | 4.25 | 3.97 | 6.66 | 0.98 | 2.52 | 13.94 | 8.70 | 4.18 | 7.28 | 7.63 | 1.38 | 2.84 | 15.87 |
| 02.10.09 | 9.20 | 4.43 | 4.38 | 6.28 | 0.87 | 2.26 | 13.51 | 8.85 | 4.25 | 7.74 | 6.93 | 1.15 | 2.63 | 15.52 |
| 09.10.09 | 8.67 | 4.44 | 4.09 | 6.58 | 1.11 | 1.83 | 11.68 | 7.97 | 5.29 | 7.35 | 7.11 | 2.67 | 2.35 | 15.28 |
| 16.10.09 | 8.89 | 4.64 | 4.20 | 6.26 | 0.98 | 2.13 | 12.25 | 8.74 | 5.40 | 8.02 | 7.57 | 1.83 | 2.83 | 16.28 |
| 22.10.09 | 9.28 | 3.94 | 4.04 | 6.91 | 1.11 | 2.07 | 13.45 | 8.78 | 5.19 | 6.74 | 7.34 | 1.64 | 2.34 | 13.93 |
| 30.10.09 | 9.20 | 7.04 | 4.34 | 6.60 | 1.04 | 1.82 | 13.08 | 9.14 | 5.69 | 7.62 | 7.40 | 1.98 | 1.77 | 8.64 |
| 07.11.09 | 7.51 | 4.94 | 3.90 | 5.78 | 1.11 | 1.56 | 12.95 | 7.71 | 5.03 | 6.70 | 6.24 | 1.62 | 1.92 | 15.03 |
| 14.11.09 | 7.92 | 4.28 | 4.01 | 5.70 | 1.04 | 1.54 | 11.35 | 7.80 | 5.22 | 7.15 | 6.51 | 1.75 | 1.45 | 9.36 |
| 24.11.09 | 7.33 | 4.27 | 3.93 | 5.28 | 0.99 | 1.53 | 10.53 | 7.11 | 5.36 | 6.89 | 5.85 | 1.64 | 2.02 | 15.85 |
| 27.11.09 | 6.38 | 4.29 | 3.81 | 4.86 | 0.98 | 1.45 | 12.59 | 7.05 | 5.32 | 6.45 | 6.02 | 1.59 | 1.87 | 13.43 |
| 04.12.09 | 8.17 | 4.41 | 3.93 | 6.25 | 1.01 | 1.53 | 13.81 | 7.37 | 5.34 | 7.03 | 6.30 | 1.63 | 2.00 | 16.05 |
| 11.12.09 | 7.71 | 4.80 | 4.46 | 5.87 | 0.74 | 1.39 | 10.83 | 7.19 | 8.23 | 6.52 | 5.47 | 3.24 | 1.88 | 13.40 |
| 18.12.09 | 7.28 | 5.76 | 5.86 | 5.65 | 0.76 | 1.75 | 11.76 | 6.67 | 11.28 | 7.84 | 5.89 | 1.21 | 1.99 | 12.36 |
| 22.12.09 | 23.42 | 5.29 | 4.37 | 14.93 | 0.91 | 1.76 | 11.90 | 20.87 | 7.09 | 7.32 | 14.71 | 1.83 | 2.16 | 14.24 |
| 31.12.09 | 9.81 | 4.80 | 4.09 | 6.77 | 0.78 | 1.19 | 9.24 | 8.35 | 8.29 | 6.96 | 6.46 | 1.54 | 1.85 | 17.42 |
| 08.01.10 | 9.39 | 5.12 | 4.44 | 6.92 | 0.81 | 1.88 | 12.87 | 8.18 | 8.10 | 6.94 | 7.12 | 1.32 | 2.20 | 19.78 |
| 15.01.10 | 10.95 | 4.88 | 4.27 | 8.46 | 0.93 | 2.32 | 12.50 | 11.39 | 7.69 | 7.77 | 9.51 | 1.97 | 2.70 | 18.50 |
| 22.01.10 | 10.96 | 4.36 | 5.32 | 7.69 | 0.98 | 2.27 | 10.10 | 10.43 | 7.37 | 8.87 | 8.55 | 1.56 | 2.79 | 15.90 |
| 29.01.10 | 16.20 | 5.31 | 4.47 | 11.60 | 0.89 | 2.40 | 13.20 | 21.57 | 7.17 | 8.19 | 16.50 | 1.45 | 2.68 | 21.20 |

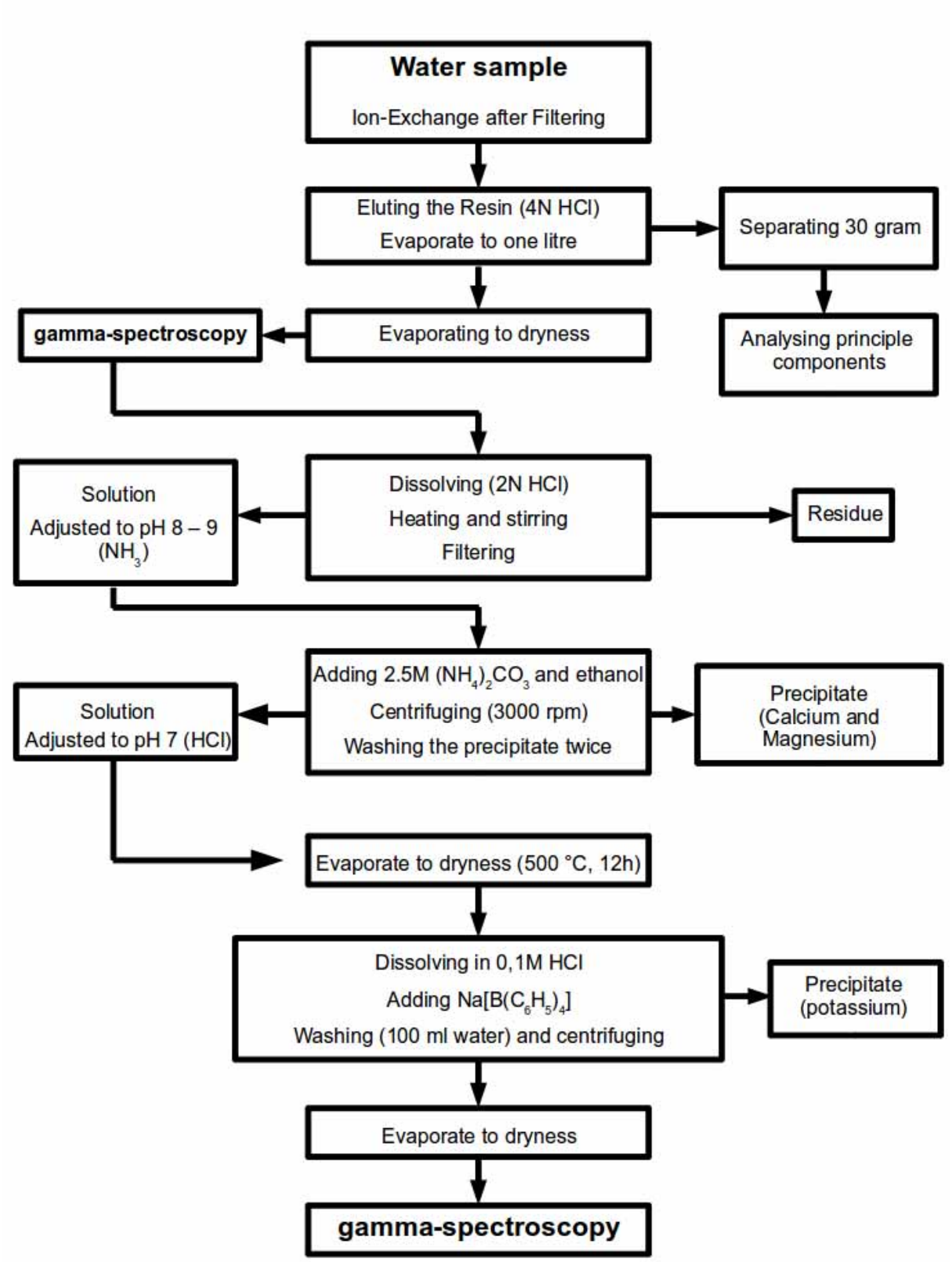


Fig. A.1: Original chemical separation of potassium presented by Sakaguchi et al. (2003)

## *Software used*

This work was done, as far as possible, using open source software, namely:

- Ubuntu 9.10
- OpenOffice.org 3.1
- JabRef 2.5
- QTIPlot 0.9.7.12
- GIMP (GNU Image Manipulation Program) 2.6.8
- Inkscape 0.47
- Durridge CaptureWin 4.0.6 (not open source)